

The effects of long-term Free Air CO₂
Enrichment (FACE) on soil aggregation, soil
carbon input, and ecosystem CO₂ dynamics in
a temperate grassland ecosystem



Inauguraldissertation

zur Erlangung des akademischen Grades doctor rerum naturalium
(Dr. rer. nat.)

der naturwissenschaftlichen Fachbereiche der
Justus-Liebig-Universität Gießen

vorgelegt von
Katharina Lenhart

Gießen, im September 2008

Dekan: Prof. Dr. Peter R. Schreiner

Erster Gutachter: Prof. Dr. Dr. h.c. Hans-Jürgen Jäger

Zweiter Gutachter: Prof. Dr. Christoph Müller

Tag der mündlichen Prüfung:

22. Dezember 2008

Erklärung

Hiermit erkläre ich, dass ich die vorgelegte Dissertation selbstständig und ohne unerlaubte fremde Hilfe und nur mit den Hilfen angefertigt habe, die ich in der Dissertation angegeben habe.

Alle Textstellen, die wörtlich oder sinngemäß aus veröffentlichten Schriften entnommen sind, und alle Angaben, die auf mündlichen Auskünften beruhen, sind als solche kenntlich gemacht.

Bei den von mir durchgeführten und in der Dissertation erwähnten Untersuchungen habe ich die Grundsätze guter wissenschaftlicher Praxis, wie sie in der „Satzung der Justus-Liebig-Universität Gießen zur Sicherung guter wissenschaftlicher Praxis“ niedergelegt sind, eingehalten.

Gießen, den 26. September 2008

Table of contents

List of tables.....	III
List of figures.....	IV
Abbreviations.....	VI
Abstract.....	XII
Kurzfassung.....	IX
1 Introduction	1
1.1 Climate change and grassland ecosystems	1
1.2 Effects of elevated CO₂ on ecosystem C dynamics	2
1.2.1 Grassland FACE experiments.....	2
1.2.2 Ecosystem C balance	3
1.2.3 Soil aggregate structure	4
1.2.4 Soil and ecosystem respiration and its components.....	6
1.3 Objectives of this study	8
2 Materials and methods	9
2.1 Site description	9
2.2 Air temperature, precipitation, and soil data	10
2.2.1 Air temperature and precipitation	10
2.2.2 Soil texture.....	12
2.2.3 Bulk density	12
2.2.4 Soil moisture	13
2.3 Soil and plant biomass sampling and analysis	14
2.3.1 Soil sampling	14
2.3.2 Soil aggregate fractionation	14
2.3.3 Plant biomass	16
2.3.4 Analysis of ¹³ C signature and SOC content.....	17
2.3.5 Calculations	17
2.4 Gas sampling and analysis	19
2.4.1 Gas sampling.....	19
2.4.2 Analysis of δ ¹³ C signature and CO ₂ concentration.....	20
2.4.3 Separation of soil and ecosystem respiration into its components.....	20
2.5 Statistical analysis	25
3 Results	27
3.1 Air temperature, precipitation, and soil moisture	27
3.2 Plant biomass	30
3.2.1 δ ¹³ C signature of above and belowground biomass	30
3.2.2 Root biomass yield.....	32
3.3 Soil aggregate structure	34
3.3.1 Distribution of aggregates in the soil profile.....	34
3.3.2 Soil aggregation changes between 1998 and 2007	35

3.3.3	Effect of elevated CO ₂ on soil aggregation	36
3.4	Soil organic carbon content and $\delta^{13}\text{C}$ signature under ambient and elevated CO₂	38
3.4.1	SOC content.....	38
3.4.2	Effects of elevated CO ₂ on SOC content	44
3.4.3	$\delta^{13}\text{C}$ signature of SOC in bulk soil and the soil aggregate fractions.....	45
3.5	Soil C input in the CO₂ enriched plots	49
3.5.1	Fraction of new C	49
3.5.2	Input of new C	50
3.5.3	Input of new C into free and macroaggregate-associated microaggregates.....	53
3.6	Soil air CO₂ and ecosystem respiration	55
3.6.1	Annual dynamics of ecosystem respiration and $\delta^{13}\text{C}$ and CO ₂ concentration in soil air	55
3.6.2	Partitioning of R _{soil} into autotrophic and heterotrophic components.....	65
3.6.3	Partitioning of R _{eco}	69
4	Discussion	73
4.1	Effects of elevated CO₂ on the soil aggregate structure.....	73
4.2	Effects of elevated CO₂ on the soil C content	77
4.3	Soil C input under elevated CO₂	83
4.4	Effects of elevated CO₂ on the autotrophic and heterotrophic components of soil and ecosystem respiration.....	91
5	Conclusions and outlook	99
6	References	101
7	Appendix	116
7.1	Date of aboveground biomass clipping.....	116
7.2	Drying-Wetting Cycles between 1997 and 2004	116
7.3	List of gas samples	116
7.4	Bulk density	121

List of Tables

Tab. 2.1 $\delta^{13}\text{CO}_2$ of tank- CO_2 and atmospheric CO_2 in the CO_2 -enriched plots	10
Tab. 2.2 Soil texture and pH in the soil profile	12
Tab. 3.1 Mean air temperatures (T_{air}) and temperature changes.....	27
Tab. 3.2 Predicted and measured $\delta^{13}\text{C}$ signature of plants	30
Tab. 3.3: $\delta^{13}\text{C}$ signature of aboveground plant biomass.....	31
Tab. 3.4 Effect of depth on $\delta^{13}\text{C}$ signature of root biomass	32
Tab. 3.5 Differences in root biomass between the CO_2 treatments	33
Tab. 3.6 Relative changes in soil aggregation.....	36
Tab. 3.7 Average changes in SOC content between April 1998 and 2004	39
Tab. 3.8 Changes in total SOC under ambient atmospheric CO_2 conditions	39
Tab. 3.9 Area-related changes in SOC of several soil fractions	41
Tab. 3.10 Fraction of new C in several soil aggregate fractions after 8 years of elevated $[\text{CO}_2]$ +20%.....	49
Tab. 3.11 Fraction of new C in several soil aggregate fractions after 8 years of elevated $[\text{CO}_2]$ +30%.....	50
Tab. 3.12 Rate of C input per year under $[\text{CO}_2]$ +20%	51
Tab. 3.13 Rate of C input per year under $[\text{CO}_2]$ +30%	52
Tab. 3.14 Fraction of new C in June 2004 in free and macroaggregate- associated microaggregates.....	53
Tab. 3.15 $\delta^{13}\text{C}$ signature of soil air CO_2 in the ring pairs 1-3	56
Tab. 3.16 $\delta^{13}\text{C}$ signature of soil air CO_2 in ring pair 4	63
Tab. 3.17 Contribution of R_{root} on R_{soil} [%]	66
Tab. 3.18 The mean $\delta^{13}\text{C}$ signature of the CO_2 source of R_{eco}	69
Tab. 3.19 Relative contribution of autotrophic respiration on R_{eco}	71
Tab. 4.1 Reported effects of elevated CO_2 on soil C stocks of in-situ CO_2 enrichment experiments on grassland ecosystems	77
Tab. 4.2 Components of R_{eco} in the Giessen-FACE, an annual grassland, and a Californian redwood forest ecosystem.....	98
Tab. 7.1 Dates of aboveground biomass clipping.....	116
Tab. 7.2 List of gas samples	117
Tab. 7.3 Bulk density values.	121

List of Figures

Fig. 1.1 Components of ecosystem C budget.	3
Fig. 1.2 Sources of soil respiration.....	7
Fig. 2.1 Aboveground biomass yield in the Giessen-FACE.....	9
Fig. 2.2 $\delta^{13}\text{C}$ signature of enrichment- CO_2	10
Fig. 2.3 Temperature function (fT) according to Jarvis-Stewart.....	11
Fig. 2.5 Soil fractions obtained from wet sieving and microaggregate isolation.....	15
Fig. 3.1 Precipitation.....	28
Fig. 3.2 Soil moisture.....	29
Fig. 3.3 $\delta^{13}\text{C}$ signature of root biomass.....	31
Fig. 3.4 Coherency between root $\delta^{13}\text{C}$ signature and depth.....	32
Fig. 3.5 Mean root biomass after 9 years of CO_2 enrichment.....	33
Fig. 3.6 Distribution of soil aggregates in the soil profile	34
Fig. 3.7 Soil aggregate structure of plots.	35
Fig. 3.8 LM content differences between E- and A-plots.....	37
Fig. 3.9 SOC content of several soil fractions in the soil profile.....	38
Fig. 3.10 Average changes in SOC content.....	40
Fig. 3.11 SOC content stored in each aggregate fraction.	42
Fig. 3.12 SOC loss between April 1998 and 2004 and magnitude of LM loss.	43
Fig. 3.13 SOC content in 1998 and after 9 years of elevated CO_2	44
Fig. 3.14 Changes in SOC since 1998.....	44
Fig. 3.15 $\delta^{13}\text{C}$ signature of SOC in the soil profile.....	46
Fig. 3.16 Shift in $\delta^{13}\text{C}$ signature of SOC in several soil aggregate fractions	47
Fig. 3.17 The $\delta^{13}\text{C}$ signature of aggregate fractions in E and A-plots.....	48
Fig. 3.18 Input of new C into free and macroaggregate-associated microaggregates.	54
Fig. 3.19 Ecosystem respiration, soil air CO_2 concentration and $\delta^{13}\text{C}$ signature of soil air CO_2 in ring pair 1.	57
Fig. 3.20 Ecosystem respiration, soil air CO_2 concentration and $\delta^{13}\text{C}$ signature of soil air CO_2 in ring pair 2.	58
Fig. 3.21 Ecosystem respiration, soil air CO_2 concentration and $\delta^{13}\text{C}$ signature of soil air CO_2 in ring pair 3.	59
Fig. 3.22 Mean values of the ring pairs 1-3.....	60
Fig. 3.23 $\delta^{13}\text{C}$ signature of soil air CO_2 in the soil profile.....	62

Fig. 3.24 Correlation of soil depth and decrease in $\delta^{13}\text{CO}_2$	64
Fig. 3.25 Contribution of R_{root} on R_{soil} over time ($[\text{CO}_2] +20\%$).	65
Fig. 3.26 Correlation of root-derived CO_2 and depth ($[\text{CO}_2] +30\%$).	67
Fig. 3.27 Contribution of R_{root} on R_{soil} in the soil profile ($[\text{CO}_2] +30\%$)	68
Fig. 3.28 $\delta^{13}\text{C}$ signature of the CO_2 source of R_{eco} and soil air CO_2	70
Fig. 3.29 Contribution of leaf respiration to R_{eco}	71
Fig. 3.30 Contributions of R_{leaf} , R_{root} and R_{bulk} to R_{eco}	72
Fig. 4.1 Theoretical periodic changes on decadal scale	82
Fig. 7.1 Drying-wetting events of the upper 15 cm of soil.	116

Abbreviations

$f_{C_{new}}$	Fraction of new C
f_{bulk}	Fraction of SOM-derived CO ₂ on R _{soil}
f_{leaf}	Fraction of leaf derived CO ₂ on R _{eco}
f_{plant}	Fraction of plant derived CO ₂ on R _{eco}
f_{root}	Fraction of root derived CO ₂ on R _{soil}
f_{soil}	Fraction of soil derived CO ₂ on R _{eco}
LM	Large macroaggregates (> 2000 μm)
Mic	Microaggregates (53-250 μm)
Mic-LM	Microaggregates within large macroaggregates
Mic-SM	Microaggregates within small macroaggregates
R _{eco}	Ecosystem respiration
R _{leaf}	Leaf respiration
R _{plant}	Plant respiration (roots + leaves)
R _{root}	Root respiration
R _{soil}	Soil respiration
SC	Silt and clay particles (< 53 μm)
SM	Small macroaggregates (250-2000 μm)
SOC	Soil organic carbon
SOM	Soil organic matter
T _{air}	Air temperature
VWC	Volumetric water content

Abstract

Elevated atmospheric CO₂ concentrations enhance photosynthesis, however, they also increase respiratory carbon (C) losses from ecosystems. The changes of both will have a yet unknown effect on ecosystem C dynamics and balances. The aim of this study was to investigate the effects of a moderate long-term CO₂ enrichment on ecosystem C dynamics of a temperate grassland ecosystem. To address this subject the effects of elevated CO₂ on the soil aggregate structure were investigated, and the soil C content and the input of new C to several soil aggregate fractions were determined. Furthermore, the ¹³C isotope signature of soil air CO₂ and ecosystem respiration was measured. The ¹³C signature was used to separate soil and ecosystem respiration into its autotrophic (plant-derived) and heterotrophic (old soil organic carbon) components. The study was conducted at the Free-Air CO₂ Enrichment (FACE) site near Giessen, Germany. The CO₂ enrichment started in May 1998 using ¹³C depleted CO₂ with a signature of -25‰. In July 2004 the δ¹³C signature of the enrichment-CO₂ was switched from -25 to -48‰ without altering the CO₂ concentration. This experimental setup provided the unique opportunity to trace ecosystem C fluxes without concomitant priming effects of a CO₂ step increase.

In the Giessen-FACE study no CO₂-induced increase in soil aggregation occurred after nine years of elevated CO₂. Root biomass increased under [CO₂] +30% but remained mainly unaltered in the [CO₂] +20% treatment. The CO₂ enrichment enhanced ecosystem respiration (R_{eco}) by 13%. However, elevated CO₂ did not result in increased soil C sequestration after 9 years of elevated CO₂ in any soil aggregate fraction, nor did it prevent the loss of soil C observed between 1998 and 2004 at the site. This C loss coincided with a breakup of large macroaggregates. In the [CO₂] +20% enriched plots the input of C to the soil corresponded to 109 ±43.5 g m⁻² yr⁻¹ in the first observation period between 1998 and June 2004, and to 44.4 ±32.5 g m⁻² yr⁻¹ in the second observation period between June 2004 and June 2006. Under elevated [CO₂] +30%, C inputs were 82.1 and 76.2 g m⁻² yr⁻¹ for both periods, respectively, indicating no higher C input with increasing [CO₂] in both investigation periods.

Under elevated [CO₂] +20%, the overall contribution of root-derived soil respiration was 55% in the top 15 cm of the soil. The ¹³C signature of R_{eco} and soil air CO₂ showed the strongest depleted values during the growth period, indicating a higher contribution of plant-derived CO₂ at that time. The mean contributions of root, leaf and soil respiration to R_{eco} were 29 ±18%, 32 ±23% and 38 ±20%, respectively. A significant decrease in soil air δ¹³CO₂ with soil depth indicated a relatively higher contribution of root-derived CO₂ in the deeper soil layers. The δ¹³CO₂ gradient showed distinct annual dynamics with a significant impact of soil temperature. The steepest δ¹³CO₂ gradients occurred during winter but became less distinctive during the summer month.

Overall, the data gave evidence for an accelerated C-turnover with increasing CO₂ concentration but without a net C sequestration under elevated CO₂. Therefore, we

cannot expect grassland ecosystems to reduce the increase in atmospheric CO₂ concentration by incorporating part of the additional C into the soil C stocks.

Kurzfassung

Erhöhte atmosphärische CO₂-Konzentrationen steigern die Photosynthese, erhöhen jedoch durch einen Anstieg der Respiration auch den C-Verlust von Ökosystemen. Veränderungen beider Prozesse haben bislang unbekannte Auswirkungen auf die ökosystemaren C-Dynamiken und deren C-Bilanzen. Ziel dieser Arbeit war es daher, die Auswirkungen einer moderaten CO₂-Anreicherung auf die Ökosystem C-Dynamik eines temperierten Grünlandökosystems zu untersuchen. Dazu wurden die Effekte von erhöhtem CO₂ auf die Aggregatstruktur des Bodens untersucht und der C-Gehalt des Bodens sowie der C-Eintrag in die einzelnen Aggregatklassen ermittelt. Weiterhin wurden die ¹³C Isotopensignatur von Bodenluft-CO₂ und Ökosystematmung gemessen. Anhand der Isotopensignatur wurde die Boden- und Ökosystematmung in ihre autotrophen (pflanzlichen) und heterotrophen (alter organischer Kohlenstoff) Bestandteile unterteilt. Alle Untersuchungen wurden im Rahmen des Giessener Freiland-CO₂ Anreicherungs-experiments (Free Air CO₂ Enrichment; FACE) in Deutschland durchgeführt. Die CO₂-Anreicherung begann bereits im Mai 1998 mit einem ¹³C-abgereicherten CO₂ mit einer Signatur von -25‰. Im July 2004 wurde die ¹³C Signatur des für die Anreicherung verwendeten CO₂'s von -25‰ auf -48‰ reduziert, ohne jedoch die CO₂-Konzentration zu verändern.

Im Giessener FACE Experiment konnte nach 9 Jahren unter erhöhtem CO₂ keine CO₂-induzierte Zunahme der Bodenaggregation beobachtet werden. Zwar zeigte sich eine Zunahme der Wurzelbiomasse unter +30% erhöhtem CO₂, die jedoch im Mittel nicht in den um +20% CO₂-angereicherten Flächen auftrat. Die CO₂-Anreicherung erhöhte die Ökosystematmung (R_{eco}) um 13%. Erhöhtes CO₂ führte nach 9 Jahren in den Bodenaggregatfraktionen weder zu einer Zunahme des C-Eintrags, noch verhinderte es den zwischen 1998 und 2004 beobachteten Verlust von Bodenkohlenstoff auf der Versuchsfläche, der mit einem Zerfall der großen Makroaggregate einherging. Unter CO₂ +20% betrug der C Eintrag in den Boden 109 ±43.5 g m⁻² a⁻¹ während des ersten Untersuchungszeitraumes zwischen 1998 und Juni 2004, und 44.4 ±32.5 g m⁻² a⁻¹ während des zweiten Untersuchungszeitraumes zwischen Juni 2004 und Juni 2006. Unter CO₂ +30% betrug der C-Eintrag 82.1 und 76.2 g m⁻² a⁻¹ für die jeweiligen Zeiträume, was nicht auf einen erhöhten C-Eintrag mit zunehmender CO₂-Konzentration und steigender Wurzelbiomasse hindeutet.

Unter CO₂ + 20% betrug der Anteil des wurzelbürtigen CO₂ an der Bodenatmung 55% in den oberen 15 cm. Die ¹³C Signatur von R_{eco} und Bodenluft-CO₂ war während der Wachstumsperiode am negativsten, was auf einen höheren Anteil an pflanzenbürtigem Atmungs-CO₂ zu dieser Zeit hindeutet. Die mittleren Anteile von Wurzel-, Blatt- und Bodenatmung an R_{eco} betragen 29 ±18%, 32 ±23% und 38 ±20%. Eine signifikante Abnahme der δ¹³C_{CO₂} Signatur der Bodenluft mit der Tiefe deutet auf einen höheren Anteil von wurzelbürtigem CO₂ in den tieferen Bodenschichten hin. Der δ¹³C Gradient zeigte eine ausgeprägte jahreszeitliche Dynamik mit signifikantem Einfluss der Bodentemperatur. Die steilsten δ¹³C_{CO₂}

Gradienten traten in den Wintermonaten auf, während die Ausprägung in den Sommermonaten nur gering war.

Insgesamt belegen die Daten einen schnelleren C-Umsatz mit steigender CO₂-Konzentration, jedoch gab es keine zusätzliche C-Einbindung. Daher können wir nicht davon ausgehen, dass Grasslandökosysteme den Anstieg der atmosphärischen CO₂-Konzentration reduzieren, indem sie einen Teil des zusätzlichen Kohlenstoffs in den Boden einbinden.

1 Introduction

1.1 Climate change and grassland ecosystems

Within the past 420,000 years the atmospheric CO₂ concentration ([CO₂]) ranged between 180 ppm in glacial periods and 280 ppm in interglacial periods (Petit et al. 1999). Since 1750 with the onset of the industrial revolution, fossil fuel burning and land use change led to an unprecedented increase in atmospheric [CO₂] of currently 1.9 ppm yr⁻¹ (IPCC 2007). The temperature increase due to rising greenhouse gas concentrations in the atmosphere is temporarily delayed by 3 to 4 decades (Hansen et al. 2007). However, over the last 100 years (1906–2005), the global mean surface temperatures have already risen by 0.74°C ±0.18°C, with the last twelve years including the eleven warmest years since the beginning of the global surface temperature records in 1850 (IPCC 2007). The increase in the greenhouse gases CO₂ (+35%; 380 ppm in 2005), methane (+248%; 1774 ppb in 2005) and nitrous oxide (+18%; 319 ppb in 2005) since 1750 is expected to rise global temperatures by 1.8 to 4.0 °C until 2100, depending on further CO₂ emission scenarios (IPCC 2007).

The increase in global temperatures has far ranging consequences for natural and human environments, whereas the impacts differ across the worlds' regions (IPCC 2007). For central Europe an increase in the frequencies of floods and heat waves as well as higher rates of soil erosion and glacier retreat are predicted. Thus, great effort is made to find solutions to mitigate or at least to decelerate the predicted [CO₂] increase and therefore global warming. Besides the use of renewable energies instead of fossil energy sources, an appropriate land management could lead to a higher soil C sequestration and thereby contribute to a deceleration in the atmospheric [CO₂] increase (Batjes 1998). Grasslands are crucial in mitigation strategies because of their global extension and C pool size.

Grasslands cover between 31 and 34% of the earth' surface, with 7 to 10% in temperate regions (White et al. 2000). Approximately 34% of the total terrestrial C (~810 GtC) is stored in grasslands, with 70% stored belowground (White et al. 2000). The C stored in the worlds soils contributes ~1500 Gt to the terrestrial C pool (Amundson 2001), which is twice the amount of C in the atmosphere. The soil carbon content reflects the balance of input and output; it is a dynamic pool rather than a static reservoir. Thus, even small changes in input or output rates lead to significant changes in the soil C content (Amundson 2001), thereby affecting atmospheric [CO₂]. Because of its wide ranging appearance and high soil organic C (SOC) content, (temperate) grassland ecosystems play an important role in the global C cycle and are a key in mitigation strategies to counteract the atmospheric [CO₂] increase and therefore climate change.

Direct CO₂-fertilization effects and higher temperatures affect the plant community structure in grasslands, with uncertain, nonlinear and rapid changes in ecosystem structure and C stocks likely to occur (Fischlin et al. 2007). The IPCC report further suggests that soil C stocks will very likely be strongly reduced under more frequent disturbance regimes, e.g. drought. C sequestration will likely be reduced due to enhanced respiration and increased rainfall variability. On the other hand, a direct fertilization effect of rising atmospheric [CO₂] could lead to a higher biomass production (Long et al. 2005) and thereby counteract the soil C stock decrease. Therefore, it is important to understand the underlying mechanisms that lead to the predicted changes in ecosystem C dynamics and their responses to elevated CO₂. The performance of CO₂ enrichment affects the response of ecosystems to elevated CO₂. Taub et al. (2008) for example reported a larger CO₂ effect in studies that were performed in open-top chambers than in studies performed in other types of experimental facilities. However, studies that focus in situ on soil C dynamics under long-term CO₂-enrichment without using enclosures are hardly available.

1.2 Effects of elevated CO₂ on ecosystem C dynamics

1.2.1 Grassland FACE experiments

A promising method to examine ecosystem effects caused by elevated CO₂ are Free Air CO₂ Enrichment (FACE) experiments, where intact ecosystems are exposed in-situ to a higher atmospheric CO₂ concentration without any greenhouse- or chamber side effects. But even if disturbances are kept as small as possible, the onset of a CO₂-enrichment itself acts as a disturbance. The sudden increases in atmospheric [CO₂] at the very beginning of a CO₂-enrichment (CO₂ step increase) may lead to atypical short-term responses of the ecosystem that differ from the long term response¹ and also to those of a gradual [CO₂] increase as currently observed in the real world (Luo 2001). Those step increase effects (Newton et al. 2001; Klironomos et al. 2005) may in the short-term lead to misinterpretation or overestimation of effects, which can only be accounted for in long-term experiments over several years.

Apart from the fact that only very few free-air CO₂-enrichment studies were performed on grassland sites (Luo et al. 2006), it is hardly possible to compare their results because studies largely differ in their experimental setup. Besides the degree of the CO₂-enrichment, which often corresponds to +30% or more, other important differences are fertilization, soil structure, run-time of the CO₂ enrichment, and the grassland vegetation itself (often ploughed, newly seeded species mixtures or monocultures). Additionally, climatic conditions such as precipitation, radiation and temperature differ widely between the sites where FACE experiments are/were performed.

¹ In the literature to my knowledge no consistent definition on short-term or long-term experiments exists. Therefore, here studies with a duration of < 5 years are defined as short-term and > 5 years as long-term experiments.

1.2.2 Ecosystem C balance

The effects of elevated CO_2 on ecosystem C dynamics are manifold. Elevated CO_2 usually increases gross and net photosynthesis, biomass production, water use efficiency, and rhizodeposition (Allard et al. 2006). The microbial fauna and soil physico-chemical processes are affected by an increased plant-C input via enhanced root growth (Fitter et al. 1997) and rhizodeposition (Pendall et al. 2004). Nevertheless, higher C supply caused by a higher C input is known to enhance microbial activity and changes in microbial community structure (Montealgre et al. 2000; Drissner et al. 2006; Kandeler et al. 2007), which is thought to have a great effect on the C balance of soil as it influences the mineralization of (older) organic substances. Thus, a higher C input to the soil must not necessarily lead to a higher net ecosystem C sequestration.

A simplified scheme of the ecosystem C budget is given in Fig. 1.1. Carbon enters the ecosystem as gross primary production (GPP) through photosynthesis. About half of the C returns immediately to the atmosphere as plant respired CO_2 (R_{plant}). The remaining C (net primary production, NPP) equals the difference between GPP and plant respiration. Subsequently, the plant C gain is partitioned between the plant, its symbionts (e.g. mycorrhizal fungi) and partly transferred to the soil. Some of the NPP is taken up by animals, lost via microbial respiration (R_{mic}), by disturbances (e.g. harvest or fires; F_{disturb}) or leaching (F_{lateral}). The GPP minus the C loss via R_{plant} , R_{mic} , F_{disturb} and F_{lateral} equals the net ecosystem productivity (NEP) which is the net accumulation of C per unit of time. NEP is positive when the C input exceeds the C losses of an ecosystem (C sink) but it can become negative when losses exceed inputs (C source). It is discussed if a CO_2 -induced increase in NPP will exceed the loss through respiration, leading to a higher NEP and an increase in net C sequestration (Schlesinger and Lichten 2001; Gill et al. 2002). Increased C losses due to enhanced respiration and/or dissolved organic carbon (DOC) losses can counterbalance the input of extra carbon and thereby reduce NEP.

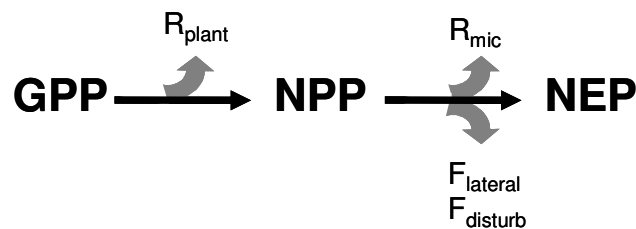


Fig. 1.1 Components of ecosystem C budget modified after Chapin III et al. (2002).

In grassland ecosystems roughly the 2.5-fold amount of aboveground-C is stored belowground (White et al. 2000), documenting the importance of understanding the soil C dynamics particularly in grasslands. The soil carbon content at a given time reflects the long-term balance between input and loss rates. It is widely known that elevated CO_2 leads to an increase in respiration (Luo et al. 1996; Stocker et al. 1997; Pendall et al. 2001; Comstedt et al. 2006), whereby a significant part of the

“extra” carbon provided by the higher atmospheric [CO₂] is lost shortly after entering the ecosystem. Priming effects, i.e. increased labile soil organic matter (SOM) supply, may also enhance the mineralization of recalcitrant SOM due to an increased microbial activity (Kuzyakov 2002; Carney et al. 2007).

There is still an ongoing debate if elevated CO₂ leads to an enhanced soil C sequestration, mitigating the rise in atmospheric [CO₂]. Two studies using a meta-analysis technique revealed a CO₂-induced increase in the soil C pool (Jastrow et al. 2005; Luo et al. 2006), whereas other studies reported a decline (Trueman and Gonzales-Meler 2005; Carney et al. 2007) or no changes in the soil C pool (Hungate et al. 1997; Niklaus et al. 2001; Gill et al. 2002; van Kessel et al. 2006). Hungate and colleagues (1997) reported an accelerated carbon cycling in grassland soils as a result of the CO₂ enrichment without a net increase. Other studies indicated that soil C sequestration may not be linear in response to soil C input (Gill et al. 2002; Kool et al. 2007), resulting in a restricted C sequestration capacity of soils because of the limited protection of SOM against microbial decay (Six et al. 2002; Kool et al. 2007). Lal (2004) considered soil C sequestration to be a short term strategy because of the proportionally lower C sequestration potential compared to the atmospheric CO₂ increase. The inconsistent results point out that a better process understanding is crucial to predict the ecosystem responses to elevated CO₂ and climate change, to be able to adapt management practices to an optimized soil C sequestration.

1.2.3 Soil aggregate structure

Soil consists of the four major components air, water, inorganic matter (i.e. sand, silt and clay) and organic matter. The solid mineral and organic particles are bound in soil aggregates of different sizes which determine the soil structure. Apart from the effects of the soil aggregate structure on soil moisture, soil aeration, erosion, mineralization, and plant growth (Dexter 1988; Six et al. 2004) it determines the turnover time of SOM. SOM within an aggregate is physically protected against mineralization due to the compartmentalization of substrate and microbial biomass (van Veen and Kuikman 1990). Moreover, a reduction in microbial activity (Sollins et al. 1996) takes place within the aggregate due to the reduced diffusion of oxygen into macro- and particularly into microaggregates. For long-term C sequestration, easily decomposable, labile substances must be protected against microbial decomposition. This could either be achieved via chemical protection (i.e. the conversion into recalcitrant substances), via physical protection within soil aggregates, or via association with silt and clay particles (Six et al. 2002).

Small soil particles are held together by organic binding agents, thereby a distinction has to be made between transient (mainly polysaccharides), temporary (roots and fungal hyphae) and persistent (e.g. aromatic components, polymers) binding agents which determine the age, size and stability of aggregates (Tisdall and Oades 1982). Transient binding agents are decomposed rapidly by microbes, whereas temporary binding agents can persist for months or even years. Tisdall and Oades (1982)

proposed a hierarchical aggregates concept. They postulated that various binding agents act at different hierarchical stages of aggregation, thereby binding primary particles into microaggregates by persistent binding agents (Pulleman and Marinissen 2004). Microaggregates, however, are bound into macroaggregates by a network of roots and fungal hyphae (temporary binding agents). This is in line with the results of Jastrow and colleagues (1997) who observed that with increasing diameter of macroaggregates transient binding agents became less relevant, whereas temporary binding agents became more important. Additionally, mycorrhizal hyphae were found to be the most important binding agent in the two largest aggregate size fractions.

Macroaggregate stability responds rapidly to changes in soil management such as tillage and organic inputs (Tisdall and Oades 1982; Elliott 1986) or changes in microbial community structure (Rillig et al. 2005). Thus, a CO₂-induced increase in organic matter input, or root and fungal biomass, could result in an enhanced soil aggregation which is essential for the protection of SOM against microbial decomposition and therefore C sequestration (Blanco-Canqui and Lal 2004). The connection between soil aggregation and SOC content is further supported by the different C contents of aggregate classes². Macroaggregates contain a higher C content than microaggregates which is due to their higher content of organic substances (e.g. binding agents). Additionally, each aggregate fraction has a characteristic turnover rate which affects its C turnover time. For temperate pasture grasslands, Six and Jastrow (2002) determined mean residence times for macroaggregate- and microaggregate-associated C of 140 and 412 years, respectively.

The effects of elevated CO₂ on soil aggregation reported in the literature are rather inconsistent, with increases (Rillig et al. 1999; Rillig et al. 2001; Six et al. 2001), no changes (Eviner and Chapin III 2002) or even decreases (Niklaus et al. 2003; del Galdo et al. 2006) being reported. In a newly seeded grassland, six years of elevated CO₂ caused an increase of 54% in aggregation but did not significantly increase the soil C content (Six et al. 2001). In two annual grasslands a CO₂-induced increase in aggregation was observed which was due to a higher glomalin content produced by fungi (Rillig et al. 1999). On the other hand, six years of elevated CO₂ decreased soil aggregation in a calcareous grassland, possibly caused by higher soil moisture under elevated CO₂ (Niklaus et al. 2003). Del Galdo et al. (2006) observed a decrease in large macroaggregates together with a decrease in soil C in a chaparral ecosystem. They found the strongest response to elevated CO₂ in the microaggregate fraction where C significantly decreased with elevated CO₂. Therefore, the authors suggest this fraction as an indicator for SOC changes.

Soil aggregate structure and C sequestration are connected by complex interrelations (Six et al. 2002). Kool et al. (2007) provided evidence for a limitation in

² In this study soil was fractionated into large (>2500µm) and small (250-2500 µm) macroaggregates, microaggregates (53-250 µm), and silt and clay particles (<53 µm).

C sequestration by a restricted increase in soil aggregation, when the soil C pool becomes saturated. Therefore, it is essential to consider soil aggregate structure when examining or predicting ecosystem C dynamics and their responses to climate change, in particular to elevated CO₂.

1.2.4 Soil and ecosystem respiration and its components

The net C balance of ecosystems is controlled by the balance between C uptake during photosynthesis and C loss during respiration (Fig. 1.1). Soil respiration (R_{soil}) is the sum of all plant (autotrophic) and microbial (heterotrophic) respiration processes belowground (Fig. 1.2), whereas ecosystem respiration (R_{eco}) also includes the aboveground respiration of standing biomass.

Approximately 40% of photosynthetically fixed C is quickly lost via shoot, root or microbial respiration (Saggar et al. 1997). Pasture plants transport 30-50% of assimilated C belowground (Kuzyakov and Domanski 2000). Root and rhizosphere respiration are mainly driven by the supply of recently fixed C (Högberg et al. 2001; Hartley et al. 2006) accounting to a significant C loss of GPP, whereas microbially respired CO₂ mainly originates from the decomposition of SOM. To estimate changes in the net soil C storage based on respiration measurements a distinction must be made between the mineralization of “old”, SOM derived C and the mineralization of labile, plant-derived substrates. These underlie a rapid turnover and therefore do not affect the long-term C balance of soils (Kuzyakov 2006). Therefore, a partitioning of soil or ecosystem respiration into “autotrophic”, plant-derived CO₂ and “heterotrophic”, microbial or SOM-derived CO₂ can provide a model to understand soil C dynamics and their responses to environmental changes.

The partitioning of soil respiration into several sources is still controversially discussed (Högberg et al. 2006). Fig. 1.2 shows the CO₂ sources according to Kuzyakov (2006). He conceptually subdivided soil respiration into the five sources (1) root respiration, the CO₂ respired from living root biomass; (2) rhizomicrobial respiration, the microbial decomposition of plant-derived rhizodeposits; (3) microbial decomposition of dead plant residues; (4) SOM-derived CO₂ affected by priming effects; and (5) microbial decomposition of SOM not caused by priming effects. In this study soil respiration was separated into plant-derived CO₂ and SOM derived CO₂ by means of stable isotope techniques. On average for non-forest vegetation, roots (1+2) contributed 60% to total soil respiration, ranging between 10 to 90% depending on vegetation and season (Hanson et al. 2000). Usually the fraction of root respiration increases during the growing season. The large variability in the results within the published literature was probably caused by the diversity of ecosystems and heterogeneity caused by different time scales and techniques.

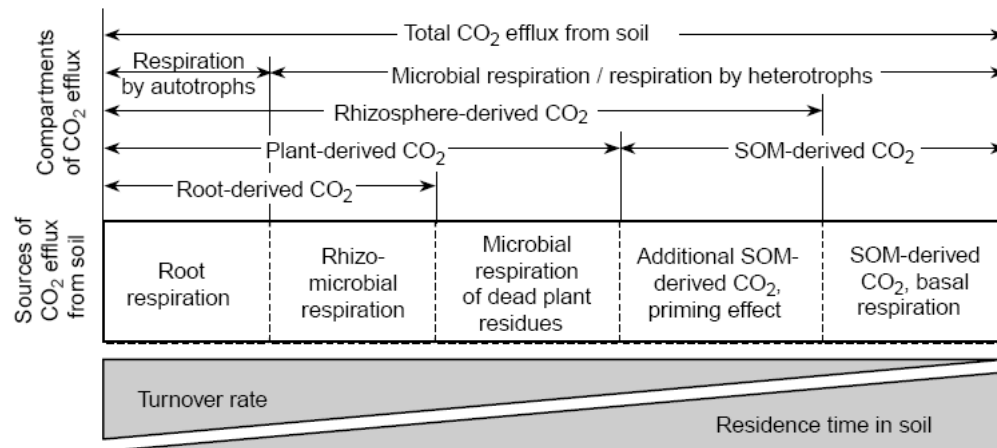


Fig. 1.2 Sources of soil respiration according to turnover rate and mean residence time (with friendly permission of Y. Kuzyakov).

Various methodical approaches using either experimental manipulation or isotope methods have been developed to separate soil respiration into its components (Andrews et al. 1999; Hanson et al. 2000; Kuzyakov and Larionova 2005; Kuzyakov 2006; Luo and Zhou 2006). A promising method seems to be the separation into autotrophic and heterotrophic CO₂ via stable isotope techniques. In FACE experiments where the CO₂ used for the enrichment originates from a fossil source (usually at a signature between -25 and -48‰) plant biomass becomes depleted in its $\delta^{13}\text{C}$ signature. The depletion in $\delta^{13}\text{C}$ continues from plant biomass to root exudates, plant residues, and plant respired CO₂. If the $\delta^{13}\text{C}$ signature differs between the autotrophic and heterotrophic CO₂ sources, the fraction of plant derived CO₂ on total soil or ecosystem respiration can be calculated (Ludlow et al. 1976). Because of the continuous application of the $\delta^{13}\text{C}$ label during the CO₂-enrichment under FACE there is a significant signature difference between plant-derived CO₂ and CO₂ that originates from the decomposition of old SOC that entered the soil before the CO₂ enrichment started. However, the use of isotopic tracers requires that different sources have a different $\delta^{13}\text{C}$ signature and that no significant discrimination against the heavier stable isotope ¹³C takes place after assimilation (Luo and Zhou 2006).

The ¹³C signature of soil air CO₂ results from the mixing of the FACE-induced ¹³C depleted, plant derived CO₂ and the microbial or SOM derived CO₂. A shift towards a higher contribution of plant derived CO₂ in times of intense plant growth would therefore lead to a decrease in soil air $\delta^{13}\text{C}\text{CO}_2$. On the other hand, an increase in microbial degradation of SOM would result in an increase in soil air $\delta^{13}\text{C}\text{CO}_2$. Consequently, $\delta^{13}\text{C}\text{CO}_2$ of soil air provides information on the mineralization processes of organic substances in the soil. In addition, mineralization of recently fixed, plant derived C sources can be distinguished from old, SOM derived C substrates.

1.3 Objectives of this study

The high relevance of grassland ecosystems in the terrestrial C storage highlights the importance to understand their C dynamics, in particular the responses to elevated CO₂. Contradictory findings of CO₂ effects on soil aggregation and soil C content as well as inconsistent results in separating root and microbial respiration prove that further research is needed for the understanding of (grassland) ecosystem C dynamics. Because CO₂ step-increase effects may occur shortly after the onset of the CO₂ enrichment, more long-term studies are needed, where the CO₂-enrichment is conducted for several years and initial effects can be neglected. Therefore, the main objective of this study was to investigate the long-term effects of elevated atmospheric [CO₂] on the ecosystem-C dynamics and the soil C stocks of a semi-natural temperate grassland ecosystem. In particular, the following questions were addressed.

Does elevated CO₂ affect the soil aggregate structure in a permanent grassland soil?

Does elevated CO₂ lead to a higher C content in one or more soil aggregate classes?

How much C was sequestered to each single soil aggregate class under elevated CO₂ with respect to short- and long-term effects?

Does an increase in atmospheric CO₂ concentration lead to a different stimulation of the autotrophic and heterotrophic components of soil or ecosystem respiration?

2 Materials and methods

2.1 Site description

The study was carried out at the Environmental Monitoring and Climatic Impact Research Station Linden located at 50°32'N and 8°41.3'E near Giessen, Germany, on a permanent semi-natural grassland site. For at least 50 years nitrogen (N) was applied at a rate of 50-80 kg N ha⁻¹ yr⁻¹ and since 1995 at a rate of 40 kg N ha⁻¹ yr⁻¹ as granular CaNH₄NO₃. Since 1993 the average annual air temperature and precipitation at the site were 9.4°C and 580 mm. The vegetation is an *Arrhenatheretum elatioris* (Br.-Bl.) *Filipendula ulmaria* sub-community with approximately 60 species (Jäger et al. 2003). The site contains four ring pairs each consisting of one control (A) and one FACE plot (E), where a moderate CO₂ enrichment has been applied since May 1998. In the ring pairs 1-3 atmospheric CO₂ was enriched to +20% above ambient conditions. The CO₂ enriched plot of ring pair 4 received CO₂ raised to +30% above ambient (Jäger et al. 2003).

Since the CO₂ enrichment started in 1998, aboveground biomass yield corresponded to 676 ±33 g m⁻² for elevated [CO₂] +20% and 654 ±48 g m⁻² for ambient [CO₂] (Fig. 2.1). Biomass before 1998 was not significantly different between A and later E plots. For plot E4 ([CO₂] +30%) no biomass yield was determined.

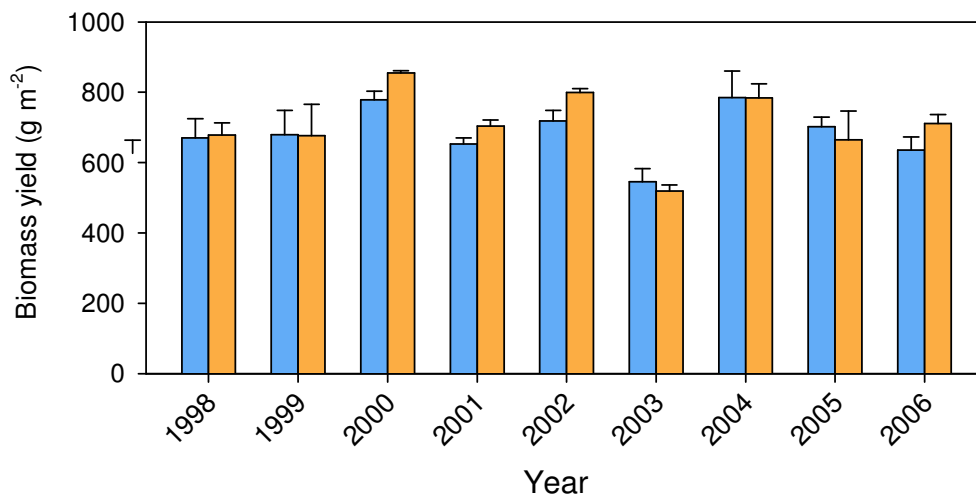


Fig. 2.1 Annual aboveground biomass yield under ambient (blue) and elevated (orange) CO₂ since the CO₂ enrichment started. Error bars mark the standard deviation.

The CO₂ enrichment was carried out throughout the entire year during daytime. From May 1998 to June 2004 the $\delta^{13}\text{C}$ signature of the CO₂ was -25‰ (atmospheric CO₂: -8‰). From July 2004 onwards the $\delta^{13}\text{C}$ signature of the CO₂ was changed to

-48‰ without altering the CO₂ concentration. Assuming a CO₂ concentration on the ambient plots of 370 ppm at a δ¹³C signature of -8‰ it is possible to calculate the theoretical δ¹³C signature of the enrichment-CO₂ in the E-plots (Tab. 2.1). Because the CO₂ increase of the plots E1-E3 corresponds only to 83 ppm, this leads to a less distinctive signature decrease than in plot E4, where [CO₂] was enriched by 110 ppm above ambient (mean 1999-2007 between 11 am to 2 pm).

Tab. 2.1 δ¹³C of tank CO₂ and of the calculated actual atmospheric [CO₂] in the CO₂-enriched plots.

δ ¹³ CO ₂	Ambient	E1-E3	E4	E1-E3	E4
	[‰]				
Tank	-	-25	-25	-48	-48
Atmosphere	-8*	-10.9	-11.7	-15.7	-17.2

*current assumption (IPCC 2007)

Solid soil samples were taken at the start of the experiment and at the end of the 6-year period shortly before the signature switch, and since that time in 6 or 12 month intervals (Fig. 2.2). In particular the second investigation period after the δ¹³C signature switch provides the opportunity to investigate C transformations under elevated CO₂ conditions without a CO₂-step increase effect which can occur at the beginning of a CO₂ enrichment experiment (Luo 2001).

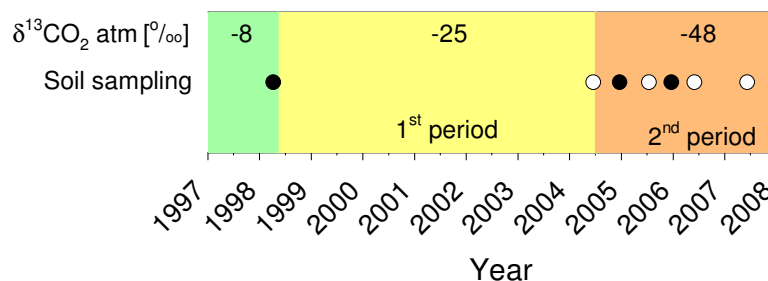


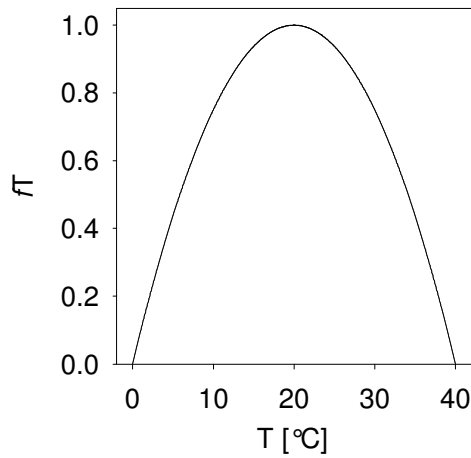
Fig. 2.2 Time sketch of the δ¹³C signature of the CO₂ used for the enrichment in the E-plots and the collection of soil samples; black symbols refer to the samplings in 0-15 cm, white symbols refer to the samplings down to 45 cm depth.

2.2 Air temperature, precipitation, and soil data

2.2.1 Air temperature and precipitation

Air temperature was measured at a height of two meters with two Thies Pt100 1/10 DIN sensors; the data were stored in 30 minute time intervals. Changes in T_{air} were determined via linear regression analysis for the data measured between 1995 and 2006.

To describe the effects of air temperature (T_{air}) on mineralization processes, the Jarvis-Stewart temperature function (Hicks et al. 1987) was used.



$$fT = \left[\frac{(T - T_e)}{(T_0 - T_e)} \right] \cdot \left[\frac{(T_h - T)}{T_h - T_0} \right]^{B_r}$$

Where

$$B_r = \frac{(T_h - T_0)}{(T_0 - T_e)}$$

Fig. 2.3 Temperature function (fT) according to Jarvis-Stewart (Hicks et al. 1987), T_h (40°C) and T_e (0°C) are the higher and lower temperature extremes at which no microbial activity takes place and T_0 (20°C) is the optimum temperature where microbial activity reaches its maximum.

The precipitation was measured via Hellmann samplers (Fa. Thies, Göttingen) either as 15-minute sum, or on a monthly basis via bulk samplers (Rothencamp B91) with $n = 12$ (Dämmgen et al. 2005).

2.2.2 Soil texture

The study area has a Fluvic Gleysol with a texture of sandy clay loam over a clay layer (FAO classification). The soil texture and pH for each soil horizon is presented in Tab. 2.2.

Tab. 2.2 Soil texture and pH in the soil profile of each ring pair.

Horizon	Lower horizon boundary	Sampling depth	pH	Sand (2000-63 μm)	Silt (63-2 μm)	Clay (<2 μm)
[cm]				[%]		
Ring pair 1						
Ah	10	2-7	5.90	43.25	39.00	17.75
M	32	12-17	6.20	40.89	42.13	16.97
SwM	78	40-45	7.05	48.10	51.90	<i>nd</i>
Ring pair 2						
Ah	12	2-7	6.25	59.26	20.89	19.85
M _{Sw}	42	15-20	7.05	34.52	40.50	24.98
Go _{Sw}	65	50-55	7.00	35.34	52.33	12.33
Ring pair 3						
Ah	12	2-7	6.20	9.98	58.13	31.89
M	20	15-20	7.05	9.78	55.56	34.66
M _{Sw}	50	40-45	7.25	14.94	50.56	34.50

nd = not determined

2.2.3 Bulk density

The bulk densities were determined for all soil samples collected since July 2005 using a sampler for undisturbed soil sampling (Ejkelkamp, Giesbeek, The Netherlands). A sub sample of approximately 15 g was used to determine the gravimetric soil moisture. The Volume of the soil sampler was 247.7 cm³.

The highest bulk densities occurred in plot A1, followed by the plots E1, E2, E3, E4, A3 and A2. Bulk density increased with soil depth and ranged from 1.0 g cm⁻³ in 0-7.5 cm to 1.7 g cm⁻³ in 37.5-45 cm depth (Fig. 2.4). The bulk density is presented separately for each plot and depth in the appendix (Tab. 7.3).

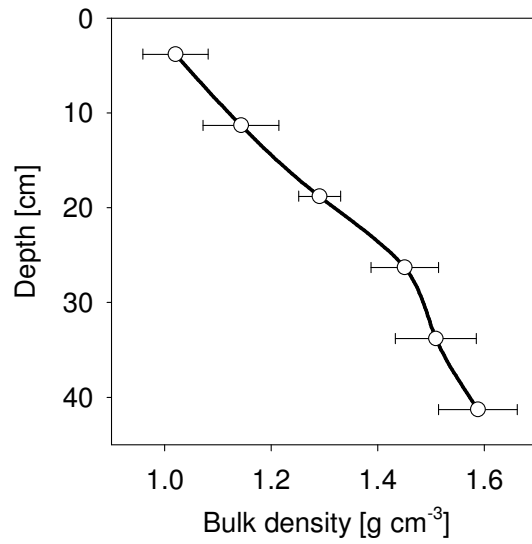


Fig. 2.4 Mean bulk density measured in the years 2005 and 2006 in the soil profile (0-45 cm) of all plots (A1-E4).

2.2.4 Soil moisture

Soil moisture was measured as the volumetric water content (VWC) with time-domain-reflectometric (TDR) probes installed vertically into the top 15 cm. The probes were monitored manually once a day except for the weekends.

2.3 Soil and plant biomass sampling and analysis

2.3.1 Soil sampling

For the sampling between 1997 and 2003 9 sub samples were taken per plot and mixed into one composite sample for the 0-5 cm depth. In April 1998 (i.e. immediately before the onset of the CO₂ enrichment) soil samples from all plots were taken in 0-5, 5-10 and 10-15 cm depth with 9 sub-samples per plot (Kammann 2006, personal communication) air dried, and stored in plastic vials. Soil samples collected since 2004 were taken in 0-7.5, 7.5-15, 15-22.5, 22.5-30, 30-37.5 and 37.5-45 cm depth (soil sampler: Ejkelkamp, Giesbeek, The Netherlands) with three sub-samples per plot in each depth. The soil was air-dried and roots were picked out with tweezers until all visible roots were removed. Before the fractioning the soil was 8 mm sieved (dry sieving).

2.3.2 Soil aggregate fractionation

Soil samples were separated into four aggregate size classes by wet sieving of 100 g of soil according to Six et al. (1998) (Fig. 2.5). Three sieves (2000 µm, 250 µm and 53 µm) were used in series to obtain the four aggregate size classes: <53 µm (silt and clay), 53-250 µm (microaggregates), 250-2000 µm (small macroaggregates) and >2000 µm (large macroaggregates). Before sieving the soil samples were submerged for 2 min in deionized water. The separation of aggregates was achieved by manually moving the sieve up and down with 50 repetitions during a period of 2 min. Each fraction was transferred into aluminum pans and dried at 60 °C until a constant weight was reached.

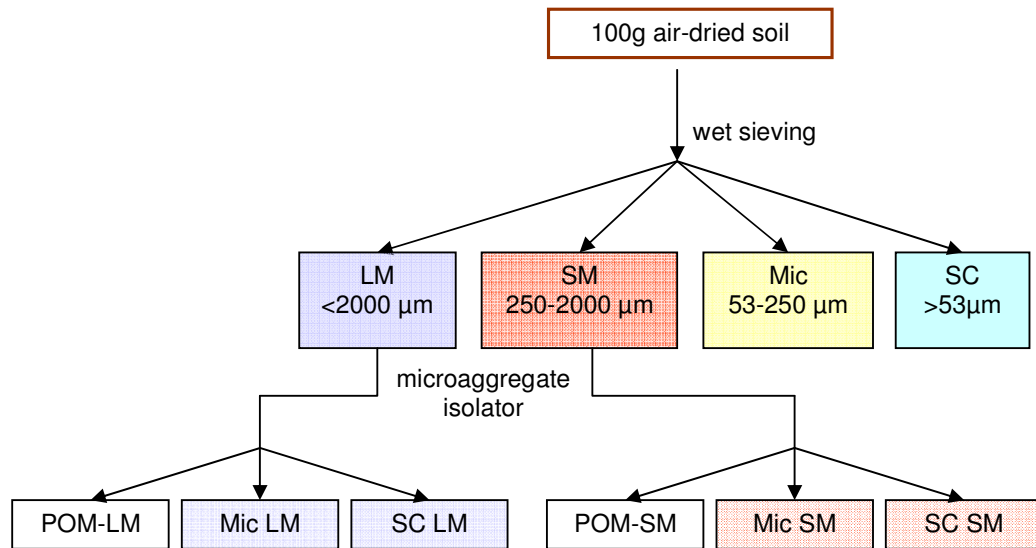


Fig. 2.5 Soil fractions obtained from wet sieving and microaggregate isolation.

Isolation of Microaggregates

Macroaggregates consist of particulate organic matter (POM), microaggregates (Mic) and silt and clay particles (SC) (Fig. 2.5). Isolation of the fractions was carried out for the samples collected in April 1998 and June 2004 on a microaggregate-analyzer (Fig. 2.6) (Six et al. 2002) using 10 g of large and small macroaggregates. POM and sand particles or stones remained on the 250 μm mesh, whereas microaggregates and silt and clay particles passed through it and were rinsed on the 53 μm sieve. The separation of microaggregates and silt and clay particles was achieved by wet sieving (see above).

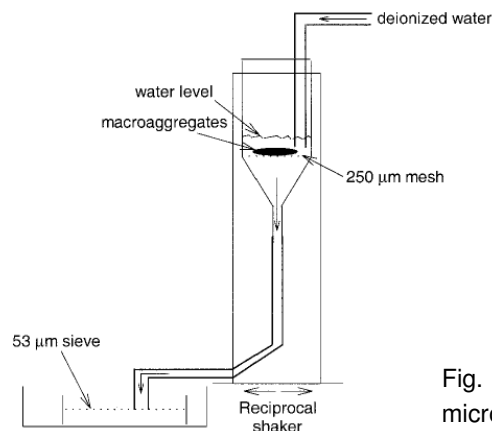


Fig. 2.6 Schematic presentation of the microaggregate isolator (Six et al. 2002).

2.3.3 Plant biomass

Roots

Roots were picked out of the air dried soil samples with tweezers, washed with deionized water until all soil particles were removed and oven dried at 60°C to a constant weight. Root biomass was determined for samples collected in July 2005, December 2005, and June 2006. The ^{13}C signature of root biomass was determined for the depths 0-7.5, 7.5-15, 15-30 and 30-45 cm (e.g. 0-5, 5-10 and 10-15 cm for the sampling in April 1998) on one composite sample per plot and depth.

Leaves

Aboveground biomass was harvested two times per year in May/June and September. In the years 2004-2006 for each harvest composite samples consisting of grass and herbs were taken from three harvest plots in each ring which are used for trace gas measurements (1 m diameter) and separately analyzed for their $\delta^{13}\text{C}$ signature. A composite sample of all 26 harvested plots per plot was also analyzed for $\delta^{13}\text{C}$. In plot E4, where no yield was determined, samples for $\delta^{13}\text{C}$ analysis were collected once in December 2006.

Theoretical $\delta^{13}\text{C}$ signature of plant biomass

The theoretical $\delta^{13}\text{C}$ signature of plant biomass can be calculated via Eqn. 1 (Farquhar et al. 1982). The plant $\delta^{13}\text{C}$ -signature (δ_{plant}) strongly depends on the ratio of the intracellular and atmospheric CO_2 concentration, the $\delta^{13}\text{C}$ signature of the atmospheric CO_2 , and the physical and biochemical discrimination against ^{13}C .

$$\delta_{\text{plant}} = \delta_{\text{atm}} - a - (b - a) \cdot \left(\frac{p_i}{p_a} \right) \quad \text{Eqn. 1}$$

where δ_{atm} is the $\delta^{13}\text{C}$ signature of atmospheric CO_2 , a is the isotopic fractionation resulting from differences in the diffusion rate of $^{12}\text{CO}_2$ and $^{13}\text{CO}_2$ (4.4‰), b is the enzymatic discrimination against ^{13}C of Rubisco (30‰), p_i is the intercellular CO_2 concentration (here: 250 ppm for ambient and 270 ppm for elevated CO_2), and p_a is the atmospheric CO_2 concentration.

2.3.4 Analysis of ^{13}C signature and soil organic carbon content

All solid samples were ground with a ball mill (Retsch, type MM). Soil (30 mg) and plant biomass (2 mg) were placed into silver (soil) and tin (plant) capsules, respectively, for the analysis of $\delta^{13}\text{C}$ signature and SOC content.

To remove inorganic C (e.g. soil carbonates) the soil samples were fumigated with hydrochloric acid (Harris et al. 2001). SOC content and $\delta^{13}\text{C}$ signature of the samples collected between 1997 and December 2005 were measured at the UC Davis Stable Isotope Facility using a continuous flow, isotope ratio mass spectrometer (CF-IRMS, PDZ-Europa Scientific, Sandbach UK) interface with a CN analyzer (Carlo Erba). All samples collected since June 2006 were measured on a combined elemental analyzer and gas purification module (SerCon-GSL) at the ISOFYS-Laboratory of Applied Physical Chemistry & AMBERLab Advanced Mass spectrometry for Bioscience Engineering Research Laboratory in Gent. The accuracy (measurement error) was $<0.2\text{‰}$ for solid samples and $<0.4\text{‰}$ for gas samples, determined every batch with sparerefs (Vermeulen 2008, personal communication). A cross-check between both labs was carried out for the root biomass samples collected in June 2004 by measuring the isotope signature of 35 samples in both labs (data not shown). The mean ^{13}C signature difference for all samples was $-0.01\text{‰} \pm 0.09$ and the largest difference for a single sample was 0.24‰ .

2.3.5 Calculations

Isotope signature

The natural abundance of the stable ^{13}C isotope in the environment is 1.108%, the rest being ^{12}C . The isotope signature is given in the delta-notation, where the $^{13}\text{C}/^{12}\text{C}$ ratio is compared to the $^{13}\text{C}/^{12}\text{C}$ ratio of an international PDB standard (Peedee belemnite, originating from the Cretaceous fossil *Bellefnita americana*) with a known $^{13}\text{C}/^{12}\text{C}$ ratio (R) of 0.0112372. The delta value is calculated from measured isotope ratio (R) via Eqn. 2,

$$\delta = \frac{1000 \cdot (R_{\text{sample}} - R_{\text{standard}})}{R_{\text{standard}}} \quad \text{Eqn. 2}$$

where R_{sample} refers to the isotope ratio of the sample and R_{standard} refers to the isotope ratio of the Peedee belemnite standard.

Changes in soil organic carbon over time

The temporal changes in total soil C were analyzed via linear regression analysis on the samples taken between 1997 and 2003 (0-5 cm depth) and between 2004 and 2007 (6 sampling dates). For the samples taken in April 1998 and June 2004 the changes in SOC were determined by difference.

C input

Based on the $\delta^{13}\text{C}$ difference either between elevated and ambient CO_2 for the same time of sampling or over time for one CO_2 treatment the fraction of new C (fC_{new}) can be calculated according to Eqn. 3 (Balesdent and Mariotti 1996). For the first investigation period (1998-2004), the soil C input was calculated via the $\delta^{13}\text{C}$ difference between the control (A-plots) and the labeled plot (E-plots) in 2004. After the signature switch in July 2004 (Fig. 2.2) it was no longer possible to calculate the C input via E/A comparisons. Therefore, for the second period the C input into the E-plots was calculated via the $\delta^{13}\text{C}$ difference before the application of a label (t_0) and after a certain time period (t_1) according to Eqn. 3

$$fC_{\text{new}} = \frac{\delta(t_1) - \delta(t_0)}{\delta_B - \delta(t_0)} \quad \text{Eqn. 3}$$

where fC_{new} is the fraction of new C, $\delta(t_1)$ is the $\delta^{13}\text{C}$ signature of SOC at t_1 (elevated), $\delta(t_0)$ is the $\delta^{13}\text{C}$ signature of SOC at t_0 (ambient), and δ_B is the signature of the newly sequestered C, which corresponds to the $\delta^{13}\text{C}$ signature of root biomass at t_1 under elevated CO_2 .

Based on the amount of C in the soil and fC_{new} , the C input was calculated separately for the first and the second observation period. When calculating the C input via the ^{13}C signature difference between E- and A-plots (as done for the first investigation period) it is a basic requirement that the initial SOC ^{13}C signatures of both treatments are equal. For the presented data set equal initial conditions in April 1998 are given for both, A- and later E-plots, either for the total soil C as well as for the single soil aggregate fractions (Fig. 3.16). The mean C input per unit of time (for the whole period between April 1998 and June 2006) was calculated as the weighted average of the C input rates determined in the two periods, 1998 – 2004 and 2004 - 2006.

2.4 Gas sampling and analysis

2.4.1 Gas sampling

Soil Gas

All gas samples were taken after the signature switch from -25‰ to -48‰ in July 2004. Soil air samplers had been inserted in autumn 2000 at 5 and 10 cm depth in each ring-plot quarter, with four replicates per depth and plot (Heinz 2000). The samplers consist of an enclosed silicone tube which allowed the sampling of soil air even at times when the soil was water saturated (Kammann et al. 2001). To preclude any effects of daily variations, all samples were collected in the morning between 8 am to 10 am with 60 ml PE-syringes (Plastipak).

In ring pair 4 the samplers were inserted at two sites at depths of 5, 10, 20, 30, 40 and 50 cm depth (repetitions differed between the depths with $n = 4$ (5 cm), $n = 2$ (10, 20, 30 and 40 cm) and $n = 3$ (50 cm)). Samples for $\delta^{13}\text{C}$ measurements in the soil profile of ring pair 4 were collected 23 times (from 1st October 2004 to 21st December 2006), and in ring pairs 1-3 26 times (from 6th August 2004 to 1st December 2006), respectively.

Two days before and after the soil air sampling for ^{13}C analysis, soil air samples were collected to determine the soil air CO_2 concentration because the internal sampler volume of ~40 ml did not allow to determine $\delta^{13}\text{C}$ and $[\text{CO}_2]$ out of one sample. Additional CO_2 concentration measurements were carried out once or twice weekly throughout the experimental period.

The values of the $\delta^{13}\text{C}$ signature, the contribution of root respiration to total soil respiration and ecosystem respiration are shown for the whole period and separately for the growth period (1st April to 31st August) and the off-season (1st September to 31st March). The time intervals were selected with respect to the time of intense plant growth and dormancy. A list of all soil gas samples and gas samples of ecosystem respiration collected for $[\text{CO}_2]$ and $\delta^{13}\text{C}$ measurements is given in the appendix (Tab. 7.2).

Ecosystem Respiration

All ecosystem respiration data obtained in the ring pairs 1-3 were taken from the ongoing long-term trace gas measurements (Kammann, C. personal communication). Ecosystem respiration (R_{eco}) was determined by the closed chamber technique (Hutchinson and Livingston, 1993) one to two times per week throughout the investigation period (2nd March 2005 to 1st December 2006) with three maxi-chambers per plot (Kammann 2001) on the chamber places (frames) that were used for the separate determination of biomass yield and ^{13}C signature of aboveground material in this study. For the determination of R_{eco} , gas samples were

taken with 60 ml syringes at four times after coverage, i.e. 0, 30, 60 and 90 minutes until summer 2005, and 0, 30 and 60 minutes since summer 2005 (Kammann et al. 2008).

2.4.2 Analysis of $\delta^{13}\text{C}$ signature and CO_2 concentration

Soil air CO_2 concentration

All samples were analyzed within 36 hours following sample collection on a gas chromatograph (HP 6890) equipped with an ECD (^{63}Ni -electron capture detector) connected to an auto sampler system for syringes (Loftfield et al. 1997). The reproducibility of atmospheric CO_2 values was ± 3 ppm CO_2 (standard deviation of $n = 6$ samplings of an atmospheric standard gas).

$\delta^{13}\text{C}$ analysis

For the $\delta^{13}\text{C}$ analysis gas samples were transferred into 12 ml exetainers (Labco) which were evacuated (vacuum pump Vacuumbrand RZ5) prior to sample transfer. Gas samples collected between June 2004 and May 2005 were analyzed on a trace gas unit ANCA-GSL coupled to a mass spectrometer PDZ Europa 20-20 in Davis, California. Since May 2005 all samples were analyzed on a trace gas unit TGII PDZ Europa coupled to the isotope ratio mass spectrometer (20-20 Sercon, Sercon Ltd.) in Gent, Belgium (Beheydt et al. 2005) (see also section 2.3.4).

2.4.3 Separation of soil and ecosystem respiration into its components

Keeling plot method

The Keeling-plot technique was used to determine the $\delta^{13}\text{C}$ signature of the CO_2 -source of ecosystem respiration. A Keeling plot (Keeling 1958) is a linear two component mixing model where the $\delta^{13}\text{C}$ signature (y-axis) is plotted against the reciprocal of the CO_2 concentration (x-axis) (Fig. 2.7). The $\delta^{13}\text{C}$ signature of the CO_2 source is given by the y-intercept of the linear regression. The gas samples can be collected as a series of samples from one chamber (Pataki et al. 2003), or from several chambers sampled at the same time (Ohlsson et al. 2005). The advantages of the second approach are a larger freedom to collect samples and a better spatial representativeness. Furthermore, all measurements were independent from each other which is assumed for least square regression analysis. During the two-year period both approaches were tested. First, from 2nd March 2005 to 21st February 2006, all chambers were sampled once after a certain time of chamber closure and CO_2 enrichment, and all samples were pooled together for ambient and elevated CO_2 ($n = 9$ per CO_2 -treatment) for the Keeling-plot analysis.

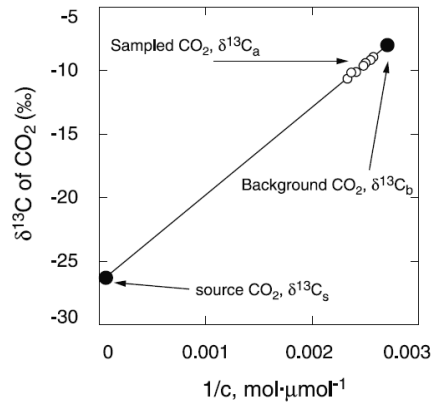


Fig. 2.7 Schematic illustration of the Keeling-plot method from Pataki et al. (2003), open circles mark the sampled CO₂, black circles mark the two endpoints of the CO₂ source and the atmospheric CO₂, respectively.

This allowed only the calculation of one mean value for each CO₂ treatment. In the second approach (16th September 2005 and since the 7th April 2006), each chamber was sampled several times ($n \geq 3$ per chamber) so that one Keeling-plot analysis could be carried out for each chamber. In the first approach the spatial variability was better taken into account, but problems occurred if samples had to be excluded due to measurement errors because of the lower number of samples ($n = 9$). Therefore, the second approach was considered as the appropriate method to determine $\delta^{13}\text{C}$ of the CO₂ source at the site. However, both methods led to comparable results (Fig. 3.29). A list of all sampling dates is given in the appendix (Tab. 7.2).

Partitioning of R_{eco} and R_{soil}

R_{eco} is the sum of all above (R_{leaf}) and belowground (R_{soil}) respiration processes of an ecosystem (Eqn. 4). Aboveground respiration is the sum of CO₂ respired from plant leaves, whereas R_{soil} consists of root and rhizosphere respiration (R_{root}) and microbial-respired CO₂ derived from the decomposition of organic matter in bulk soil (R_{bulk}) (Eqn. 5).

$$R_{\text{eco}} = R_{\text{leaf}} + R_{\text{soil}} \quad \text{Eqn. 4}$$

$$R_{\text{soil}} = R_{\text{root}} + R_{\text{bulk}} \quad \text{Eqn. 5}$$

Expanding Eqn. 4 and 5 following the conservation of mass (Bowling et al. 2001) leads to Eqn. 6 and 7:

$$\delta_{\text{eco}} R_{\text{eco}} = \delta_{\text{leaf}} R_{\text{leaf}} + \delta_{\text{soil}} R_{\text{soil}} \quad \text{Eqn. 6}$$

$$\delta_{soil} R_{soil} = \delta_{root} R_{root} + \delta_{bulk} R_{bulk} \quad \text{Eqn. 7}$$

A two-component mixing model (Ludlow et al. 1976) was used to separate the two sources of R_{eco} (above- and belowground respiration or heterotrophic and autotrophic respiration) and R_{soil} (root and bulk soil respiration) based on their isotope signatures. The contribution of aboveground respiration (R_{leaf}) and soil respiration (R_{soil}) on ecosystem respiration (R_{eco}) was determined via Eqn. 8.

$$f_{leaf} = \frac{(\delta^{13}C_{R_{eco}} - \delta^{13}C_{soil\ air\ CO_2})}{(\delta^{13}C_{leaf} - \delta^{13}C_{soil\ air\ CO_2})} \quad \text{Eqn. 8}$$

and

$$f_{soil} = 1 - f_{leaf}$$

where f_{leaf} is the fraction of R_{leaf} to R_{eco} , $\delta^{13}C_{soil\ air\ CO_2}$ is the signature of soil air CO_2 in 5 cm depth, $\delta^{13}C_{R_{eco}}$ is the isotope signature of R_{eco} determined via the Keeling-plot analysis, and f_{soil} is the fraction of R_{soil} on R_{eco} .

R_{eco} was separated into plant respiration (R_{plant}) and bulk soil respiration (R_{bulk}) according to Eqn. 9,

$$f_{plant} = \frac{(\delta^{13}C_{R_{eco}} - \delta^{13}C_{soil})}{(\delta^{13}C_{plant} - \delta^{13}C_{soil})} \quad \text{Eqn. 9}$$

and

$$f_{bulk} = 1 - f_{plant}$$

where f_{plant} is the fraction of R_{plant} to R_{eco} , f_{bulk} is the fraction of R_{bulk} on R_{eco} , and $\delta^{13}C_{plant}$ is the mean $\delta^{13}C$ signature of leaves and roots.

The contribution of R_{root} to R_{soil} was determined according to Eqn. 10. Therefore, the isotope signature of the two sources (i.e. plants and bulk soil C) and the $\delta^{13}C$ signature of the respired CO_2 (soil air CO_2) must be known. In this study R_{root} was defined as the sum of CO_2 released by roots and microbes feeding on plant derived C in the rhizosphere (Andrews et al. 1999; Hanson et al. 2000; Högberg et al. 2006).

$$f_{root} = \frac{(\delta^{13}CO_2 - \delta^{13}C_{soil})}{(\delta^{13}C_{leaf} - \delta^{13}C_{soil})} \quad \text{Eqn. 10}$$

Here, f_{root} is the contribution of R_{root} to R_{soil} , and $\delta^{13}C_{soil}$ and $\delta^{13}C_{leaf}$ are the $\delta^{13}C$ signatures of bulk soil and leaves, respectively. For the $\delta^{13}C$ signature of the plant CO_2 source the $\delta^{13}C$ signature of leaves measured in July 2005 was taken instead of $\delta^{13}C$ of root biomass, which encompasses biomass of various age classes. Root respiration is mainly driven by recently fixed C in the form of carbohydrates (with the signature of recently fixed C, Högberg et al. (2001)), of which plant leaves are more representative than roots. The calculation of f_{root} was carried out separately for each plot.

The signature of the bulk soil (i.e. total soil) was interpolated for each sampling date between the last and next soil sampling date, although the differences were only very small (<0.5‰). For the time period after June 2006 the isotope signature of this sampling date was used instead of interpolated values, because the soil $\delta^{13}C$ signature in June 2007 was exceedingly low and should be reanalyzed to exclude measurement errors. However, considering only the data of June 2006 is associated with a minor uncertainty because the $\delta^{13}C$ signature of bulk soil changes very slowly over time. Separate values were taken for each plot from the corresponding depth. The $\delta^{13}C$ signatures of soil air CO_2 were corrected for isotopic fractionation due to diffusion (i.e. 4.4‰) (Cerling 1991; Hesterberg and Siegenthaler 1991). Eqn. 10 was applied to every single $\delta^{13}CO_2$ measurement of soil air. If f_{root} was < 0 or > 1 the values were set to 0 or 1, respectively.

A sophisticated separation of R_{eco} into f_{leaf} , f_{root} and f_{bulk} was achieved as follows: f_{leaf} and f_{soil} were calculated according to Eqn. 8, f_{root} and f_{bulk} were calculated according to Eqn. 11 and 12, respectively.

$$f_{root} = f_{soil} \cdot f_{root \text{ on } R_{soil}} \quad \text{Eqn. 11}$$

As

$$f_{root} + f_{leaf} + f_{bulk} = 1 \quad (R_{eco}) \quad \text{Eqn. 12}$$

$$f_{bulk} = 1 - f_{leaf} - f_{root}$$

General comments on the use of two-component mixing models

Linear mixing models are widely used in stable isotope research to determine the proportional contribution of two sources, e.g. autotrophic and heterotrophic respiration or old and new C sources (Robinson and Scrimgeour 1995; Andrews et al. 1999; Pendall et al. 2001; Soe et al. 2004; Taneva et al. 2006). With this approach equal $\delta^{13}C$ signatures of the source and the produced CO_2 are assumed.

The first assumption is that root respired CO_2 has the $\delta^{13}\text{C}$ signature of leaves ($\delta^{13}\text{C}_{R_{\text{root}}} = \delta^{13}\text{C}_{\text{leaves}}$), the second assumption is that the soil-derived CO_2 has the $\delta^{13}\text{C}$ signature of bulk soil ($\delta^{13}\text{C}_{R_{\text{bulk}}} = \delta^{13}\text{C}_{\text{soil}}$). Daily or seasonal changes in assimilate composition might cause a variation in $\delta^{13}\text{C}$ of plant respired CO_2 that differs from the $\delta^{13}\text{C}$ signature of the source (e.g. plant biomass), leading to incorrect results. In this study a diurnal effect on $\delta^{13}\text{CO}_2$ was excluded by taking the soil air samples in the morning between 8 and 9 am. The R_{eco} measurements were always carried out after sunset, but a possible effect of environmental conditions could not be ruled out. Possibly, the contribution of plant respiration during summer was underestimated if drier soil moisture conditions have led to an increase in plant-respired $\delta^{13}\text{CO}_2$ signature. Under elevated CO_2 only a weak correlation was found between the $\delta^{13}\text{CO}_2$ signature of soil air in 5 cm depth and soil moisture ($p = 0.057$, linear regression analyses), whereas under ambient CO_2 a significant effect ($p = 0.001$, linear regression analyses) occurred. However, the time span where plant growth reached its maximum (i.e. where the f_{plant} of R_{eco} reached its maximum) occurred during the summer period, i.e. at times of low soil moisture. Therefore, it is impossible to separate both effects. Furthermore, a sufficient $\delta^{13}\text{C}$ difference between the two sources must be present, which depends primarily on the standard deviation of the sources and the mixture and the desired confidence interval (Phillips and Gregg 2001). Under ambient CO_2 the signature difference between the two sources was too small. Therefore, the partitioning method was only applied to the CO_2 -enriched plots, where a sufficient $\delta^{13}\text{C}$ signature difference existed.

The application of the two-component mixing model to soil air CO_2 samples (i.e. to separate R_{root} from R_{soil}) is restricted by the diffusion of CO_2 within the soil profile. Soil air collected at 5 cm depth originates at least partly from deeper soil layers. For detailed analyses, a soil air diffusion model must be used where both stable isotopes (^{12}C and ^{13}C) are considered with their respective diffusion coefficients. Consequently, the results obtained via a combined approach of Keeling-plot analyses (R_{eco}) and two-component mixing model are more reasonable: when the overall plant respiration is considered, possible $\delta^{13}\text{C}$ differences between root and leaf respiration (Klumpp et al. 2005) are ruled out.

Another uncertainty in stable isotope research is post-photosynthetic discrimination, which would further restrict the assumption that plant-derived CO_2 equals the $\delta^{13}\text{C}$ signature of plant biomass. It is still unclear if and/or to what extent a discrimination against the heavier ^{13}C isotope takes place during respiration (Tcherkez et al. 2003; Xu et al. 2004; Klumpp et al. 2005; Pataki 2005). For example, a ^{13}C enrichment in leaf-respired CO_2 would lead to an underestimation of plant-derived C in R_{eco} , whereas the depletion in root-derived CO_2 would lead to an overestimation of the contribution of R_{root} to R_{soil} .

2.5 Statistical analysis

The experimental setup of the Giessen-FACE experiment was a randomized block-design. For the block construction, i.e. the generation of ring pairs and the classification into E- and A-plots, the matched-pairs-technique (Harms 1998) was used. Initially, the experimental plots were arranged into four ring pairs based on their soil and vegetation characteristics, so that these factors were similar for both CO₂ treatments. Afterwards a randomized assignment of CO₂-enrichment or ambient CO₂ conditions was carried out.

The level of significance was defined as:

$p \leq 0.01$ highly significant (a);

$p > 0.01$ and $p < 0.05$ significant (b);

$p > 0.05$ and < 0.1 weakly significant (c);

For all statistical analyses the SPSS version 12.0.1 was used. Mean values, standard deviation (sd) and standard error (se) were calculated via Microsoft Excel (2003).

T-test statistics

For the t-test statistics normality had to be assumed, because with $n = 3$ no test of normality could be carried out. An independent samples t-test was used to evaluate significant differences in ecosystem respiration between the CO₂ enriched and ambient plots.

A paired samples t-test was used to evaluate the differences in soil SOC content between 1998 and 2004, or 2004 and 2006, and to test if significant differences in the C input rates between the first and the second investigation period did occur. Changes in soil aggregate composition were tested separately for each fraction and depth via paired-samples t-test. Root biomass yield was tested via paired samples t-test separately for each sampling date and depth.

Linear regression analysis

To test if a significant effect of depth on the ¹³C signature of roots under ambient and elevated CO₂ existed, a linear regression analysis was performed separately for each sampling date. A possible correlation between the amount of large macroaggregates and the loss in total soil C was also tested via linear regression analysis. Effects of soil moisture and aboveground biomass production on the

content of large macroaggregates were tested via linear regression analysis for 0-7.5 cm depth and for the whole soil profile 0-45 cm; possible changes in the contribution of root respiration to total soil respiration with depth were also tested via linear regression analyses.

General linear model (GLM) analysis

The general linear model analysis was used to test if elevated CO₂ had a significant effect on root biomass. The test was performed with “ring pair” as covariate. A possible effect of the CO₂ treatment on the loss in LM-content between 1998 and mean 2004 or mean 2004 and 2006 was tested via an univariate GLM procedure.

3 Results

3.1 Air temperature, precipitation, and soil moisture

Air temperature

Between 1995 and 2006 air temperature (T_{air}) in 2 m height significantly increased at the site with $0.11 \text{ }^{\circ}\text{C yr}^{-1}$ (Tab. 3.1). The most pronounced warming of $0.23 \pm 0.08 \text{ }^{\circ}\text{C yr}^{-1}$ ($p = 0.014$) occurred during the winter months January, November, and December. When also the autumn months September and October (annual T_{air} mean of Jan; Sep-Dec) were considered, T_{air} increased by $0.21 \pm 0.07 \text{ }^{\circ}\text{C yr}^{-1}$ ($p = 0.016$). For annual T_{air} means a marginally significant temperature increase of $0.11 \text{ }^{\circ}\text{C yr}^{-1}$ was observed. The highest significant increase ($0.26 \text{ }^{\circ}\text{C yr}^{-1}$) was found for the month November.

Based on the temperature function fT to estimate the temperature dependence of microbial respiration (Fig. 2.3), the effect of warming on mineralization becomes even more pronounced. During the cold season a temperature induced increase in respiration of up to 28% in December and 24% in November was estimated. For the entire year, the temperature-induced increase corresponded to 6.3%.

Tab. 3.1 Mean air temperatures (T_{air}) and annual temperature changes for each month between 1995 and 2006.

Month	T_{air} [$^{\circ}\text{C}$]	ΔT_{air} [$^{\circ}\text{C yr}^{-1}$]	Significance
Jan	0.5	0.19 ± 0.19	<i>n.s.</i>
Feb	2.5	-0.22 ± 0.21	<i>n.s.</i>
Mar	5.1	0.00 ± 0.14	<i>n.s.</i>
Apr	8.8	0.07 ± 0.08	<i>n.s.</i>
May	13.2	0.06 ± 0.10	<i>n.s.</i>
Jun	16.1	0.19 ± 0.10	*
Jul	17.9	0.19 ± 0.15	<i>n.s.</i>
Aug	17.9	-0.04 ± 0.13	<i>n.s.</i>
Sep	13.8	0.25 ± 0.13	*
Oct	9.9	0.11 ± 0.15	<i>n.s.</i>
Nov	5.0	0.26 ± 0.11	**
Dec	1.6	0.25 ± 0.14	<i>n.s.</i>
Annual	9.40	0.11 ± 0.05	*

n.s. not significant; * $p < 0.1$; ** $p < 0.05$

Precipitation

The annual precipitation sum is presented in Fig. 3.1. For the whole period between 1995 and 2006 the mean annual rainfall was 582 mm. The highest annual rainfall occurred in the years 1998 and 2002, whereas lowest rainfall occurred in the years 1997 and 2003. The annual precipitation was in line with the soil moisture dynamics. No trend towards a higher annual precipitation was observed during the investigation period.

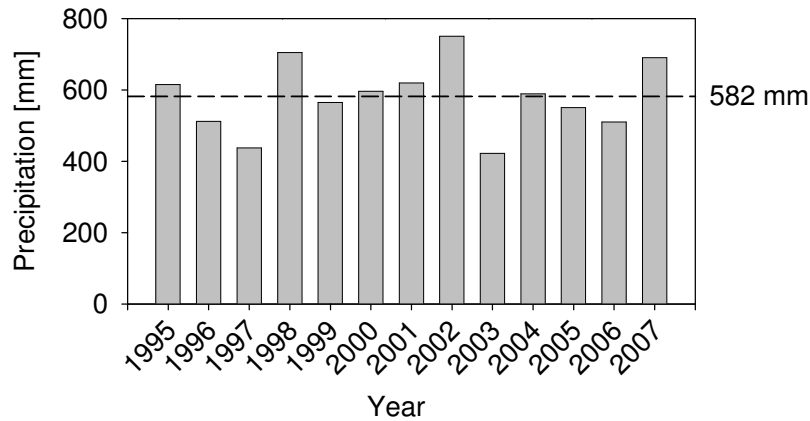


Fig. 3.1 Annual precipitation between 1995 and 2006 measured at the Giessen-FACE site, the dashed line marks the mean precipitation since 1995.

Soil moisture

At the site between 3rd March 1997 and 31st December 2006 the lowest soil moisture was generally recorded in ring pair 1, followed by the ring pairs 3 and 2 (Fig. 3.2). The mean volumetric water content (VWC) of the plots E1 and A1 was $40.1 \pm 3.9\%$ and $36.5 \pm 4.5\%$ during the experimental period. Ring pair 3 had a soil moisture content of $39.9 \pm 4.1\%$ and $40.7 \pm 4.5\%$ for E3 and A3, respectively. By far the highest VWC was found in the plots E2 ($44.5 \pm 5.5\%$) and A2 ($45.9 \pm 5.8\%$). Within each ring pair the soil moisture difference was less pronounced, with mean E/A-differences of +3.5, -1.4 and -0.8% in the ring pairs 1, 2, and 3, respectively. The average soil moisture difference between E- and A-plot means was 0.4% ($n = 3$). No significant differences were found between E- and A-plots.

Distinctive annual dynamics of the soil moisture were observed, with wettest soil moisture conditions in winter, i.e. close to saturation, and driest conditions in summer (July-August). The lowest soil moisture was recorded in 1997 and 2003, and the wettest year was 2002.

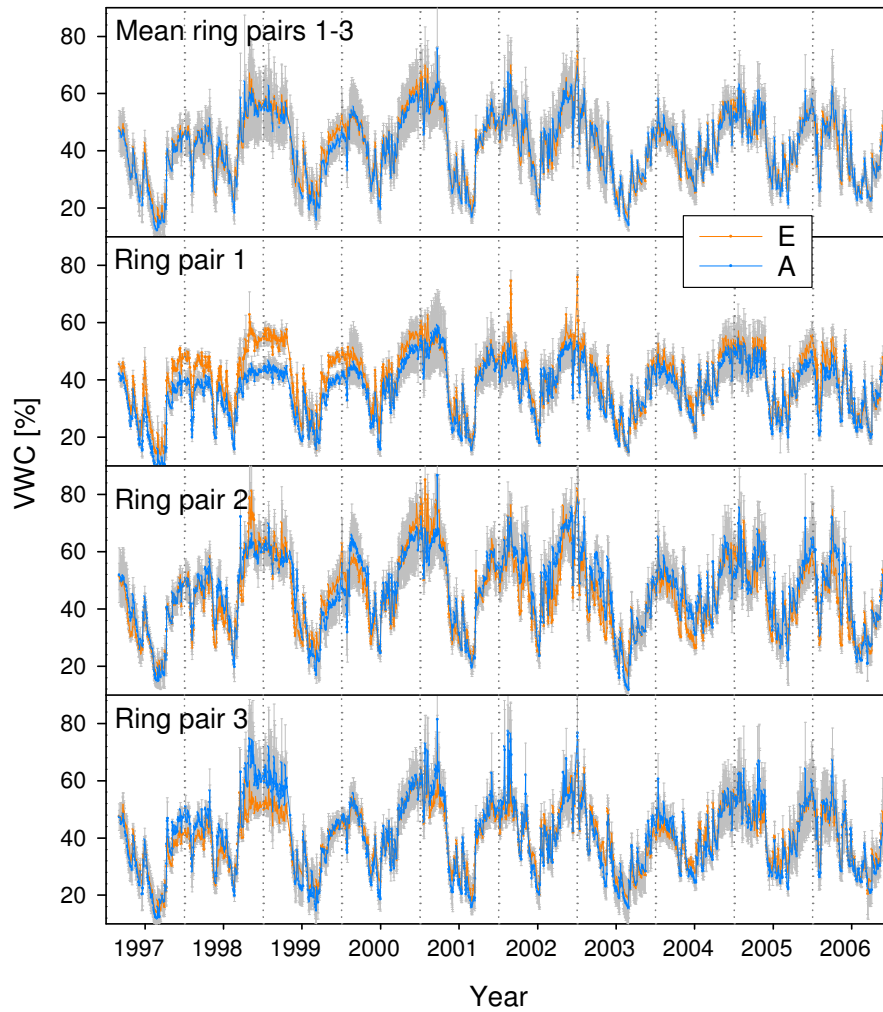


Fig. 3.2 The volumetric soil water content (VWC) in 0-15 cm depth is presented separately for the plots E1-A3 and as the E- or A-average ($n = 3$), error bars (grey) mark the standard deviation.

3.2 Plant biomass

3.2.1 $\delta^{13}\text{C}$ signature of above and belowground biomass

The isotope signature of plant material depends on the $\delta^{13}\text{C}$ signature of atmospheric CO_2 and was predicted via Eqn. 1. The predicted plant $\delta^{13}\text{C}$ signatures were close to the measured values (Tab. 3.2).

Tab. 3.2 Predicted and measured $\delta^{13}\text{C}$ signature of plant biomass (*June 2004, **May/June 2006; n = 3)

$\delta^{13}\text{C}$	Ambient	E1-E3 (-25‰)	E1-E3 (-48‰)
	[‰]		
Plant (predicted)	-28.9	-30.1	-34.6
Roots	-29.3 \pm 0.2*	-31.7 \pm 0.2*	-34.1 \pm 0.5**
Leaves	-28.1 \pm 0.5*	-29.3 \pm 0.3*	-33.9 \pm 0.2**

Leaves

The ^{13}C signature of aboveground biomass grown under ambient and elevated atmospheric CO_2 conditions differed among years (Tab. 3.3). For the ambient plots the mean signature ranged between -28.8 to -27.4‰, whereas in the elevated plots the CO_2 enrichment caused a decrease in the $\delta^{13}\text{C}$ due to the lower $\delta^{13}\text{C}$ signature of the CO_2 used for the enrichment. The signature switch in June 2004 occurred between the first and second biomass harvest of the year 2004. The biomass collected during the first harvest 2004 had a ^{13}C signature difference between E- and A-plots of only -1.2‰. From July 2004 onwards the $\delta^{13}\text{C}$ signature significantly decreased in plant leaves grown under elevated CO_2 . The signature of the second harvest 2004 was approximately 4‰ lower than at the first harvest (Tab. 3.3). The mean leaf $\delta^{13}\text{C}$ signature for both harvests is presented separately for the years 2005 and 2006 in Tab. 3.3. No significant differences between the first and the second harvest occurred. For both CO_2 treatments the ^{13}C signature was lower in 2005 than in 2006.

In plot E4, where the $\delta^{13}\text{C}$ signature of leaves was only measured in December 2006, it was with -38.5 \pm 0.7‰ significantly lower than in the E-plots 1-3 in September 2006.

Tab. 3.3: $\delta^{13}\text{C}$ signature of aboveground plant biomass grown under ambient and elevated atmospheric CO_2 . Values are presented as means for each plot ($n = 3$) and as E-A means (2004: $n = 3$; 2005 and 2006: $n = 6$). Letters mark the level of significance between E- and A-plots.

Plot	Jun 2004	Sep 2004	Mean 2005	Mean 2006
	[‰]			
E_{avg}	-29.3 ± 0.3	-33.1 ± 1.1	-35.1 ± 1.3	-33.2 ± 0.9
A_{avg}	-28.1 ± 0.5	-28.8 ± 0.5	-28.7 ± 0.5	-27.4 ± 1.4
$(E-A)_{\text{avg}}$	$-1.2 \pm 0.8^{\text{b}}$	$-4.3 \pm 1.5^{\text{a}}$	$-6.4 \pm 1.5^{\text{a}}$	$-5.8 \pm 1.5^{\text{a}}$

Root biomass

Before the onset of the CO_2 enrichment the $\delta^{13}\text{C}$ signature of root biomass in the top 15 cm was similar for all plots (Fig. 3.3). In the ambient plots the $\delta^{13}\text{C}$ signature remained at $29.5 \pm 0.2\text{‰}$ over the whole investigation period. Under $[\text{CO}_2] +20\%$ the $\delta^{13}\text{C}$ signature decreased in the first three years down to -32‰ (October 2001). Between October 2001 and June 2004 no further depletion in ^{13}C occurred. In the three years following the $\delta^{13}\text{C}$ switch the $\delta^{13}\text{C}$ signature decreased down to -34.5‰ . In plot E4, where no data were available before the signature switch, root biomass was approximately 1.5‰ lower than under $[\text{CO}_2] +20\%$.

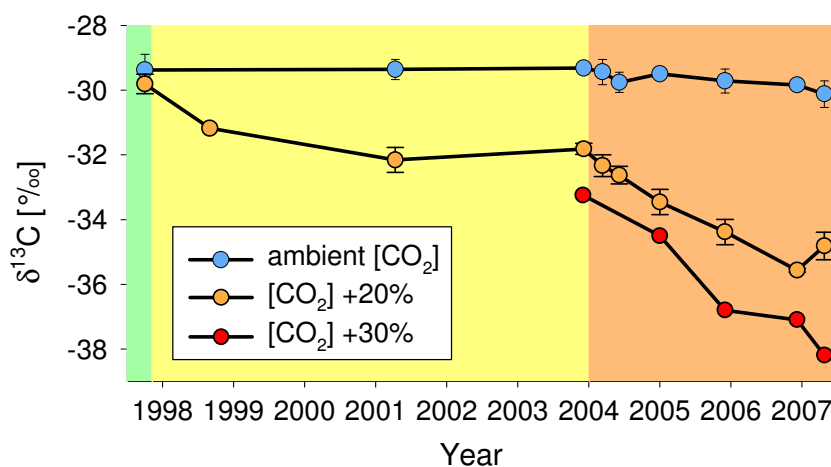
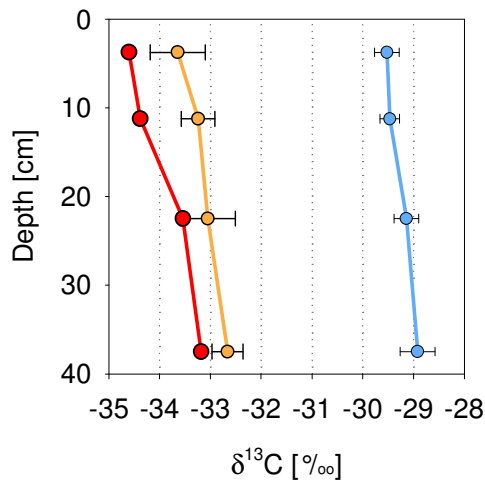


Fig. 3.3 $\delta^{13}\text{C}$ signature of root biomass in 0-15 cm depth between 8th April 1998 and 25th October 2007 under ambient and elevated CO_2 , values for ambient and elevated $[\text{CO}_2] +20\%$ are presented as averages of the plots 1-3; error bars mark the standard deviation ($n = 3$). For $[\text{CO}_2] +30\%$ only one plot exists ($n = 1$).

The lowest $\delta^{13}\text{C}$ signatures of root biomass in soil profiles sampled between 2004 and 2006 occurred in the uppermost soil layer. The signature increased with depth (Fig. 3.4). The results of the linear regression analysis, where the effect of depth on root- $\delta^{13}\text{C}$ signature was tested, are presented in Tab. 3.4. In June 2004 neither in A1-A3 nor in E1-E3 a significant impact of depth was observed, but after the signature switch depth had a significant impact on root- $\delta^{13}\text{C}$ signature in the plots E1-E3. In the plots A1-A3 also an unexpected impact of depth on root- $\delta^{13}\text{C}$ signature occurred in 2005, but the signature differences between the depths were altogether very small. In plot E4 depth had a significant impact on root- $\delta^{13}\text{C}$ signature in all years; here the largest differences of all CO_2 treatments occurred.



Tab. 3.4 Significant influence (p) of the factor depth on $\delta^{13}\text{C}$ signature of root biomass under all CO_2 treatments.

Plot	16-Jun-04	15-Jul-05	1-Jun-06
A_{avg}	>0.1	0.005	>0.1
E_{avg}	>0.1	0.010	0.059
E4	0.040	0.032	0.031

Fig. 3.4 Coherency between root $\delta^{13}\text{C}$ signature and depth, exemplary shown for July 2005 (blue: ambient; orange: $[\text{CO}_2]$ +20%, red: $[\text{CO}_2]$ +30%).

3.2.2 Root biomass yield

The highest average root biomass in the top 45 cm in July 2005, December 2005 and June 2006 occurred in the driest ring pair 1 (E1: 0.344 kg m^{-2} , A1: 0.302 kg m^{-2}), followed by ring pair 3 (E3: 0.229 kg m^{-2} , A3: 0.202 kg m^{-2}) and ring pair 2 (E2: 0.233 kg m^{-2} , A2: 0.153 kg m^{-2}). A significant effect of elevated CO_2 on root biomass ($p = 0.093$ in 0-7.5 cm; $p = 0.054$ in 7.5-15 cm; paired t-test) only occurred for the samples taken in December 2005. The highest root biomass was observed in plot E4, with a total root biomass of 0.434 (July 2005) and 0.325 kg m^{-2} (June 2006) in the top 0-45 cm depth.

For the samplings in summer 2005, 2006 and 2007 no significant differences in root biomass growth under ambient and elevated $[\text{CO}_2]$ +20% were observed ($p > 0.1$). However, root biomass of plot E4 ($[\text{CO}_2]$ +30%) was up to 68% above ambient (Tab. 3.5).

Tab. 3.5 Differences in root biomass (0-45 cm) between the CO₂ treatments

Difference	July 2005	June 2006	June 2007
E _{avg} in% of A _{avg}	98	111	93
E4 in% of A _{avg}	161	168	129

The distribution of root biomass in the soil profile is presented in Fig. 3.5. The highest root biomass occurred near the surface but then decreased rapidly with depth. Under [CO₂] +30% root biomass increased in all soil depths.

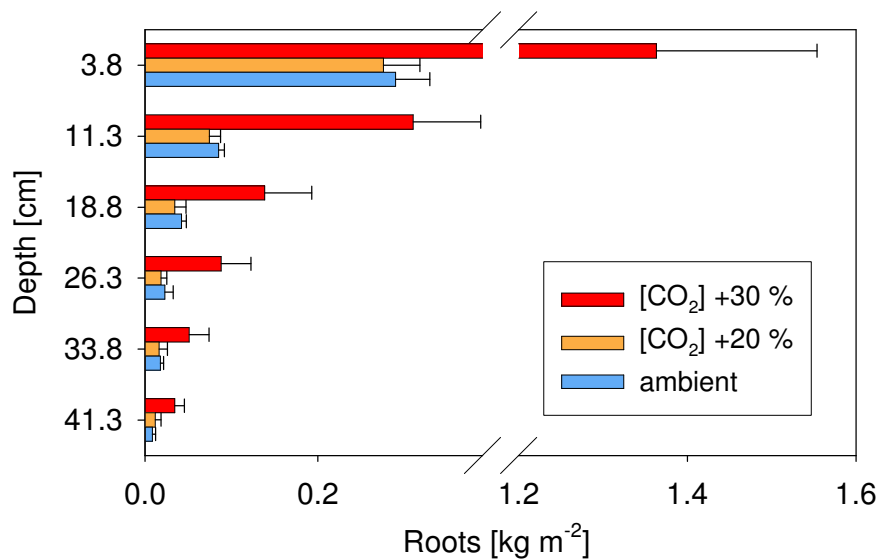


Fig. 3.5 Mean root biomass after 9 years of CO₂ enrichment (June 2007) in the soil profile under elevated and ambient atmospheric CO₂ conditions (means \pm standard deviation (n = 3) for ambient and [CO₂] +20%; for plot E4 ([CO₂] +30%) error bars mark the standard deviation within the plot (n = 3).

3.3 Soil aggregate structure

The soil samples collected in the profile down to 45 cm depth were repeatedly taken shortly after the first harvest in early June. In the years 2004 and 2005, additional soil samples of the uppermost 15 cm depth were taken in December to identify a possible impact of the season on the soil aggregate structure. A comparison with the soil profile collected in summer revealed no significant seasonal effect on soil aggregation or SOC. To take the spatial variability of the research site into account, annual means were calculated of the summer and winter sampling of the aggregate fractions and the SOC content for the depths 0-7.5 and 7.5-15 cm separately for each plot. This was not done for the $\delta^{13}\text{C}$ signature, which changed over time and is therefore different to samples collected in June and December.

3.3.1 Distribution of aggregates in the soil profile

The aggregate structure of the soil profile is presented as averages for the ring pairs 1-3 ($n = 6$) (Fig. 3.6). In the ring pairs 1-3 the fraction of LM first increased with depth, reaching the highest contribution at around 25 cm depth but then decreased again. In general, the total amount of large and small macroaggregates decreased with depth and the Mic and SC fractions increased. The soil aggregate structure differed between the ring pairs, but the differences within the E and A-plots of each ring pair were only marginal. The vertical distribution of soil aggregates of plot E4 (data not shown) was statistically not different from the ring pairs 1 and 3 (one-sample t-test; $p > 0.1$).

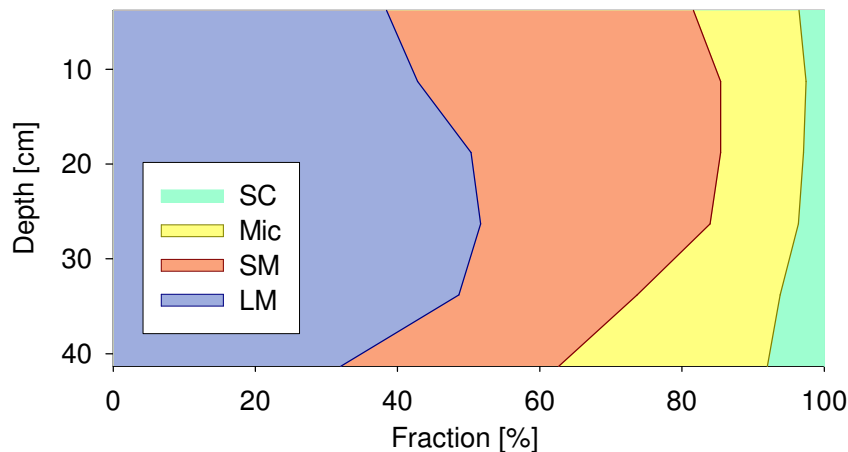


Fig. 3.6 Soil aggregate classes in the in the top 45 cm (June 2007). Values are presented as mean for the ring pairs 1-3 ($n = 6$).

3.3.2 Soil aggregation changes between 1998 and 2007

The highest LM content was recorded in April 1998 for the uppermost 7.5 cm in ring pair 3 (64.3 ±1.9%), followed by the ring pairs 2 (60.9 ±0.7%) and 1 (51.5 ±0.6%). In 7.5-15 cm the aggregate composition was very similar for the ring pairs 2 (59.8 ±1.3%) and 3 (58.3 ±0.5%), with the lowest LM content occurring in ring pair 1 (51.8 ±4.0%).

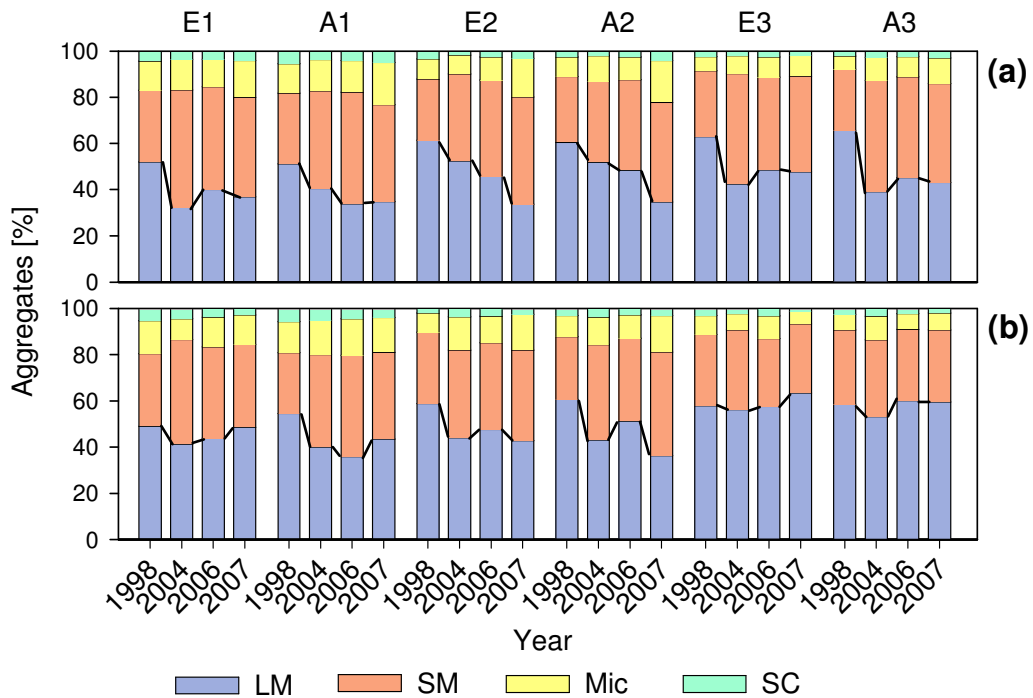


Fig. 3.7 Soil aggregate structure in the soil profile (a = 0-7.5 cm, b = 7.5-15 cm). Values are presented separately for each plot for the years 1998, 2004, 2006, and 2007.

No significant differences in soil aggregation between E- and A-plots were found ($p > 0.1$; ANOVA with VWC as covariate). The first observation period (April 1998 to June 2004) was characterized by a change in soil aggregate composition within the uppermost 15 cm, which was due to the decrease of the LM fraction for the benefit of the SM fraction and, to a minor extend, the Mic fraction (Fig. 3.7, Tab. 3.6). In plot E4, where no samples were available for the year 1998, between 2004 and 2007 the LM content remained constant in the uppermost 15 cm depth (four-year mean LM content was $40.8 \pm 0.8\%$ and $50.8 \pm 2.4\%$ ($n = 4$) for 0-7.5 and 7.5-15 cm depth, respectively).

The changes in soil aggregation between April 1998 and 2004 were similar in both CO₂ treatments (Tab. 3.6). Both showed a loss in large macroaggregates, which was on average higher in the uppermost soil layer (mean A1-E3: -16%) than in the soil layer below (mean A1-E3: -11%). In 0-7.5 cm the highest loss in LM occurred in ring pair 3 (A3 = -27.2%, E3 = -20.6%), followed by the ring pairs 1 (A1 = -10.6%,

E1 = -19.1%) and 2 (A2 = -8.6%, E2 = -9.7%). In the deeper soil layer the highest loss was observed in ring pair 2 (A2 = -17.2%, E2 = -15.4%), followed by the ring pairs 1 (A1 = -15.3%, E1 = -9.0%) and 3 (A3 = -6.1%, E3 = -2.2%).

Tab. 3.6 Relative changes in soil aggregation between 1998 and 2004 and between 2004 and 2006 (n = 3); values for the year 2004 in the upper 15cm were averaged from the samplings in June and December.

CO ₂	Depth [cm]	1998 to 2004				2004 to 2006			
		LM	SM	Mic	SC	LM	SM	Mic	SC
		[%]				[%]			
A _{avg}	0-7.5	-15.5 ±9.8	13.2 ^c ±7.7	2.7 ±1.8	-0.6 ±1.1	-1.3 ±6.5	1.9 ±5.6	-0.7 ±0.9	0.2 ±0.4
E _{avg}		-16.3 ^b ±6.5	16.7 ^b ±4.8	0.6 ±1.1	-1.0 ^c ±0.6	2.4 ±8.0	-3.3 ±6.5	0.4 ±1.6	0.5 ±0.4
A _{avg}	7.5-15	-16.5 ^c ±6.3	13.9 ±7.4	2.9 ^b ±1.0	-0.3 ±0.8	-0.5 ±6.8	1.2 ±4.7	-0.5 ±2.2	-0.1 ^b ±0.3
E _{avg}		-12.5 ±6.5	9.6 ±5.2	2.7 ±5.8	0.2 ±1.4	3.7 ^b ±1.1	-1.2 ^b ±3.0	-1.5 ±3.7	-0.9 ±0.9

Letters mark the level of significance ($p \leq 0.01$ (a); $p < 0.05$ (b); $p < 0.1$ (c)) in aggregate composition changes between 1998 and 2004 or 2004 and 2006, respectively. No letters indicate that no significant difference occurred between dates.

To test the effect of soil moisture or aboveground biomass production on soil aggregation, linear regression analysis was used. For 0-7.5 cm depth a marginally significant impact ($p = 0.081$) of soil moisture (mean 1997-2004) on the large macroaggregate content in June 2004 was detected. However, no significant effect of soil moisture on the LM loss between 1998 and 2004 was observed. The aboveground biomass yield (mean for the years 1998-2004) did not have a significant effect on either the LM loss or the LM content in 2004.

3.3.3 Effect of elevated CO₂ on soil aggregation

No significant effect of elevated CO₂ on soil aggregation or soil aggregation changes were observed, neither in the first nor in the second observation period, in neither depth (paired t-test; $p > 0.1$). When calculating the difference between 1998 and 2004 separately for ambient and elevated CO₂, in 0-7.5 cm the difference between the CO₂ treatments was with 0.8 percent points only marginal, whereas in 7.5-15 cm the LM loss was 4 percent points higher in the A-plots (Tab. 3.6).

The mean differences between E- and A-plots for the ring pairs 1-3 are presented in Fig. 3.8 for each sampling date. The initial LM content was similar in the corresponding E- and A-plots. The slope of the linear regression indicated an increase in LM content under elevated CO₂. However, as indicated by the error bars, the variability between the ring pairs was too large to yield a statistically significant increase of LM under elevated CO₂ ($p > 0.1$).

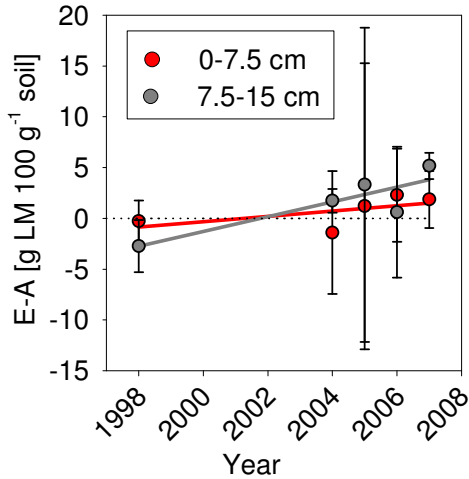


Fig. 3.8 LM content differences between E- and A-plots ($n = 3$) between 1998 and 2007, note: values > 0 indicate a higher LM content, values < 0 indicate a lower LM content in the CO_2 enriched plots. Values are presented as annual means.

For plot E4 changes in soil aggregation could not be detected during the first investigation period because no data for the year 1998 were available. In the second investigation period no increase in LM content over time occurred, the LM content ranged between 40 and 46%. When comparing plot E4 with its corresponding control site A4, a higher soil aggregation (LM content was 47 and 64% in 0-7.5 and 7.5-15 cm depth in September 2005) was found at the control site.

3.4 Soil organic carbon content and $\delta^{13}\text{C}$ signature under ambient and elevated CO_2

3.4.1 Soil organic carbon content

The SOC content differed between the ring pairs, but was similar in the corresponding E- and A-plots. Therefore, the SOC content is presented separately for each plot, whereas the SOC differences between E and A plots and their changes over time are presented as averages. Similar to the aggregation of soil, the highest SOC content was present in ring pair 3, followed by the ring pairs 2 and 1.

Aggregate-associated carbon

The SOC content of the four aggregate fractions is presented in Fig. 3.9. In all soil aggregate classes the SOC content decreased significantly with depth (for all fractions $p < 0.05$, linear regression analyses). The SOC content of the large and small macroaggregate fractions was similar in each depth, whereas the SOC content of the smaller soil fractions Mic and SC was 28 \pm 2.8% (mean soil profile) lower than in the two macroaggregate fractions. The differences in SOC content between the soil aggregate fractions decreased with depth.

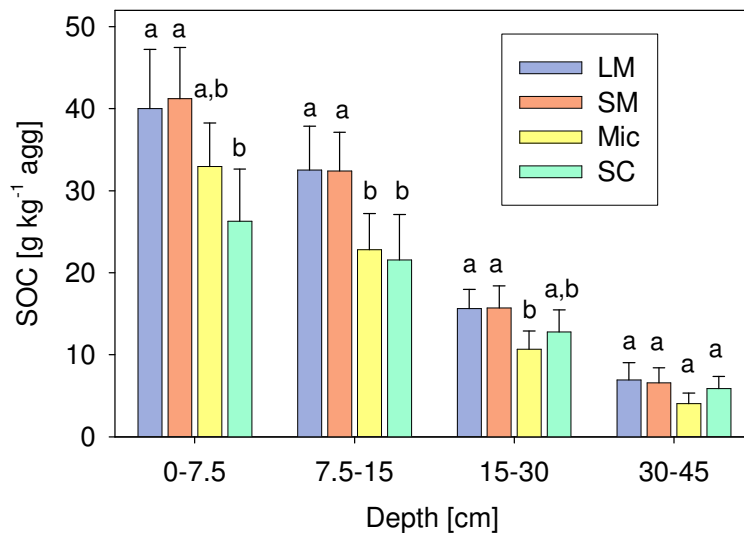


Fig. 3.9 SOC content of several soil fractions in the soil profile, values are presented as means for the ring pairs 1-3 ($n = 6$ plots) for the years 2004 to 2007 ($n = 4$ samplings); error bars show the standard deviation. Different letters mark a significant difference in C content within one depth ($\alpha = 0.05$, *General linear model, Posthoc, LSD*).

Temporal dynamics

Between 1998 and 2004 all soil fractions in the top 15 cm decreased in their SOC content (Tab. 3.7). For the E-plots the total SOC loss was higher in 7.5-15 cm depth, whereas for the A-plots it was higher in 0-7.5 cm depth. However, no significant effect of depth or CO₂ treatment on SOC loss occurred in any soil fraction ($p > 0.1$; multivariate ANOVA, main factors depth and CO₂, no covariates). For both CO₂ treatments the highest relative SOC loss occurred in the SC fraction ($p = 0.002$), but due to the small pool size of this fraction (Fig. 3.7) it had a negligible influence on the total SOC loss.

Tab. 3.7 Average losses in SOC content between April 1998 and 2004 (mean June and December); values are presented separately for each depth and CO₂-treatment.

Plot	Depth [cm]	Total C	LM SM Mic SC			
			[g C kg ⁻¹ agg yr ⁻¹]			
A _{avg}	0-7.5	-1.1 ^c	-1.0	-0.4	-1.6	-2.3 ^a
		±0.6	±0.8	±0.3	±2.0	±0.4
E _{avg}		-1.3	-0.6	-0.7	-0.8	-1.6 ^c
		±0.5	±1.4	±0.5	±1.0	±0.8
A _{avg}	7.5-15	-0.8 ^a	-0.5	-0.6	-2.5	-2.8
		±0.0	±0.6	±1.5	±1.8	±2.3
E _{avg}		-1.0	-0.9 ^b	-0.7	-0.9	-1.4
		±0.4	±0.2	±1.0	±1.1	±0.9

Letters mark the level of significance ($p \leq 0.01$ (a); $p < 0.05$ (b); $p < 0.1$ (c)) in SOC content changes between 1998 and 2004 ($n = 3$).

Between 1998 and 2007 in plot E4 the SOC content decreased with a mean rate of 2.18 g kg⁻¹ yr⁻¹ ($r^2 = 0.53$) and 1.00 g kg⁻¹ yr⁻¹ ($r^2 = 0.46$) in 0-7.5 and 7.5-15 cm depth, respectively.

The SOC loss during the first observation period was also present in soil samples taken in 0-5 cm depth, where no soil aggregate fractionation was carried out (Tab. 3.8). The average SOC loss per year between 1997 and 2003 was highest in plot A1, followed by the plots E3, A3, and E1. The lowest decrease in SOC content occurred in the two wettest plots A2 and E2. The mean C loss rate ($n = 3$) was 26% higher under A compared to E, but differences were not significant (paired t-test, $p > 0.1$).

Tab. 3.8 Changes in total SOC (0-5 cm depth) between the years 1997 and 2003 under ambient atmospheric CO₂ conditions, determined via linear regression analysis ($y = \text{SOC vs. } X = \text{time}$).

Ring pair	Ambient		Elevated	
	g C kg ⁻¹	r^2	g C kg ⁻¹	r^2
1	-2.91	0.58	-1.69	0.46
2	-1.15	0.16	-0.55	0.03
3	-1.73	0.29	-2.04	0.42
Mean	-1.93 ±0.90		-1.43 ±0.78	

The changes in SOC are presented separately for the first and the second observation period in Fig. 3.11 as means for E and A plots together with the 95% confidence interval. For the second observation period between June 2004 and June 2007 the changes in SOC were evaluated via linear regression analysis ($n = 5$ samplings per plot). In the first observation period in 0-7.5 and 7.5-15 cm depth all soil fractions lost part of their initial C content, which was significant ($p < 0.05$) for five soil aggregate fractions (Fig. 3.10). From all other aggregate fractions the 95% interval touched the zero-line, indicating that no significant changes occurred. The changes in SOC during the second observation period were inconsistent, with both increases and decreases in aggregate C content. Significant changes only occurred in the SC fraction (A-plots, 0-7.5 cm). While the C content of the smaller aggregate-size fractions Mic and SC decreased, the macroaggregate C content increased or remained unaltered. No significant differences between the CO_2 -treatments were observed.

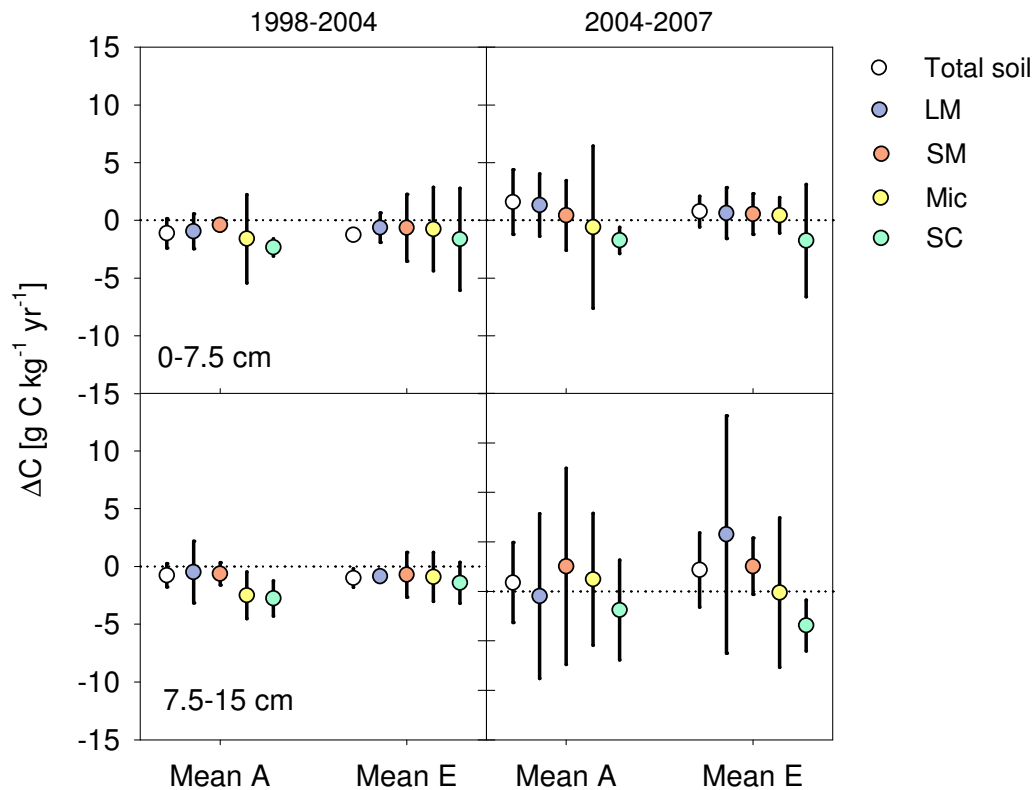


Fig. 3.10 Average changes in SOC content (mean \pm 95% confidence interval) between April 1998 and June 2004 ($n = 2$), and June 2004 to June 2007 ($n = 6$); values are presented separately for each depth and CO_2 -treatment ($n = 3$).

Area-related SOC content

The total amount of SOC stored in each fraction is presented in Fig. 3.11 separately for each plot. In April 1998 the highest amount of SOC was stored in the LM fraction, followed by the SM fraction. In line with the observed shift in soil aggregation between 1998 and 2004 from bigger towards smaller aggregates, a gradually lower amount of SOC was stored in the LM fraction, but the amount of SOC stored in the SM fraction increased (Fig. 3.11). In Tab. 3.9 the mean changes in aggregate-associated SOC are presented separately for each CO₂-treatment and depth.

Tab. 3.9 Area-related changes in SOC of several soil fractions between April 1998 and mean 2004, values are presented as means \pm standard deviation (n = 3).

Plot	Depth [cm]	Total soil	LM	SM [kg C m ⁻²]	Mic	SC
A _{avg}	0-7.5	-0.54 \pm 0.30	-0.74 \pm 0.43	0.37 \pm 0.36	0.02 \pm 0.04	-0.04 \pm 0.04
E _{avg}		-0.61 \pm 0.24	-0.72 \pm 0.52	0.47 \pm 0.17	-0.01 \pm 0.07	-0.04 \pm 0.03
A _{avg}	7.5-15	-0.40 \pm 0.04	-0.49 \pm 0.05	0.15 \pm 0.43	-0.07 \pm 0.07	-0.05 \pm 0.02
E _{avg}		-0.72 \pm 0.53	-0.45 \pm 0.12	0.09 \pm 0.23	-0.05 \pm 0.06	-0.03 \pm 0.03
A _{avg}	0-15	-0.94 \pm 0.29	-1.23 \pm 0.43	0.53 \pm 0.15	-0.05 \pm 0.11	-0.09 \pm 0.02
E _{avg}		-1.33 \pm 0.39	-1.17 \pm 0.49	0.55 \pm 0.38	-0.06 \pm 0.03	-0.07 \pm 0.02

Between April 1998 and 2004 the total soil SOC loss in the top 15 cm was on average 1.33 and 0.94 kg C m⁻² in E and A plots, respectively, which corresponds to an annual loss rate of 0.18 and 0.15 kg C m⁻² yr⁻¹.

In the top 7.5 cm the greatest loss in SOC occurred in ring pair 3 (-0.82 kg m⁻²), followed by the ring pairs 2 (-0.35 kg m⁻²) and 1 (-0.24 kg m⁻²). In 7.5-15 cm the highest SOC loss also occurred in ring pair 3 (-0.68 kg m⁻²), followed by ring pair 2 (-0.35 kg m⁻²). In ring pair 1 the SOC content of the ambient plot A1 increased about +0.37 kg m⁻², whereas the SOC content of plot E1 again decreased (-0.31 kg m⁻²).

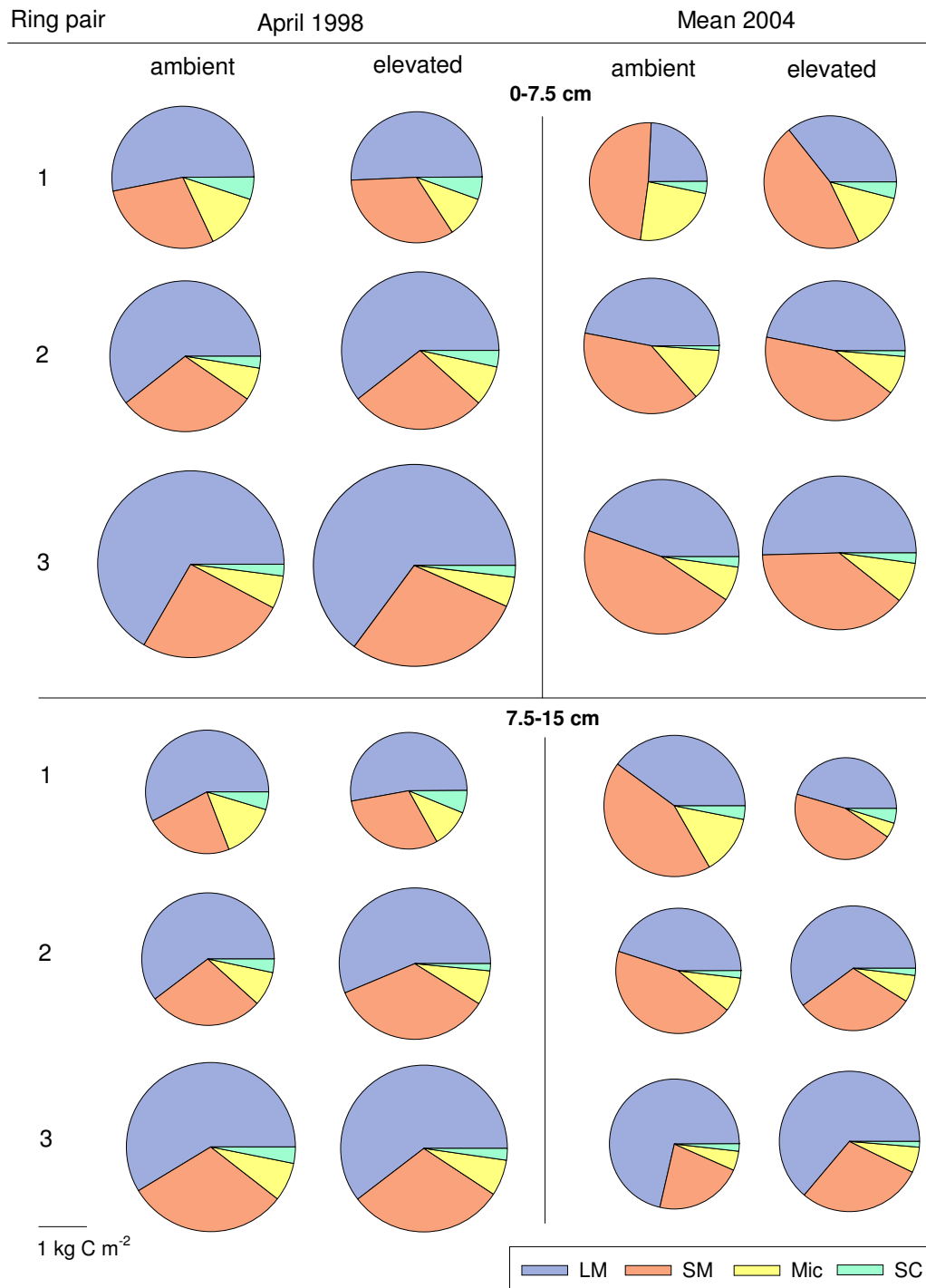


Fig. 3.11 The SOC content stored in several aggregate fractions in 0-7.5 and 7.5-15 cm depth is presented separately for each ring pair. The diameters of the circles represent the total amount of SOC (kg m⁻²).

Correlation between SOC and amount of LM in the soil

As changes in soil aggregation and a decrease in SOC occurred during the same time period, a linear regression analysis was carried out to evaluate possible interactions. A significant correlation ($p = 0.045$, linear regression) between the SOC loss and the breakup of LM only occurred under ambient CO_2 (Fig. 3.12).

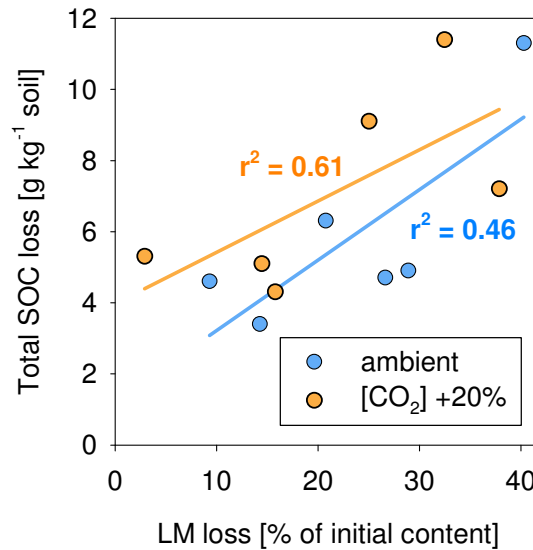


Fig. 3.12 SOC loss and magnitude of LM loss between April 1998 and 2004 in 0-7.5 and 7.5-15 cm.

3.4.2 Effects of elevated CO₂ on soil organic carbon content

After 9 years of elevated CO₂ the SOC content was not different among the CO₂ treatments (Fig. 3.13), indicating that no net C sequestration had taken place in any depth. Additionally, the SOC loss that occurred within the first six years of the experiment was not alleviated by the CO₂ enrichment (Tab. 3.7, Tab. 3.8).

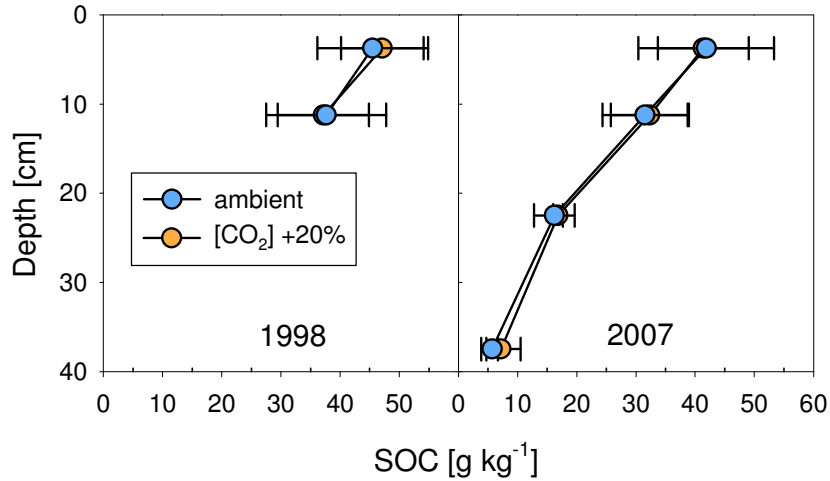


Fig. 3.13 Mean SOC content in April 1998 before the CO₂ enrichment started and after 9 years of elevated CO₂ in June 2007 (n=3).

Fig. 3.14 shows the decrease in SOC relative to the initial content in 1998, (set to 100%). The linear regression analysis revealed a C loss of 2.5% yr⁻¹ under ambient (not significant) and 2.2% yr⁻¹ under elevated CO₂ ($p < 0.05$, linear regression analyses).

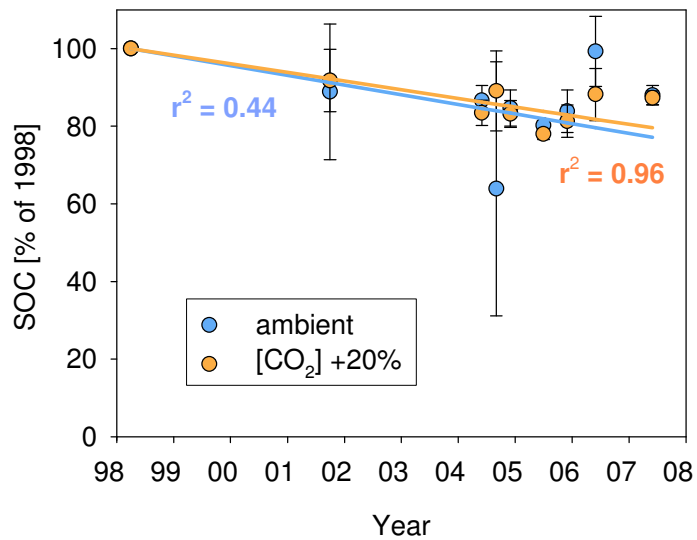


Fig. 3.14 Changes in SOC since 1998 in E and A-plots for the top 15 cm, error bars mark the standard deviation (n=3).

The SOC content of the single aggregate fractions (Fig. 3.15) was not significantly different between E and A plots (paired t-test; $p > 0.1$ for all aggregate classes in all depths, tested for the years 2006 and 2007).

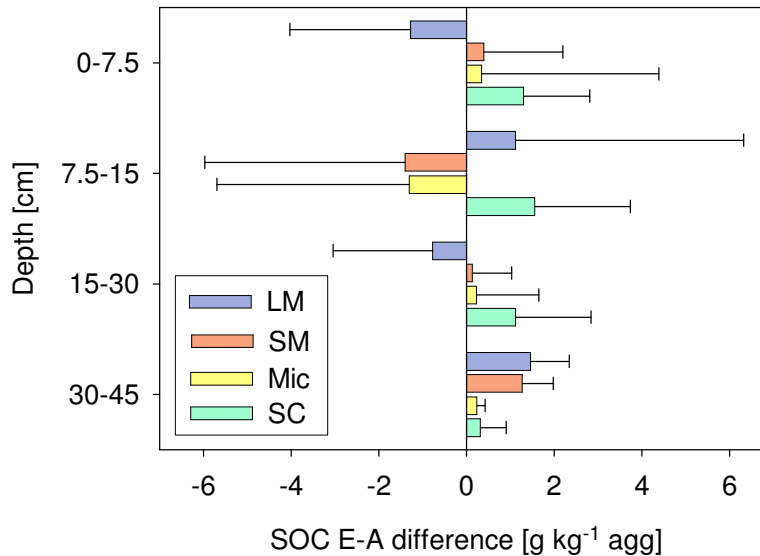


Fig. 3.15 Mean SOC content difference between ambient and elevated $[\text{CO}_2]$ +20% in the years 2006 and 2007, error bars mark the standard deviation ($n = 6$).

3.4.3 $\delta^{13}\text{C}$ signature in bulk soil and the soil aggregate fractions

Before the CO_2 enrichment of the E-plots started the $\delta^{13}\text{C}$ signature of the non-fractionated soil was equal for all A- and (later) E-plots (Fig. 3.16). In June 2004, after six years of a moderate CO_2 -enrichment using CO_2 with a signature of -25‰ , the $\delta^{13}\text{C}$ signature of the non-fractionated soil decreased by 0.3‰ in the top 7.5 cm of soil. With increasing depth the difference was less pronounced. The comparison between E- and A-plots after six years of elevated CO_2 revealed a 1.2‰ lower $\delta^{13}\text{C}$ signature in the E-plots in the uppermost soil layer. The signature switch in July 2004 to CO_2 -48‰ caused a subsequent further decrease in $\delta^{13}\text{C}$ of the bulk soil until June 2007. In June 2007 also the ambient plots decreased in their SOC $\delta^{13}\text{C}$ signature, whereas one year before in June 2006 (data not shown) the $\delta^{13}\text{C}$ signature was similar to 1998 and 2004.

After six years of elevated CO_2 with $[\text{CO}_2]$ +30% SOC in 0-7.5 and 15-30 cm depth was more depleted in its $\delta^{13}\text{C}$ signature than in the E-plots 1-3. In 7.5-15 and 30-45 cm the $\delta^{13}\text{C}$ signatures were not different (Fig. 3.16). Three years after the signature switch the ^{13}C depletion was more pronounced, whereas the degree of depletion decreased with depth. In June 2007 the $\delta^{13}\text{C}$ signature of SOC was lower in the $[\text{CO}_2]$ +30% treatment than under $[\text{CO}_2]$ +20%.

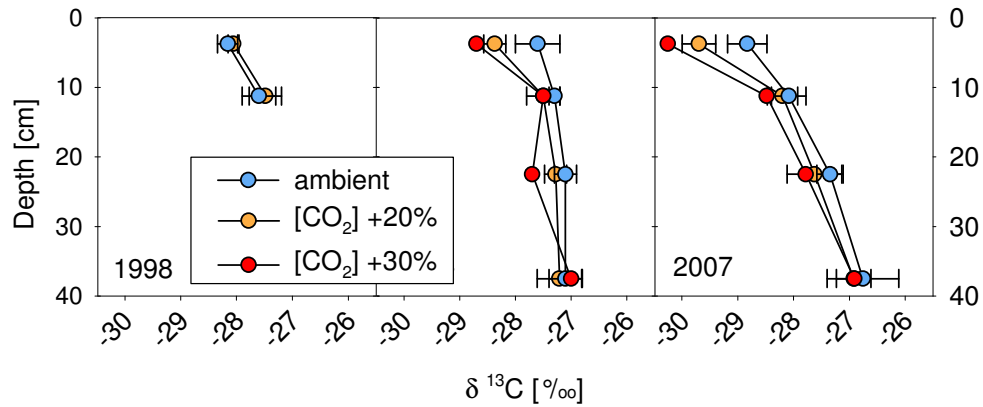


Fig. 3.16 $\delta^{13}\text{C}$ signature of SOC in the soil profile under ambient and elevated CO_2 (avg. ring pairs 1-3 ($n = 3$), $n = 1$ for $[\text{CO}_2] + 30\%$), values from non fractionated soil.

The SOC content decreased with depth (Fig. 3.13), whereas the $\delta^{13}\text{C}$ signature increased (Fig. 3.16). After 6 years of moderate CO_2 enrichment, a significant difference in the ^{13}C signature between E- and A-plots occurred in 0-7.5 cm ($p = 0.001$, paired t-test), 7.5-15 cm ($p = 0.024$) and (marginally) in 15-30 cm depth ($p = 0.075$).

Soil aggregate fractions

Because the total soil is less sensitive for changes in $\delta^{13}\text{C}$ than the fractionated soil, the following section focuses on the $\delta^{13}\text{C}$ signature of the separate soil aggregate fractions.

The ^{13}C signatures in 0-7.5 cm depth are presented in Fig. 3.17 and Fig. 3.18 for each soil aggregate fraction for the entire investigation period. Before the experiment started in April 1998, the $\delta^{13}\text{C}$ signatures of SOC in all aggregate fractions were similar for all A- and (later) E-plots. Six years of elevated CO_2 caused a decrease in ^{13}C signature in all aggregate fractions. The decrease in $\delta^{13}\text{C}$ was approximately 1‰ in the SM, Mic and SC fractions but only 0.5‰ in the LM fraction. After the signature switch the difference between E- and A-plots stayed at around 1‰ in all aggregate fractions. In the A-plots the $\delta^{13}\text{C}$ signature remained around -28‰, except for the samples collected in June 2007, where a decrease in the SOC $\delta^{13}\text{C}$ signature in all soil aggregate fractions of both E- and A-plots was observed (Fig. 3.17). In the deeper soil layers this depletion was less pronounced (data not shown).

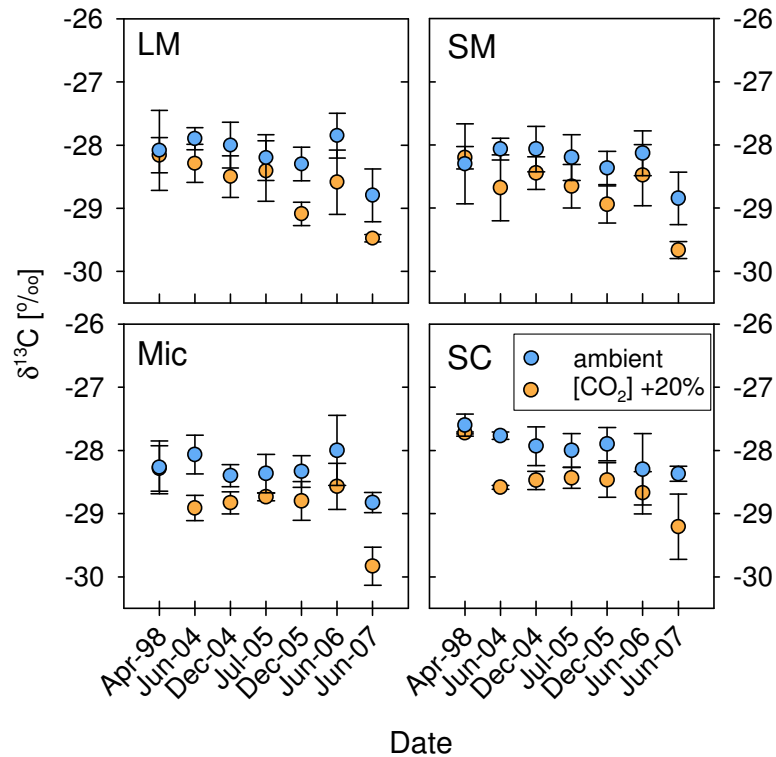


Fig. 3.17 Shift in $\delta^{13}\text{C}$ signature of SOC in several soil aggregate fractions in 0-7.5 cm depth since the beginning of the CO₂ enrichment. Values are presented as means with the standard deviation (n = 3). Note that the time axis is not linear (category axis).

To illustrate the differences in $\delta^{13}\text{C}$ among the four aggregate fractions data from Fig. 3.17 were re-draw according to CO₂ treatment and sampling date (Fig. 3.18). Except for the E-plots in June 2004 and the A-plots in June 2006, the SC fraction showed the highest $\delta^{13}\text{C}$ signature of all soil fractions. Under ambient CO₂ and for the later E-plots in 1998 the differences between the aggregate fractions LM, SM and Mic were very small. They accounted for $-28.2\text{‰} \pm 0.3$ (LM), $-28.3\text{‰} \pm 0.3$ (SM), $-28.3\text{‰} \pm 0.3$ (Mic), and $-28.0\text{‰} \pm 0.3$ (SC) on average for all samplings between April 1998 and June 2007 (only ambient plots, n = 7).

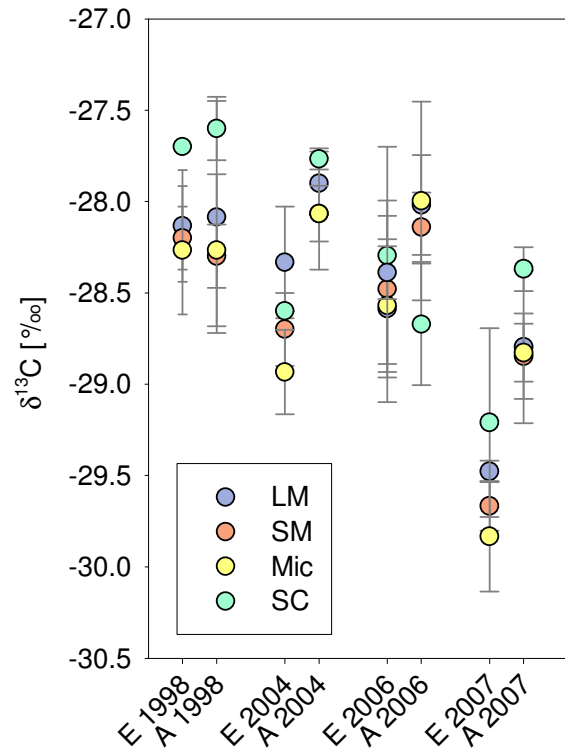


Fig. 3.18 The $\delta^{13}\text{C}$ signature of each aggregate fraction for E- and A-plots for the sampling dates April 1998, June 2004, June 2006, and June 2007, error bars mark the standard deviation (n=3).

3.5 Soil C input in the CO₂ enriched plots

The soil C input could only be determined for the CO₂-enriched plots, as in the ambient plots no ¹³C label was applied.

3.5.1 Fraction of new C

The fractions of new C (fC_{new}) under elevated [CO₂] +20% and +30% between April 1998 and June 2006 are presented in Tab. 3.10 and Tab. 3.11, respectively. After 8 years of elevated CO₂ with [CO₂] +20%, the percentage of new C ranged from 3.7% to 20.9% in the non-fractionated soil. In the treatment [CO₂] +30% fC_{new} of total soil was with 28% (0-7.5 cm) and 19% (7.5-15 cm) higher than fC_{new} under [CO₂] +20%. In the deeper soil layers the differences were only small. In both treatments the highest fC_{new} occurred in the top 7.5 cm and decreased with depth.

Under [CO₂] +20%, fC_{new} was not significantly different between the aggregate fractions in the top 15 cm, although in 0-7.5 cm the highest fC_{new} was found in the Mic and SC fractions. However, in 7.5-15 cm the macroaggregate fractions contained the highest proportion of new C. Significant differences in fC_{new} between the fractions only occurred in 15-30 cm depth, where fC_{new} was highest in the SC fraction, followed by Mic, LM and SM. An exceedingly high fC_{new} of 38% was found in the SC fraction in 30-45 cm depth. This was caused by the plots E1 and E2, whereas in plot E3 fC_{new} was with 0.4% very low.

Similar to the plots E1-E3 also in plot E4 the highest fC_{new} in the top 7.5 cm was found in the Mic and SC fraction. Also in 7.5-15 cm the LM fraction had the highest fC_{new} . The second highest amount of fC_{new} occurred in the Mic fraction. In the deeper soil layers 15-30 and 30-45 cm the Mic fraction had the highest fC_{new} .

Tab. 3.10 Fraction of new C in several soil aggregate fractions after 8 years of elevated [CO₂] +20% (plots E1-E3); values are presented as means ±standard deviations.

Depth [cm]	LM	SM	Mic [%]	SC	Total
0-7.5	15.1 ±10.5	18.1 ±3.5	24.1 ±10.2	23.6 ±4.2	20.9 ±7.8
7.5-15	9.2 ±8.2	8.3 ±5.4	2.5 ±3.4	4.1 ±1.3	8.0 ±7.4
15-30	5.0 ±2.3	1.7 ±1.6	5.8 ±3.0	16.3 ±5.7	9.3 ±5.6
30-45	9.9 ±9.4	4.6 ±1.8	1.4 ±2.5	37.8 ±34.3	3.7 ±1.1

Tab. 3.11 Fraction of new C in several soil aggregate fractions after 8 years of elevated [CO₂] +30% (plot E4)

Depth [cm]	LM	SM	Mic [%]	SC	Total
0-7.5	12.0	10.0	29.3	24.4	27.7
7.5-15	16.3	10.0	13.8	8.1	19.2
15-30	7.4	2.5	26.3	5.8	11.3
30-45	17.9	4.0	23.5	0.3	1.8

3.5.2 Input of new C

Plots E1-E3

In total for the whole soil profile (0-45 cm), the highest amount of new C was found in plot E2 (122 g C m⁻² yr⁻¹), followed by plot E1 (105 g C m⁻² yr⁻¹) and plot E3 (53 g C m⁻² yr⁻¹). No correlations ($p > 0.1$) were observed between the input of new C and aboveground biomass yield or soil moisture (linear regression analysis for 0-7.5 and 0-45 cm depth).

The average input of new C in the plots E1-E3 is presented separately for bulk soil and each soil aggregate fraction for each observation period (Tab. 3.12). Over the whole observation period, i.e. eight years of elevated [CO₂], the mean total soil C input into the top 45 cm was 93.5 g C m⁻² yr⁻¹. The highest total soil C input occurred in the top 7.5 cm but decreased with depth. Most of the new C was sequestered into the LM fraction (40.7 g m⁻² yr⁻¹), followed by the SM, Mic and SC fractions with 37.9, 10.5 and 4.4 g m⁻² yr⁻¹, respectively.

The total amount of new C and the amount of new C input to several aggregate fractions was different in the two observation periods. In the first observation period a similar amount of newly fixed C was sequestered into the LM and SM fractions. In the second observation period, however, the C input rate into the LM fraction was three times higher than into the SM fraction (Tab. 3.12). Significant differences between the two observation periods were also observed for the SM fraction (0-7.5 cm depth; $p = 0.043$), the Mic fraction (0-7.5 cm; $p = 0.023$ and 0-45 cm; $p = 0.093$), and the SC fraction (30-45 cm, $p = 0.092$, and 0-45 cm, $p = 0.076$).

Furthermore, in the first investigation period most of the newly fixed C was sequestered into the top 7.5 cm, whereas in the second investigation period the largest amount was sequestered into 7.5-15 cm depth (Tab. 3.12). The total soil C input rate was approximately 65 g m⁻² yr⁻¹ higher in the first observation period compared to the second observation period.

Tab. 3.12 Rate of annual C input in the two investigation periods (April 1998 to June 2004, and June 2004 to June 2006) for the plots E1-E3; values are presented as means \pm standard deviation (n = 3).

Period	Depth [cm]	LM	SM	Mic	SC	Total
		[g C m ⁻² yr ⁻¹]				
1998 to 2004	0-7.5	20.7 \pm 16.8	35.4 \pm 5.2	11.4 \pm 3.1	2.5 \pm 1.1	70.0 \pm 21.4
	7.5-15	5.4 \pm 5.5	5.3 \pm 8.3	0.7 \pm 1.1	0.1 \pm 0.1	11.5 \pm 14.4
	15-30	13.5 \pm 10.3	1.8 \pm 2.1	1.3 \pm 1.0	0.4 \pm 0.3	17.0 \pm 13.4
	30-45	5.0 \pm 3.0	4.9 \pm 3.1	0.4 \pm 0.7	0.2 \pm 0.3	10.6 \pm 6.7
	0-45	44.6 \pm 28.1	47.5 \pm 14.1	13.8 \pm 3.2	3.1 \pm 1.4	109.0 \pm 43.5
2004 to 2006	0-7.5	10.2 \pm 9.9	1.9 \pm 3.3	< 0.1	0.2 \pm 0.3	12.3 \pm 13.3
	7.5-15	14.8 \pm 15.0	5.6 \pm 1.6	< 0.1	0.2 \pm 0.1	20.6 \pm 14.8
	15-30	2.6 \pm 2.4	< 0.1	< 0.1	1.9 \pm 0.7	4.6 \pm 2.1
	30-45	0.7 \pm 1.1	< 0.1	< 0.1	6.3 \pm 5.9	6.9 \pm 6.8
	0-45	28.3 \pm 27.4	7.6 \pm 2.8	< 0.1	8.6 \pm 5.6	44.4 \pm 32.5

Plot E4

During eight years of elevated [CO₂] +30%, the mean soil C input into the soil profile corresponded to 80.7 g C m⁻² yr⁻¹, whereas the differences between the first and the second period were only marginal (Tab. 3.13). During the first observation period the highest C input occurred in 0-7.5 and 15-30 cm depth. The low input in 7.5-15 cm during the first period was counterbalanced by a high C input during the second observation period. Most of the new C was incorporated into the LM fraction, followed by the SM (first period) or the Mic (second period) fractions. During the second period nearly the 5-fold amount of C was sequestered in the Mic fraction compared to the first observation period.

Tab. 3.13 C input rates into various soil fractions under $[\text{CO}_2]$ +30% (plot E4) from April 1998 to June 2004 and from June 2004 to June 2006.

Period	Depth [cm]	LM	SM	Mic [g C m ⁻² yr ⁻¹]	SC	Total
1998 to 2004	0-7.5	12.2	16.6	4.2	2.1	35.2
	7.5-15	8.8	0.4	< 0.1	0.2	9.5
	15-30	29.3	1.5	1.1	0.4	32.3
	30-45	< 0.1	4.8	0.3	< 0.1	5.1
	0-45	50.3	23.4	5.6	2.8	82.1
2004 to 2006	0-7.5	2.9	5.3	2.7	< 0.1	10.9
	7.5-15	18.6	14.6	3.7	0.1	36.9
	15-30	< 0.1	< 0.1	9.3	0.1	9.4
	30-45	9.2	< 0.1	9.8	< 0.1	19.0
	0-45	30.7	19.8	25.4	0.3	76.2

Differences between $[\text{CO}_2]$ +20% and $[\text{CO}_2]$ +30%

Over the entire observation period the C_{new} input was similar under both $[\text{CO}_2]$ treatments, with 80.7 g C m⁻² yr⁻¹ ($[\text{CO}_2]$ +30%) and 93.5 g C m⁻² yr⁻¹ ($[\text{CO}_2]$ +20%), respectively. In both treatments, during the first observation period, the highest C input occurred in 0-7.5 and 15-30 cm depth. The lower C input in 7.5-15 cm was counterbalanced by a comparatively high C input during the second observation period into this depth. Comparable to the plots E1-E3, the largest C input in plot E4 occurred in the LM fraction (45.6 g C m⁻² yr⁻¹ between 1998 and 2006).

As shown in Tab. 3.12, a higher C input in the lower CO_2 -enriched plots E1-E3 occurred during the first observation period (in total 109 and 82 g C m⁻² yr⁻¹ for E1-E3 and E4, respectively), while in plot E4 a higher C input rate occurred during the second observation period (in total 44 and 76 g C m⁻² yr⁻¹ for E1-E3 and E4, respectively). In contrast to the plots E1-E3, during the second observation period, a considerable amount of C was sequestered into the Mic fraction of plot E4.

When examining the C input into the macroaggregate fractions, over the entire period a higher proportion of C was incorporated into the LM fraction (45 g m⁻² yr⁻¹), whereas under $[\text{CO}_2]$ +20% both macroaggregate fractions incorporated with 40.7 (LM) and 37.9 g m⁻² yr⁻¹ (SM) a similar amount of new C.

3.5.3 Input of new C into free and macroaggregate-associated microaggregates

This section focuses on the microaggregates associated with large or small macroaggregates. In April 1998 the $\delta^{13}\text{C}$ signature of free and macroaggregate-associated microaggregates was similar for E- and A-plots in both depths (i.e. -28.3‰ in 0-7.5 cm and -27.9‰ in 7.5-15 cm). After six years of elevated CO_2 the $\delta^{13}\text{C}$ signature was -28.9‰ for the free microaggregates and -28.5 and -29.0‰ for the LM- and SM-associated microaggregates in 0-7.5 cm. The depletion in ^{13}C was significant ($p < 0.05$, paired t-test) for the free microaggregates and the Mic-SM fraction but not for the Mic-LM fraction. In the next deeper soil layer, the signature decrease was with -28.1‰ , -27.9‰ , and -28.0‰ , no significant depletion occurred.

The percentage of newly sequestered C in the first observation period is given in Tab. 3.14. The largest $f\text{C}_{\text{new}}$ occurred in the free microaggregates, closely followed by the SM-associated microaggregates. In 0-7.5 cm $f\text{C}_{\text{new}}$ in the Mic-LM fraction was approximately a third of $f\text{C}_{\text{new}}$ found in free Mic and Mic-SM aggregates.

Tab. 3.14 Relative (percentage) fraction of new C in June 2004 in free and macroaggregate-associated microaggregates of the plots E1-E3; values are presented as means with the standard deviation separately for each depth.

Depth [cm]	Mic	Mic-LM [%]	Mic-SM
0-7.5	24.1 \pm 10.2	7.8 \pm 5.9	21.6 \pm 9.1
7.5-15	2.5 \pm 3.4	3.4 \pm 4.0	5.3 \pm 5.5

The newly sequestered C between April 1998 and June 2004 is given in Fig. 3.19. The highest amount of new C was sequestered into the small macroaggregate-associated microaggregates (Mic-SM), followed by the free microaggregates (Mic) and the large macroaggregate associated microaggregates (Mic-LM). Altogether a low amount of C was sequestered into the microaggregates in 7.5-15 cm depth.

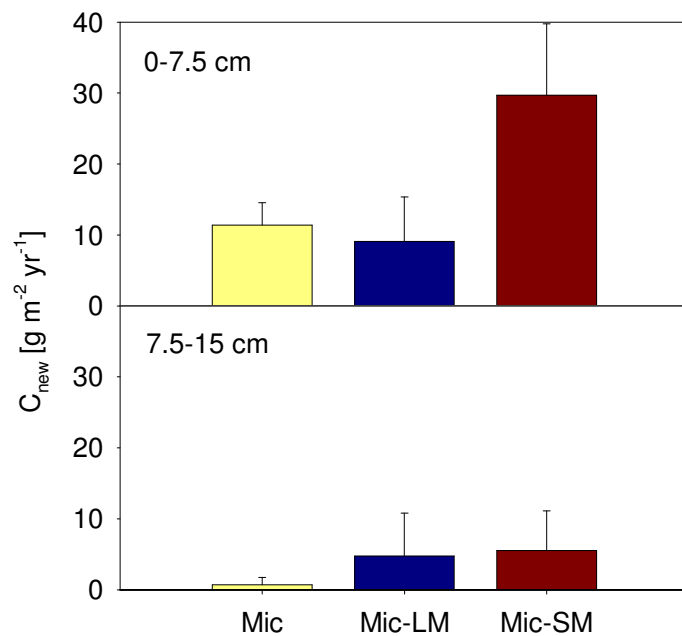


Fig. 3.19 Input of new C into free and macroaggregate-associated microaggregates between April 1998 and June 2004; values are presented as E1-E3 means \pm standard deviation ($n = 3$) separately for each depth.

3.6 Soil air CO₂ and ecosystem respiration

3.6.1 Annual dynamics of ecosystem respiration and $\delta^{13}\text{C}$ and CO₂ concentration in soil air

Ring pairs 1-3

The temporal dynamics of R_{eco} , of soil air [CO₂] and of the $\delta^{13}\text{C}$ signature were monitored between August 2004 and December 2006 (Fig. 3.20 - 3.21). The observation period was subdivided into the (1) growth period, defined here from 1st April until 1st September, and (2) the off-season period from 1st September until 1st April. In general, the temporal dynamics of R_{eco} , soil [CO₂] and $\delta^{13}\text{C}$ were synchronous for all plots in both depths.

R_{eco}

The R_{eco} rates showed clear annual dynamics with lowest values during the winter months November to February and a considerable increase in March. In contrast to soil [CO₂], where the highest concentrations were reached in May or June, the highest R_{eco} rates occurred during July and August with mean values up to 16.4 $\mu\text{mol CO}_2 \text{ m}^{-2} \text{ s}^{-1}$. Over the whole investigation period, the average R_{eco} rate was 4.5 and 3.9 $\mu\text{mol CO}_2 \text{ m}^{-2} \text{ s}^{-1}$ in E and A plots, respectively, i.e. a 13% increase under elevated CO₂. In the growth period the mean R_{eco} rates for E and A plots were 7.2 ± 0.9 and $6.6 \pm 0.3 \mu\text{mol CO}_2 \text{ m}^{-2} \text{ s}^{-1}$ (E = 108% of A), whereas in the non-growing period the mean values were only 2.7 ± 0.2 and $2.1 \pm 0.1 \mu\text{mol CO}_2 \text{ m}^{-2} \text{ s}^{-1}$ (E = 124% of A). Significant differences between E and A plots occurred mainly during the non-growing season mostly due to higher R_{eco} in the CO₂ enriched plots. In the year 2004 the E-plots showed higher R_{eco} rates than their corresponding A-plots in 35% of all measurements (all A > all E = 0%). In the years 2005 and 2006 R_{eco} was higher in 42% and 25% of all measurements in all E-plots (all A > all E: only 3% of all measurements in 2005 and 3.1% in 2006, respectively).

Soil [CO₂]

Within a few days in March the soil [CO₂] in the top 10 cm increased very fast from around 2500 ppm up to 10.000 ppm. The soil [CO₂] differed between the ring pairs, with highest concentrations up to 60.000 ppm occurring in the wettest plots A2 and E2 in May. Concentrations decreased with declining soil moisture down to values around 5000 ppm and 10.000 ppm in 5 and 10 cm depth, respectively. The harvest of the aboveground biomass had only minor effects on soil air [CO₂] ($p > 0.1$) with a slight decrease in soil air [CO₂] in 5 and 10 cm depth after the first harvest, based on measurements one day before and nine days after aboveground biomass removal. No significant differences between E- and A-plots were detected.

$\delta^{13}\text{C}$ signature of soil air CO_2

The mean $\delta^{13}\text{CO}_2$ signatures and the differences between E- and A-plots are presented in Tab. 3.15. A decrease of $\delta^{13}\text{CO}_2$ during the growth period occurred under both CO_2 treatments. The $\delta^{13}\text{C}$ signature in 5 and 10 cm depth was quite comparable over the whole investigation period (difference < 0.6‰), but for both CO_2 treatments it was in general slightly lower in 10 cm depth.

The $\delta^{13}\text{C}$ signature of soil air CO_2 under elevated CO_2 was, on average over the entire investigation period, depleted by $3.3 \pm 1.0\text{‰}$ (5 cm depth) and $3.2 \pm 0.9\text{‰}$ (10 cm depth) in comparison to soil air CO_2 from ambient plots. The difference in the $\delta^{13}\text{C}$ signature between E and A treatments was most pronounced during the summer period (3.7‰) and less pronounced during winter (2.8‰). Only in ring pair 2 between February and April 2005 were the $\delta^{13}\text{C}$ signatures of soil air CO_2 similar for both CO_2 treatments (Fig. 3.21).

Tab. 3.15 Mean $\delta^{13}\text{C}$ signature of soil air CO_2 in the ring pairs 1-3 in 5 and 10 cm depth between 2004 and 2006; numbers in brackets mark the number of measurements. Values are presented as the means \pm standard deviation ($n = 3$).

Plot	Depth [cm]	Growth period ($n = 13$)	Off-season ($n = 13$)	Entire period ($n = 26$)
		[‰]	[‰]	[‰]
E _{avg}	5	-27.5 \pm 2.9	-25.7 \pm 2.7	-26.5 \pm 2.3
	10	-27.7 \pm 2.5	-26.3 \pm 2.1	-27.0 \pm 2.0
A _{avg}	5	-23.8 \pm 1.9	-23.4 \pm 1.9	-23.6 \pm 1.7
	10	-24.1 \pm 1.7	-23.9 \pm 1.7	-24.0 \pm 1.5
E-A-diff	5	-3.7 \pm 1.4	-2.8 \pm 0.9	-3.3 \pm 1.0
	10	-3.6 \pm 1.0	-2.8 \pm 0.9	-3.2 \pm 0.9

The temporal dynamics of $\delta^{13}\text{CO}_2$ signature in soil air were synchronous under elevated and ambient CO_2 conditions in both depths (Fig. 3.20 – 3.22). The $\delta^{13}\text{C}$ signature reached the most negative values during the times of high soil $[\text{CO}_2]$. Values increased during the off-season. Six days after N-fertilization in April 2005, the $\delta^{13}\text{C}$ signature reached its lowest most negative values down to -32‰ (Fig. 3.23).

The removal of aboveground plant biomass had only a minor effect on the $\delta^{13}\text{C}$ signature of soil air CO_2 ($p > 0.1$), as indicated by the samples taken directly before and after the first harvest in the years 2005 and 2006 (Fig. 3.23).

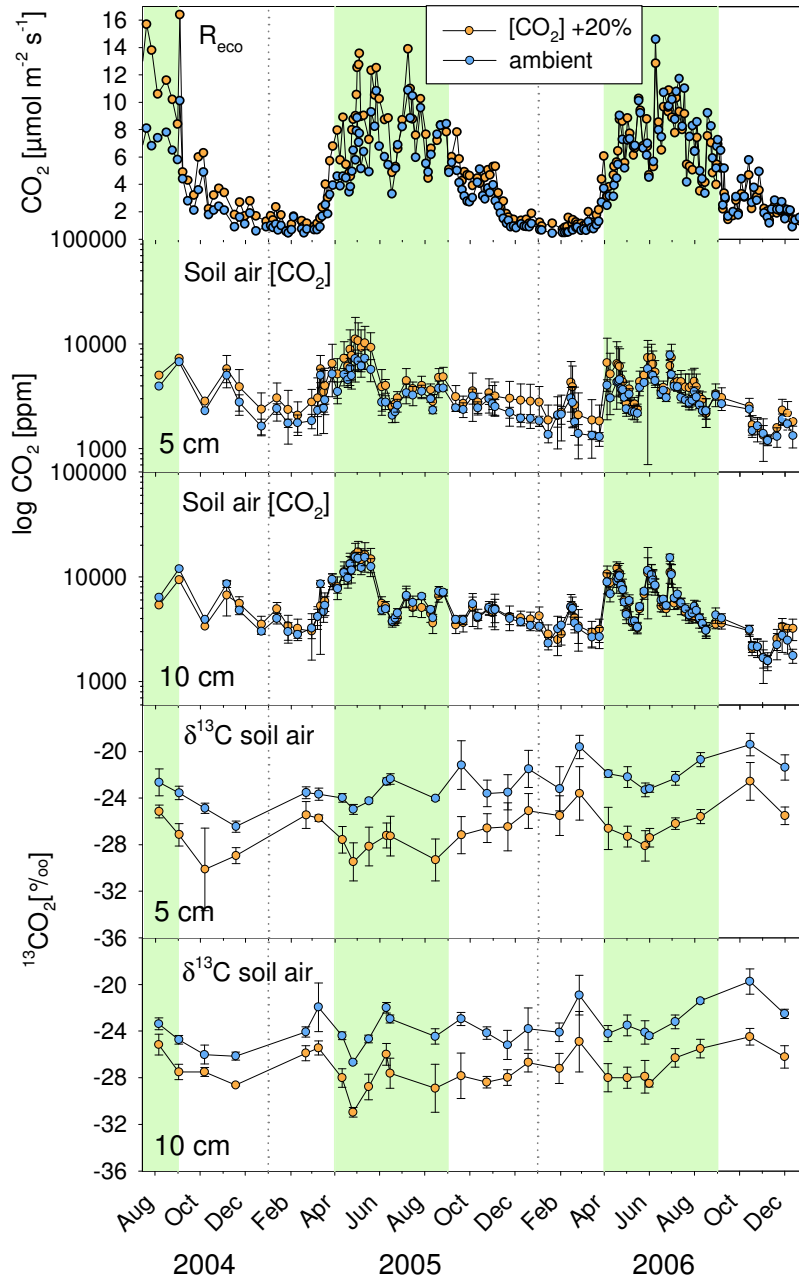


Fig. 3.20 Ecosystem respiration, soil air CO₂ concentration and δ¹³C signature of soil air CO₂ in ring pair 1 in 5 and 10 cm depth. Error bars mark the standard deviation (n = 4 soil air samplers per depth). Green shading roughly depicts the pre-defined growth period.

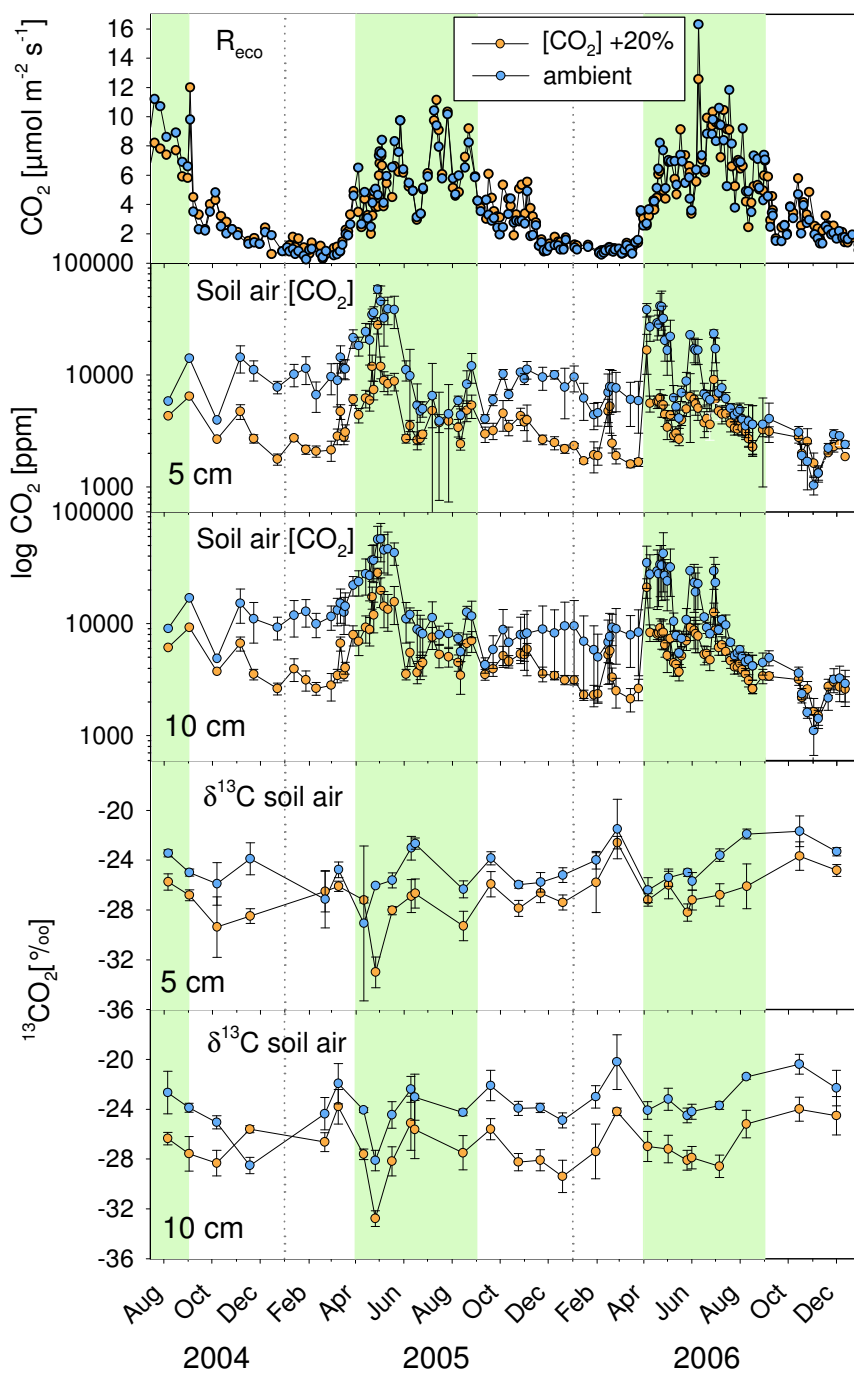


Fig. 3.21 Ecosystem respiration, soil air CO₂ concentration and δ¹³C signature of soil air CO₂ in ring pair 2 in 5 and 10 cm depth. Error bars mark the standard deviation (n = 4 soil air samplers per depth).

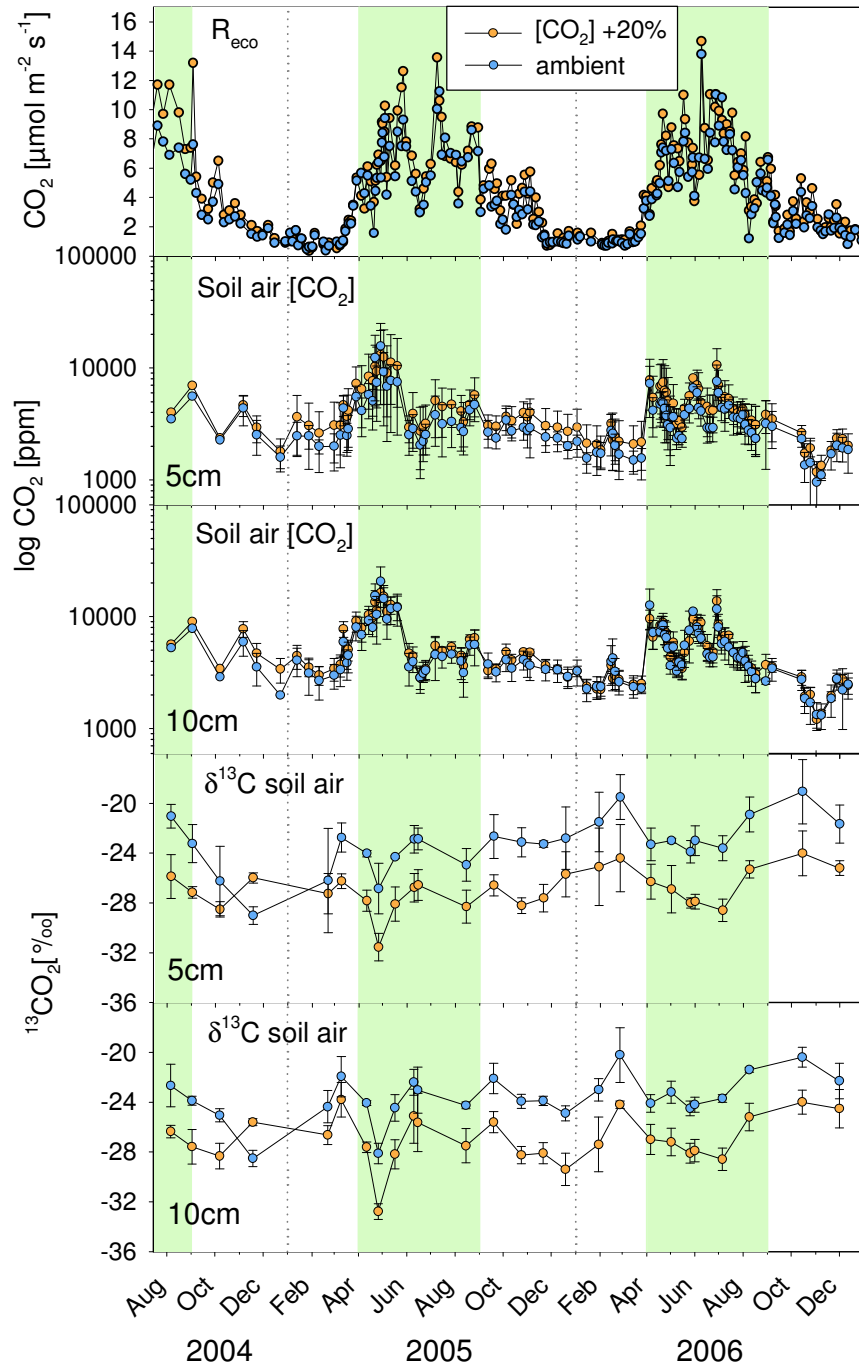


Fig. 3.22 Ecosystem respiration, soil air CO₂ concentration and δ¹³C signature of soil air CO₂ in ring pair 3 in 5 and 10 cm depth. Error bars mark the standard deviation (n = 4 soil air samplers per depth).

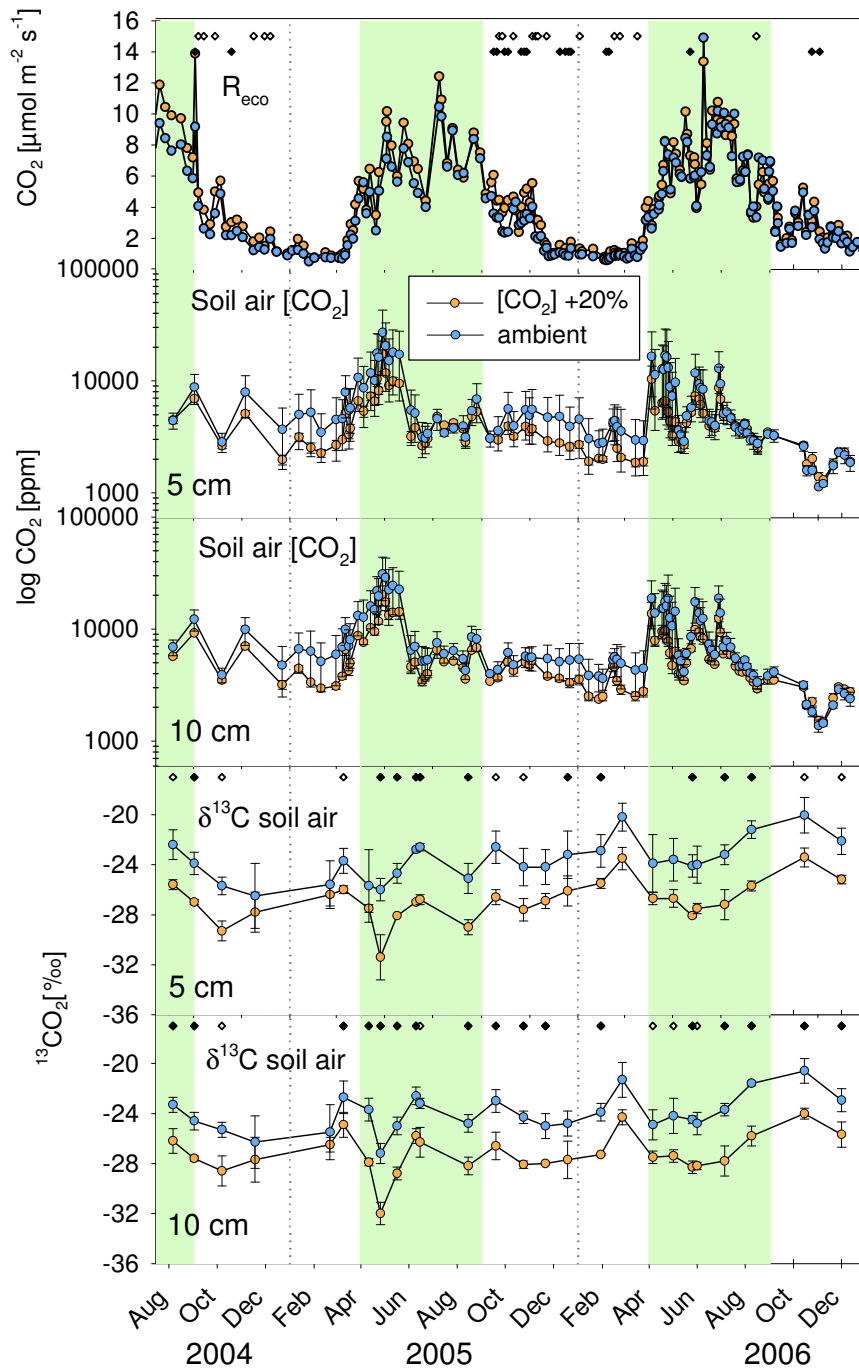


Fig. 3.23 Mean values of the ring pairs 1-3; diamonds mark significant differences between E and A plots (white: $p < 0.1$; black: $p < 0.05$; paired t-test); error bars mark the standard deviation ($n = 3$).

Ring pair 4

A more detailed observation of the $^{13}\text{CO}_2$ signature in soil air was carried out in the plots E4 and A4, where soil gas concentrations were measured down to 50 cm depth between October 2004 and December 2006 (Fig. 3.24, Tab. 3.16). The annual dynamics in $\delta^{13}\text{C}$ were similar to the ring pairs 1-3, but differences in $\delta^{13}\text{C}$ between plot E4 and the E1-E3 occurred in both 5 and 10 cm depth, with plot E4 having a 1‰ lower $\delta^{13}\text{C}$ signature than the plots E1-E3 (Fig. 3.23). The temporal dynamics in $\delta^{13}\text{C}$ raised and fell synchronous in the entire soil profile.

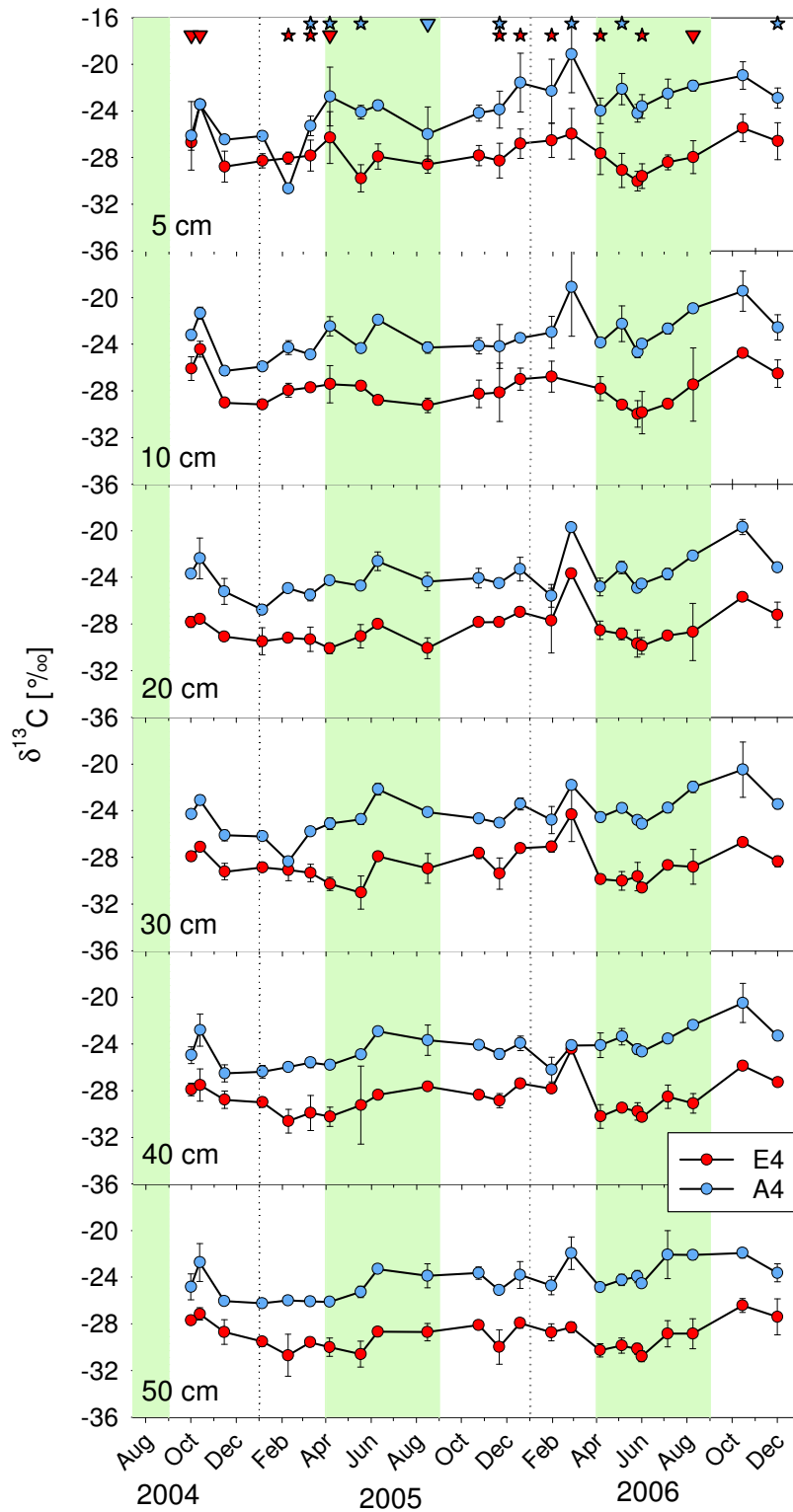


Fig. 3.24 $\delta^{13}\text{C}$ signature of soil air CO_2 monitored in the soil profile of plot E4 ($[\text{CO}_2]$ +30%) and plot A4 between October 2004 and December 2006; significant correlations of $\delta^{13}\text{C}$ with depth are marked by the symbols star ($p < 0.05$) and triangle ($p < 0.1$). Values are presented as the means for each plot, error bars mark the standard deviation $n = 4$ (5 cm), $n = 2$ (10-40 cm) and $n = 3$ (50 cm).

The mean signature differences between the plots E4 and A4 ranged between 3.8 and 4.8‰ (entire period), with higher E-A differences during the growth period (Tab. 3.16). In both CO₂ treatments the $\delta^{13}\text{C}$ signature became more negative with depth (Tab. 3.16). This decrease in $\delta^{13}\text{C}$ was more pronounced in plot E4 where the difference between 5 and 50 cm depth was 1.4‰. In plot A4 the $\delta^{13}\text{C}$ signature decline with depth was only 0.4‰. Over the entire period the impact of depth on $\delta^{13}\text{C}$ of soil air CO₂ was significant in both plots (E4: $p = 0.019$; A4: $p = 0.040$, linear regression analysis).

Tab. 3.16 $\delta^{13}\text{C}$ signature of soil air CO₂ in ring pair 4 are presented separately for each depth (observation period between October 2004 and December 2006); numbers in brackets mark the number of measurements. Values are presented as means over the respective time period \pm standard deviations, where $n = 4$ (5 cm); $n = 2$ (10 - 40 cm); and $n = 3$ (50 cm).

Plot	Depth [cm]	Growth period (n = 10)	Off-season (n = 13)	Entire period (n = 23)
		[‰]	[‰]	[‰]
E4	5	-28.5 \pm 1.1	-27.0 \pm 1.5	-27.6 \pm 1.5
	10	-28.6 \pm 1.0	-27.2 \pm 1.5	-27.8 \pm 1.5
	20	-29.2 \pm 0.7	-27.7 \pm 1.6	-28.3 \pm 1.5
	30	-29.6 \pm 1.0	-27.9 \pm 1.4	-28.6 \pm 1.5
	40	-29.3 \pm 0.9	-28.0 \pm 1.6	-28.6 \pm 1.5
	50	-29.7 \pm 0.8	-28.5 \pm 1.2	-29.0 \pm 1.2
A4	5	-23.5 \pm 1.2	-24.1 \pm 2.9	-23.8 \pm 2.3
	10	-23.1 \pm 1.3	-23.2 \pm 2.2	-23.2 \pm 1.8
	20	-23.9 \pm 1.0	-23.7 \pm 2.1	-23.8 \pm 1.7
	30	-24.0 \pm 1.1	-24.4 \pm 2.0	-24.2 \pm 1.7
	40	-24.0 \pm 1.0	-24.6 \pm 1.7	-24.3 \pm 1.5
	50	-24.0 \pm 1.3	-24.4 \pm 1.5	-24.2 \pm 1.4
E - A	5	-5.1 \pm 1.4	-2.9 \pm 2.5	-3.8 \pm 2.3
	10	-5.5 \pm 1.3	-3.6 \pm 0.7	-4.5 \pm 1.4
	20	-5.3 \pm 0.8	-3.9 \pm 1.0	-4.5 \pm 1.1
	30	-5.6 \pm 0.7	-3.4 \pm 1.3	-4.4 \pm 1.5
	40	-5.3 \pm 0.9	-3.4 \pm 1.4	-4.2 \pm 1.5
	50	-5.6 \pm 0.9	-4.1 \pm 1.0	-4.8 \pm 1.2
	mean	-5.4 \pm 0.7	-3.6 \pm 0.8	-4.4 \pm 1.2

The magnitude of the $\delta^{13}\text{C}$ decrease with depth showed clear annual dynamics that were strongly correlated with soil temperature (plot E4: $p = 0.001$; plot A4: $p = 0.009$) (Fig. 3.25). More negative slopes indicate a stronger decrease in $\delta^{13}\text{C}$ with depth. During the growth period the $\delta^{13}\text{C}$ signature gradient was less pronounced than during the winter period. No correlations with the soil moisture content were found ($p > 0.05$).

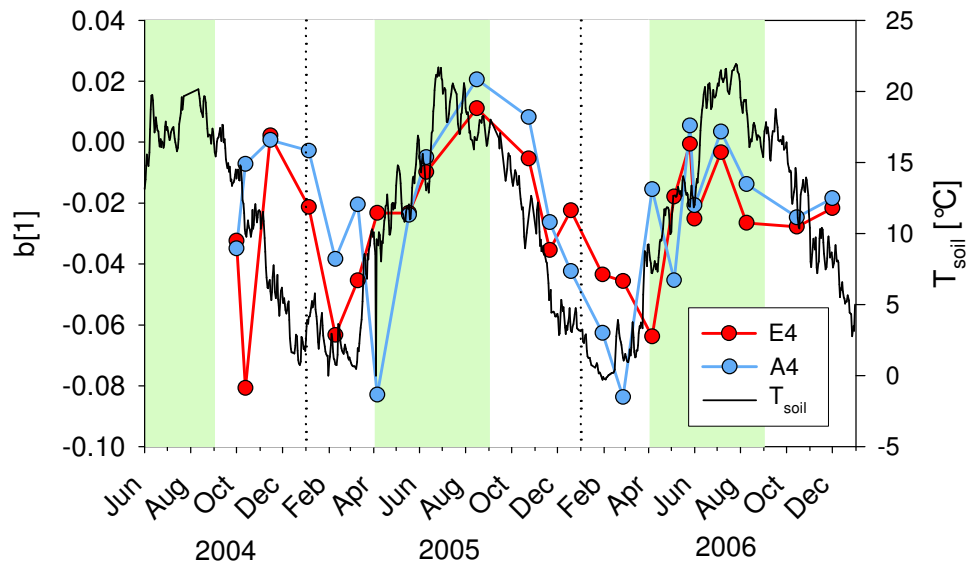


Fig. 3.25 Correlation between soil depth dependent decrease in $\delta^{13}\text{CO}_2$, indicated by the slope $b[1]$ of the linear regression analyses (5 to 50 cm depth; $n = 15$ per E-, respective A-plot), and soil temperature (T_{soil} , 10 cm depth). The slope $b[1]$ refers to the entire soil profile.

3.6.2 Partitioning of R_{soil} into autotrophic and heterotrophic components

The partitioning was based on the assumptions that the soil CO_2 originates to a certain amount from (1) recently fixed carbon with a $\delta^{13}\text{C}$ signature close to leaf biomass and (2) mineralization of old carbon having a $\delta^{13}\text{C}$ signature close to SOC. The fractions of R_{root} and R_{soil} were calculated via a two component mixing model (Eqn. 10) where the signature for R_{soil} was derived from SOC and for R_{root} the $\delta^{13}\text{C}$ signature was derived from leaves. Consequently, it is expected that the $\delta^{13}\text{CO}_2$ signature is in the range between $\delta^{13}\text{C}$ of plant leaves and SOC. In the E-plots $\delta^{13}\text{C}$ between soil (-28.2‰) and leaves (-35.1‰) differed on average about 6.9‰ (0-7.5 cm), whereas in the A-plots this difference was only 1.1‰ (avg. A1-3 in 0-7.5 cm). Therefore, the use of the two-component mixing model was not an appropriate tool to calculate the contribution of R_{root} on R_{soil} under ambient conditions. In plot E4 the $\delta^{13}\text{C}$ signature difference between SOC and plant leaves was about 9.7‰.

Equation 10 was applied to 611 samples (plots E1-E3). In 63 cases (10%), the $\delta^{13}\text{CO}_2$ signature was not in the range between the $\delta^{13}\text{C}$ signature of leaves and SOC. From E4 328 soil gas samples were used of which in 8 samples (2%) the $\delta^{13}\text{C}$ signature was not between the $\delta^{13}\text{C}$ signature of leaves and SOC. Those samples were excluded from the results.

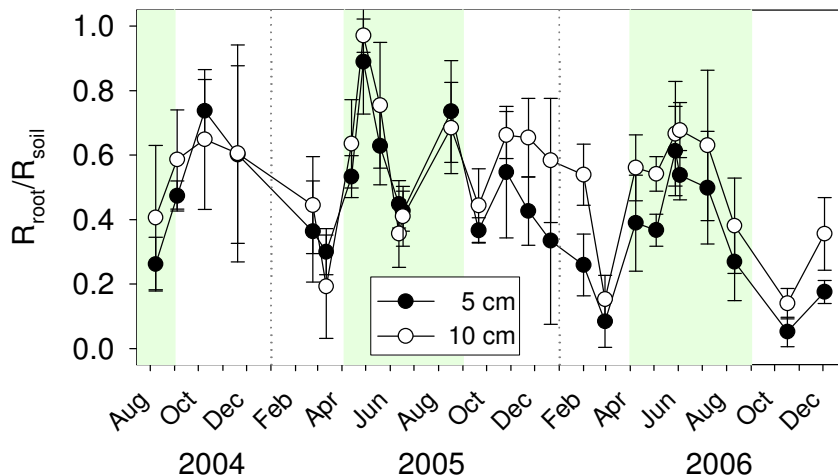


Fig. 3.26 Relative contribution of R_{root} on R_{soil} over time in 5 and 10 cm in plots E1-E3 (means \pm standard deviation; $n = 3$).

The temporal dynamics of R_{root} as part of R_{soil} (Fig. 3.26) were similar in 5 and 10 cm depth. In general, R_{root} was highest at the beginning of the growth period. Also, at the beginning of the off-season, a (less pronounced) increase was observed, followed by a decrease until the beginning of the next growth period. During the off-season 2005/2006 a higher contribution of R_{root} took place in 10 cm compared to 5 cm depth than in 2004/2005. However, in June 2005 an unexpected decrease

occurred, which differed to the course observed in 2006, where R_{root} reached its maximum in June (Fig. 3.26).

The mean values of R_{root} for the growth season and the off-season in the top 15 cm depth are presented for the plots E1-E3 and plot E4 (Tab. 3.17). In the three moderate [+20%] CO_2 -enriched plots as well as in plot E4 [+30%], a higher contribution of R_{root} was observed during the growth period in both depths (Tab. 3.17). In plot E4 the contribution of R_{root} was lower than in the plots E1-E3 with a mean difference of 10% (5 cm) and 14% (10 cm) over the entire period. The differences between the growth and off-season were only marginally significant ($p = 0.062$ for 5 cm depth and $p = 0.087$ for 10 cm depth, independent t-test).

Tab. 3.17 Contribution of R_{root} to R_{soil} [%] in the growth and off-season and over the whole investigation period in plots E1-E3 ($n = 3$) and plot E4 ($n = 1$).

Plot	Depth [cm]	Growth period	Off-season	Entire period
E1-E3	5	51 ±18	36 ±20	44 ±20
	10	59 ±17	46 ±19	53 ±19
E4	5	42 ±11	27 ±13	34 ±14
	10	47 ±09	33 ±15	39 ±14

R_{root} in the soil profile of plot E4

The contribution to R_{root} on R_{soil} increased with depth. Over the entire observation period this effect was significant at 15 sampling times ($p = 0.002$; 7 times during the growth period ($p = 0.007$) and 8 times during the off-season ($p = 0.002$), linear regression analysis, Fig. 3.28). The average contribution of R_{root} in plot E4 ranged from 37 ±9% in 5 cm up to 56 ±10% in 50 cm depth (Fig. 3.27).

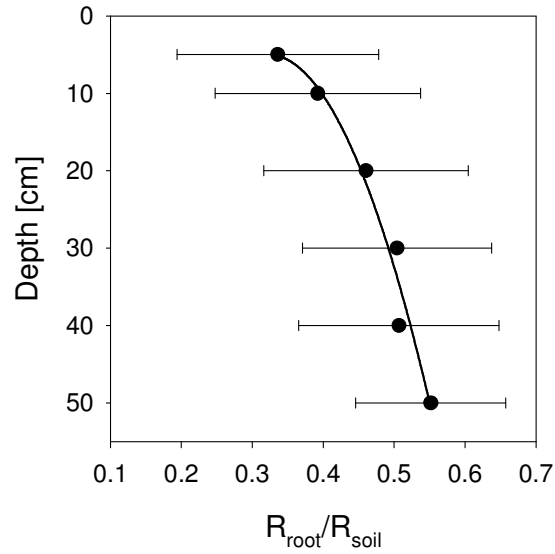


Fig. 3.27 Relative contribution of R_{root} to R_{soil} in varying soil depths in plot E4 over the entire investigation period; error bars mark the (temporal) standard deviation. The applied function was a quadratic regression ($f(x) = ax^2+bx+c$; r^2 : 0.97 where a, b and c had the following values: 94.0, 553.8, 861.5).

The dynamics of R_{root} in plot E4 (Fig. 3.28) were close to the observations made in the moderate CO_2 enriched plots 1-3 (Fig. 3.26). Comparable dynamics in R_{root} occurred in all soil depths, although the fluctuations were less pronounced in the deeper soil layers. In February 2006 a decrease in R_{root} was observed, which was found only in the depths 20, 30 and 40 cm (Fig. 3.28).

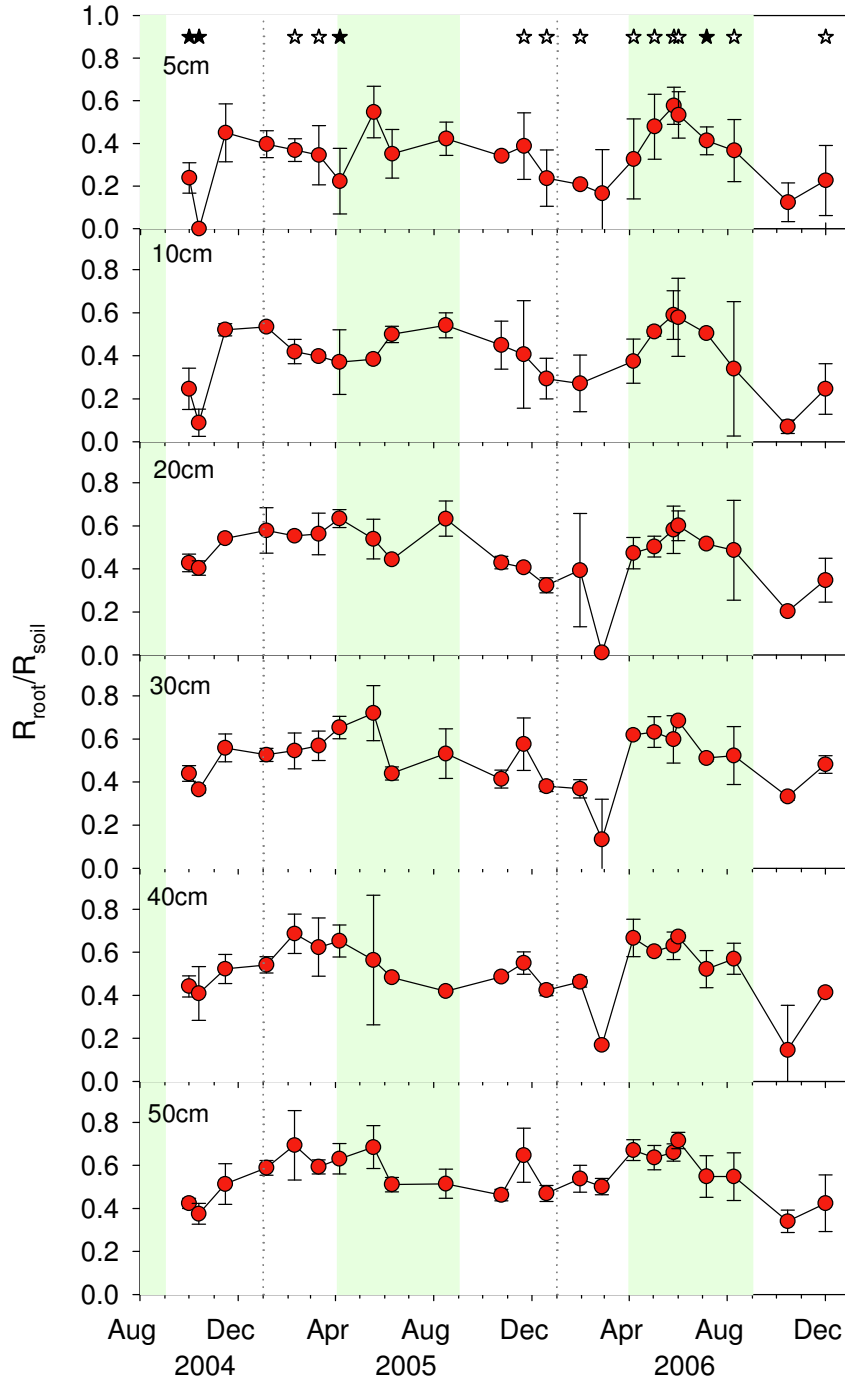


Fig. 3.28 Relative contribution of R_{root} on R_{soil} in the soil profile of plot E4 ($[\text{CO}_2 + 30\%$), a significant impact of depth on R_{root} is marked by white ($p < 0.05$) or black ($p < 0.1$) stars. Values are presented as means for each depth, error bars mark the standard deviation ($n = 4$ (5 cm), $n = 2$ (10-40 cm), and $n = 3$ (50 cm)).

3.6.3 Partitioning of R_{eco}

Keeling plot analysis

The Keeling-plot method (Keeling 1958) was used to determine the $\delta^{13}\text{C}$ signature of the CO_2 source of ecosystem respired CO_2 via linear regression analysis (see section 2.4.3).

Based on the Keeling-plot method the average source $\delta^{13}\text{C}$ signature of the CO_2 originating from R_{eco} was -28.3 and -25.7‰ for E- and A-plots, respectively, over the entire investigation period. Differences in source $\delta^{13}\text{C}$ between growth period and off-season were larger in the CO_2 -enriched plots (Tab. 3.18). The mean $\delta^{13}\text{C}$ signature difference between E- and A-plots was -2.6‰ . The source signature difference between E and A was slightly higher during the growth period (-2.7‰) than during the off-season (-2.5‰ , Tab. 3.18).

Tab. 3.18 The mean $\delta^{13}\text{C}$ signature of the CO_2 source of R_{eco} is presented separately for the plots E1-E3 and A1-A3.

Plot	Growth period	Off-season	Whole period
	[‰]		
E1-E3	-29.0 ± 3.7	-27.5 ± 3.1	-28.3 ± 3.4
A1-A3	-26.3 ± 1.5	-25.0 ± 5.3	-25.7 ± 3.7
E - A	-2.7 ± 4.2	-2.5 ± 5.3	-2.6 ± 4.6

The annual course (temporal dynamics) in $\delta^{13}\text{C}$ of the CO_2 source of R_{eco} was similar for E- and A-plots, although the oscillation was more pronounced in the CO_2 -enriched plots (Fig. 3.29 a). The annual dynamics showed an increase in $\delta^{13}\text{C}$ within the off-season for both, E- and A-plots, whereas the source signature decreased towards the beginning of the growth period. In 2005 a slight increase in $\delta^{13}\text{C}$ was observed for both CO_2 treatments within the growth period (Fig. 3.29).

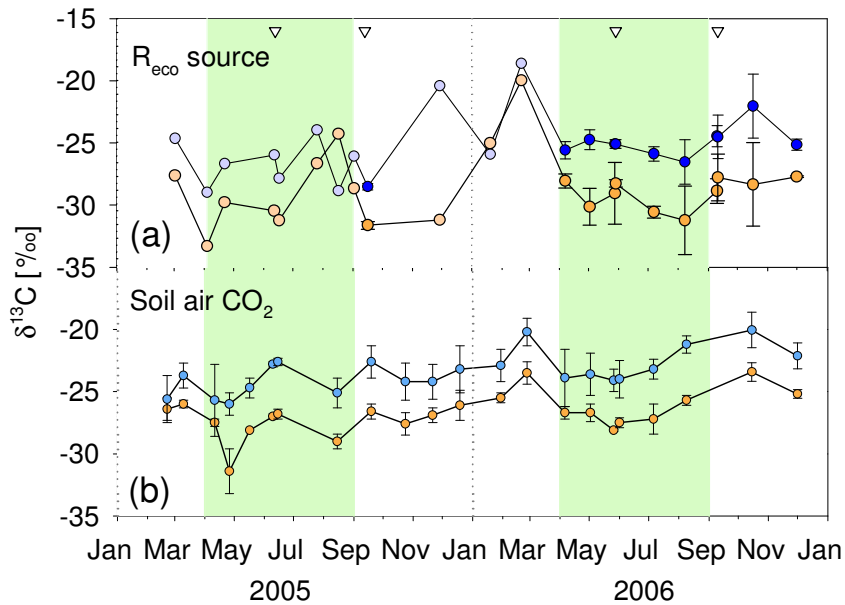


Fig. 3.29 $\delta^{13}\text{C}$ signature of the CO_2 source (a) of ecosystem respiration and (b) of soil air CO_2 in 5 cm depth in a temperate grassland ecosystem under elevated $[\text{CO}_2]$ +20% (orange) and ambient (blue) CO_2 . Pale colors mark the measurements where only one sample per chamber was taken (no calculation of standard deviation possible, see methods); dark colors mark the measurements with three or more samples per chamber. Times of aboveground biomass clipping are indicated by triangles.

At the beginning of the experiment the Keeling-plot analysis was not applied separately to the samples taken in each plot ($n = 3$) but to all samples collected in all E- and A-plots ($n = 9$), respectively, thereby it was not possible to calculate a mean value \pm standard deviation for A- and E-plots (Fig. 3.29 a). The effect of aboveground biomass clipping on $\delta^{13}\text{C}$ of both R_{eco} and soil air CO_2 was not significant. The $\delta^{13}\text{C}$ signature of the CO_2 source of R_{eco} closely followed the dynamics of the $\delta^{13}\text{C}$ signature of soil air CO_2 (Fig. 3.29 b), although the dynamics in $\delta^{13}\text{C}$ of R_{eco} were more pronounced.

Partitioning into autotrophic and heterotrophic respiration

The relative contribution of plant derived CO₂ (f_{plant}) to R_{eco} , calculated via a two-component mixing model, is presented in Tab. 3.19. For the entire period f_{plant} was 22% of R_{eco} . f_{plant} was three times higher during the growth period than during the off-season. The contribution of f_{plant} to R_{eco} was with 22% only half of f_{root} which contributed approximately to 50% to R_{soil} (see section 3.6.2).

Tab. 3.19 Relative contribution of autotrophic respiration to R_{eco} under elevated [CO₂] +20%.

Growth period	Off-season	Whole period
[%]		
31 ±25	11 ±17	22 ±24

Partitioning into above and belowground respiration

The relative contribution of aboveground respiration (f_{leaf}) to R_{eco} over time is presented in Fig. 3.30. On average for the whole investigation period f_{leaf} corresponded to 32% ±23 of R_{eco} . The contribution was higher during the growth period (34% ±27) than during the off-season (30% ±19). Values for f_{leaf} ranged between 0 and 0.8. At four times, the contribution of aboveground respiration to R_{eco} was zero. Furthermore, aboveground biomass clipping did not lead to a marked decrease in f_{leaf} except for the second harvest in the year 2006 (Fig. 3.30).

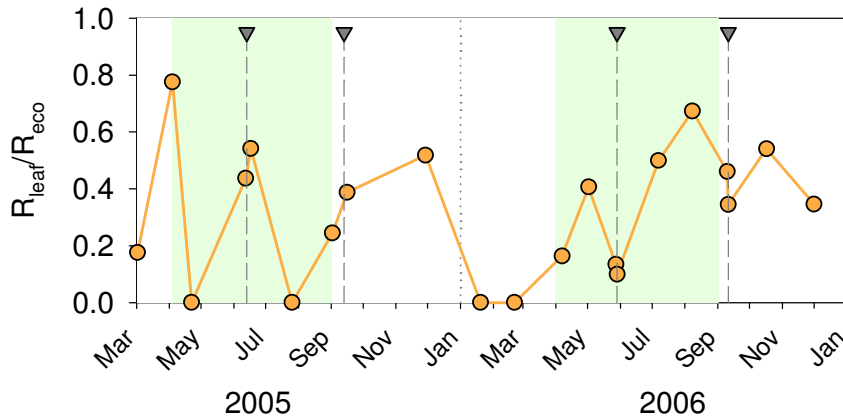


Fig. 3.30 Relative contribution of aboveground respiration to total ecosystem respiration under elevated [CO₂] +20% between March 2005 and December 2006, triangles mark the harvest of aboveground biomass.

Relative contribution of respiratory components to R_{eco}

The relative contributions of R_{leaf} , R_{root} and R_{bulk} to R_{eco} are shown in Fig. 3.31. On average for the entire period the relative contributions of R_{bulk} and R_{plant} to R_{eco} were $38 \pm 20\%$ and $62 \pm 20\%$, respectively. The highest contribution of R_{bulk} (92%) occurred in February 2006, whereas for the rest of the year the contribution of R_{plant} to R_{eco} was higher than the fraction of R_{bulk} . The mean contributions of R_{root} and R_{leaf} to R_{eco} were with $29 \pm 18\%$ and $32 \pm 23\%$ very similar (Fig. 3.31).

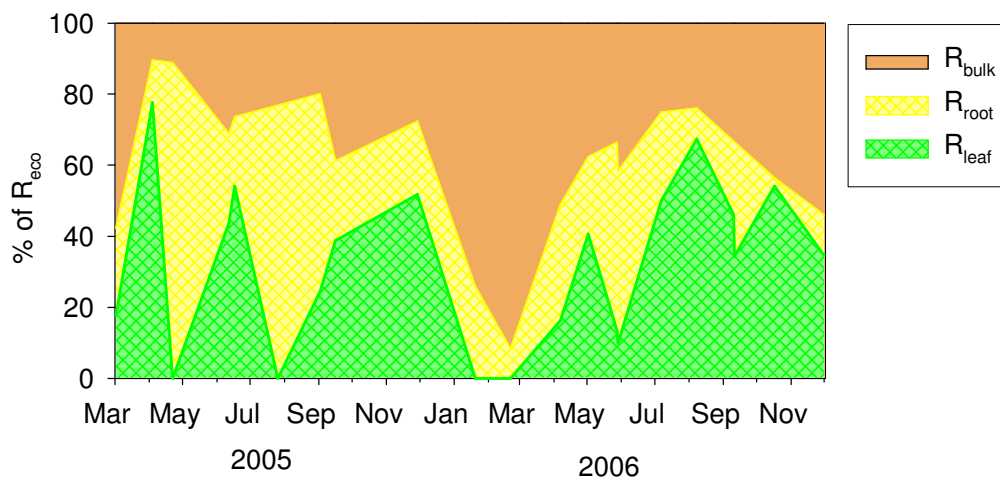


Fig. 3.31 Mean contribution of R_{leaf} , R_{root} and R_{bulk} to R_{eco} between March 2005 and December 2006 under elevated $[\text{CO}_2] + 20\%$ ($n = 3$).

4 Discussion

4.1 Effects of elevated CO₂ on the soil aggregate structure

The soil aggregate structure affects the soil C content because aggregate-associated organic matter is better protected against mineralization than free organic substances. Therefore, changes in soil aggregation will affect the mineralization rates of organic matter and therefore the soil C content.

Distribution of aggregates in the soil profile

The varying content of large macroaggregates in the soil profile (Fig. 3.6) is most likely due to disturbance by strong fluctuations in soil moisture, to a high root turnover (upper soil layers), and to changes in soil texture (i.e. a coherent increase in sand content with depth, which is in line with the finding that the amount of large macroaggregates is negatively correlated with sand content (De Gryze et al. 2006)). Furthermore, with increasing bulk density so-called physicogenic aggregates rise. These are aggregates that are held together by physical or chemical forces instead of organic binding agents (Dexter 1988). A decrease in SOC content on a per-aggregate basis, caused by the decrease in organic binding agents (Fig. 3.5), indicates the presence of physicogenic aggregates. For the Giessen-FACE site the SOC content of LM in 30-45 cm depth was only 13 to 30% of the LM-SOC content in 0-7.5 cm, showing that LM at depth are bound together not so much by organic matter than by physicogenic forces. A possible CO₂ effect can only be expected for biogenic aggregates, i.e. aggregates that are kept together by organic binding agents (Tisdall and Oades 1982), as elevated CO₂ does not affect bulk density or the mineral composition. Since below 15 cm depth the physicogenic aggregates dominated, no effect of elevated CO₂ on the aggregate structure in deeper soil layers can be expected.

Effects of elevated CO₂ on soil aggregation

In this study nine years of elevated CO₂ did not lead to a significant increase in soil aggregation in any depth (Fig. 3.8). However, similar experiments led to inconsistent results. Several studies reported an increase in soil aggregation (Rillig et al. 1999; Six et al. 2001), whereas other studies found no changes (Eviner and Chapin III 2002) or even a decrease in soil aggregation under elevated CO₂ (Niklaus et al. 2003). Reasons for the different results are manifold, leading from differences in CO₂ enrichment and ecosystem to the different initial conditions.

For a rise in soil aggregation the abundance of macroaggregate binding agents, i.e. roots and fungal hyphae (Tisdall and Oades 1982), must increase. The absence of increased soil aggregation is in line with the absence of a CO₂-induced increase in

root biomass at that time. However, in plot E4, where root biomass was increased up to 65% also no increase in aggregation was observed compared to the ring pairs 1-3. Unfortunately no data of E4 were available for the year 1998, so it is not possible to draw final conclusions. Apart from roots fungal-derived binding agents are important. It is well known that elevated CO₂ may alter the microbial community structure (Carney et al. 2007). Glomalin, a glycoprotein that is produced by arbuscular fungi, can be used as an indicator for fungal biomass (Lovelock et al. 2004). Wright and Upadhyaya (1998) found that the aggregate stability was linearly correlated to the glomalin content of soil. Glomalin content and macroaggregate abundance were found to increase under elevated CO₂, indicating that fungi caused the CO₂-induced increase in soil aggregation (Rillig et al. 1999). For the Giessen-FACE site there is evidence for an enhanced fungal rhizodeposit-C assimilation by arbuscular mycorrhizal fungi under [CO₂] +30% (Denef et al. 2007), but for the moderate CO₂-enriched plots no investigations were made with respect to this topic.

Because of the physical protection of organic matter within soil aggregates, an increase in soil aggregation is thought to be crucial for an increased soil C sequestration under elevated CO₂ (Jastrow 1996; Six et al. 2000). The absence of a CO₂ induced increase in soil aggregation indicates no better stabilization of organic matter under elevated CO₂. Thus, it is unlikely that elevated CO₂ will lead to an increased soil C sequestration in the Giessen-FACE grassland.

Changes in soil aggregation over time

Between 1998 and 2004 the content of large macroaggregates decreased under ambient and elevated CO₂, with no significant differences between both CO₂ treatments (Tab. 3.6). Elevated CO₂ did therefore not reduce the macroaggregate breakup. It is difficult to verify the reason for this loss in soil aggregation, which could either be caused by physical forces, e.g. freezing-thawing cycles (FTC) or drying-wetting cycles (DWC), or by a decrease of binding agents. A reduction of binding agents could either have been caused by a decreased build up or a faster mineralization of roots and fungal hyphae, maybe caused by the higher temperatures (Tab. 3.1).

FTC, in particular in wet soil (Six et al. 2004), or DWC (Adu and Oades 1978) lead to a breakup of macroaggregates. Oztas and Fayetorbay (2003) showed that freezing and thawing decreased aggregate stability, but the magnitude depended on soil type, aggregate size and stability, soil moisture and the number of FTC. For the research site, between 1998 and 2005 only two FTC were observed, where the soil temperature was below 0°C in 5 cm depth. The two FTC took place in January 2000 and February 2003. Before the start of the CO₂ enrichment in 1996/1997 a strong winter caused soil freezing down to 20 cm depth, with high N₂O emissions during freeze-thaw periods (Kammann et al. 1998). Possibly this pronounced freeze-thaw event marked the start of the decrease in soil aggregation in the following years. However, as no field data on the effect of FTC or DWC on soil aggregation are

available in the literature, it is hardly possible to estimate the duration or the magnitude of the effect on soil aggregate structure at the Giessen-FACE site.

After rewetting of dry soil water causes a slaking effect, a disruption of aggregates due to air pushed out of aggregates by incoming water. Studies that focus on the effect of DWC on aggregate breakup are mainly lab-based. In laboratory experiments the soil moisture decreased down to 1-2% before rewetting (Denef et al. 2001), whereas at the Giessen-FACE site even during drought summers (1997, 2003) the soil moisture never was below 10%. Therefore, it is difficult to estimate the effect of DWC on soil aggregate structure in the field. Here, a fast rewetting of dry aggregates caused by a heavy rainfall event is required after dry periods with low soil moisture to cause the aggregate breakup. To estimate DWC in the field, soil moisture below 20% was defined as "drought". In the years 1998, 1999, 2001 and 2003 the soil moisture dropped below 20% in midsummer, followed by sudden increases in soil moisture (Fig. 7.1). Prior to 1998 soil moisture data were only available for the year 1997 where, following a cold winter, a drought occurred during midsummer that persisted even longer than the drought in 2003. Therefore, DWC could be responsible for the disruption of macroaggregates in the field, although to my knowledge no studies are available that focus on the duration of these disturbances in the field. Perhaps the combination of the extreme cold during winter 1996/1997 followed by an exceedingly hot and dry summer initiated the breakup of large macroaggregates in the following years.

Furthermore, the amount or the kind or quality of binding agents could be responsible for the LM breakup. In a parallel study at the Giessen-FACE site, Janze (2006) observed a decline of plant biodiversity between 1998 and 2005 under both CO₂ treatments. The mean decline was lower under elevated CO₂ (from 16.2 to 11.2 species) than under ambient CO₂ conditions (from 18.2 to 10.3 species). A CO₂-induced species shift has also been observed in calcareous grassland (Leadley et al. 1999). The disappearance of plant species from native grasslands was found to reduce the size of earthworm communities (Zaller and Arnone 1999). Earthworm activity increases soil structure stability and soil C and N storage in large water stable aggregates (Ketterings et al. 1997). Therefore, the decrease in plant species might have contributed to the observed breakup of aggregates. But until now no investigation with respect to the earthworm population was carried out at the Giessen-FACE site.

Samples taken between 1997 and 2003 (data not shown) indicate a decrease in root biomass from $639 \pm 39 \text{ g m}^{-2}$ to $325 \pm 12 \text{ g m}^{-2}$ (A plots) and $595 \pm 79 \text{ g m}^{-2}$ to $407 \pm 12 \text{ g m}^{-2}$ (E plots) in the Ah-horizon (0-12 cm) (personal communication Kammann, 2007), thereby reducing the amount of macroaggregate-binding agents. As soil warming increases the death rates of roots (Fitter et al. 1999), the observed temperature increase may have contributed to the decrease in root biomass and thereby the breakup of LM.

Another important aspect are changes in the soil microbial community structure, in particular the abundance of fungi that are known to alter the soil structure (Treseder 2005). Changes in microbial community composition might have taken place either due to the observed temperature increase or changes in plant species composition (Chung et al. 2007). It is known that microbial community shifts may be caused by freezing stress and the competition for FTC induced substrate release (Feng et al. 2007). Finally, the reason for the C loss cannot certainly be clarified, and an interaction of several factors is possible.

4.2 Effects of elevated CO₂ on the soil C content

In this study, 9 years of elevated CO₂ did not lead to an increase in the soil C pool in any soil aggregate fraction (Fig. 3.13, Fig. 3.15). In Tab. 4.1 all published in situ studies on the effect of CO₂ enrichment on grassland soil C pools are summarized. The experimental setups differ widely between the experiments, ranging from tallgrass prairie in open top chambers to natural CO₂ springs. Comparable studies in grassland ecosystems showed inconsistent results (Tab. 4.1). The partly contradictory findings could to some extent be due to the degree of CO₂ enrichment, vegetation, fertilization, climatic conditions, soil type etc. and in particular the age of the ecosystem (late vs. early-successional studies). Only for the tallgrass prairie and the natural CO₂ spring a significant CO₂-induced increase in soil C stocks was reported. This is in contrast to the results of the meta-analysis of Luo et al. (2006) who reported a CO₂-induced accumulation of C and N in terrestrial ecosystems. For the meta-analytical analysis of the soil C pool only 14 studies were taken into account, whereof five studies were carried out in forests, two in agro-ecosystems and seven in grassland ecosystems (three in the same FACE-experiment, i.e. five different experiments for grassland were taken into account). The different result between the meta-analysis (Luo et al. 2006) and the single studies (Hungate et al. 1997; Jastrow et al. 2000; van Kessel et al. 2000; Niklaus et al. 2001; Six et al. 2001; Gill et al. 2002; van Groenigen et al. 2002) are likely due to the increased statistical power of the meta-analysis to detect small changes in C and N processes under elevated CO₂.

Tab. 4.1 Reported effects of elevated CO₂ on soil C stocks of in-situ CO₂ enrichment experiments on grassland ecosystems.

Vegetation	CO ₂ [ppm]	Duration [yr]	Δ SOC	System	Reference
Tallgrass Prairie	720	8	+	OTC	(Jastrow et al. 2000)
Calcareous grassland	600	6	No increase	FACE	(Niklaus et al. 2001)
Seeded grassland	600	10	No increase	FACE	(van Kessel et al. 2006)
Annual grassland	720	3	No increase	OTC	(Hungate et al. 1997)
Grassland	200- 550	4	No increase	EC	(Gill et al. 2002)
Grassland	370 - 2450	> Several decades	+	Natural spring	(Kool et al. 2007)

+ CO₂-induced increase in SOC; OTC: open top chamber, EC: elongated chamber, FACE: free air CO₂ enrichment

The soil C pool increase reported for the tallgrass prairie was at least partly due to the increase in root biomass and POM, which were included in the calculation of the soil C pool (Jastrow et al. 2000). However, root residues and POM can quickly be mineralized and do not represent a long-term storage pool. In the cold natural CO₂ spring at Hakanoa Springs, New Zealand, where soil samples were taken along a CO₂ gradient, an increase in soil C content and soil aggregation took place with increasing atmospheric CO₂ (Kool et al. 2007).

In all other studies no net increase in soil C stocks occurred (Hungate et al. 1997; Niklaus et al. 2001; Gill et al. 2002; van Kessel et al. 2006). Hungate et al. (1997) found an increase in carbon cycling under elevated CO₂ due to an increased C partitioning towards rapidly cycling C soil pools. Kool et al. (2007) suggested that an increase in SOC can only take place with an associated increase in soil aggregation that leads to a protection of the additional C against decomposers, thereby decelerating the C cycling.

A crucial factor that governs the amount of C sequestered is the availability of N. van Groeningen et al. (2006) showed in a meta-analysis a strong correlation between N-fertilization and C sequestration in CO₂ enrichment experiments. They found no effect of elevated CO₂ on soil C in the low N-treatments (< 30 kg N ha⁻¹ yr⁻¹), which is close to the 40 kg N ha⁻¹ yr⁻¹ applied in this study. Therefore, the absence of increased soil C stocks in the CO₂ enriched plots at the Giessen-FACE site are probably due to the low N-application. Both, [CO₂] +20% and [CO₂] +30% treatments, showed a similar C input.

The limited number of experiments for grassland ecosystems and the different experimental setups make it difficult to generalize the response of soil C stocks to elevated CO₂. Future predictions should take into account possible C saturation levels of soils (Six et al. 2002). Ecosystems may act as a C sink until a certain soil C stock is reached; beyond, no further net C sequestration will take place. More research and especially long-term data sets over several decades are needed to address this problem. Moreover, since 11 of the last 12 years were among the warmest 12 years since the beginning of the climate record since 1850 (IPCC 2007), a combination of elevated CO₂ and experimental temperature increase should be considered.

Aggregate-associated SOC

The soil aggregate classes in the Giessen-FACE differed in their C content, with higher C contents in the two macroaggregate fractions (LM, SM) compared to the Mic and SC fractions (Fig. 3.9). This was due to the higher content of organic matter (e.g. binding agents) within macroaggregates compared to the smaller soil fractions (Jastrow and Miller 1997). The SOC content difference between the macroaggregates and the smaller soil fractions decreased with increasing soil depth. This together with the decrease in organic binding agents accounts for an increase of physicogenic aggregates.

Because of the different C content of the soil fractions (Tisdall and Oades 1982) the aggregate structure of soil affects the soil C storage. The redistribution of aggregate-associated C from bigger to smaller aggregate size classes and the associated C loss has consequences for the remaining C. Although microaggregates contain less C on a per aggregate basis than macroaggregates (Fig. 3.9), the present C in microaggregates is better stabilized against mineralization, as indicated by the approximately 3 times higher turnover time of C in free microaggregates (Jastrow 1996).

In the CO₂-enriched plots no increase in C content took place over time in any soil aggregate fraction compared to ambient. This is in line with the results for the total soil C content and indicates that no mitigation in the atmospheric CO₂ rise can be expected due to an increased soil C sequestration.

Temporal dynamics

Between 1998 and 2004 a significant soil C loss along with a decrease in soil aggregation was observed under both CO₂ treatments (Fig. 3.9, Fig. 3.11), spanning all soil aggregate fractions (Tab. 3.7, Fig. 3.12). This C loss was connected with the change in soil aggregate structure because of the protection of soil organic matter within aggregates (Elliott 1986). A reasonable explanation for the C loss is that the breakdown of macroaggregates resulted in a release of organic substances which were then available for microbial decay, leading to the observed soil C loss. This is supported by other studies showing that if grasslands were changed into agricultural soil by ploughing, the aggregates became disrupted and soil C stocks decreased (Six et al. 1999; del Galdo et al. 2003). The release of labile SOM via the breakup of LM could result in an enhanced mineralization of otherwise stable SOM, i.e. it may have caused a priming effect (Kuzyakov 2002).

In addition, several biotic (root biomass, plant and microbial community structure) and abiotic (temperature, fertilization, rainfall) factors may have contributed to the C loss. At first, the reduced fertilizer application from 80 to 40 kg N ha yr⁻¹ since 1996 was thought to be a main factor. But this could be excluded by investigating several control plots which received different amounts of fertilizer (i.e. 0, 40, 80 and 120 kg N ha⁻¹ yr⁻¹ from 1993 onwards up to now). The results showed that the SOC content decreased in all plots under all N-treatments; the factor "N fertilization" was not significant. Instead, the factor "time" was significant (samples taken in 1997 and 2005, data not shown). Principally, SOC may be lost from the soil via leaching, i.e. as dissolved organic carbon. But as no changes in soil moisture conditions or average rainfall were observed, leaching was unlikely to be the responsible process. Also, the finding of the lowest C loss in the wettest ring pair 2 does not support leaching as a likely pathway for the C loss.

Changes in microbial community composition can cause changes in SOC (Carney et al. 2007). Microbes differ in their C utilization efficiency (CUE). Organisms with a lower CUE respire a higher proportion of metabolized C as CO₂. Therefore, bacteria

with a lower CUE would contribute less to pools of newly stabilized SOC than fungi (Jastrow et al. 2007). However, no data on the microbial community structure exists for the research site.

With respect to the mass balance equation, the decrease in the soil C pool could either be due to a decreased soil C input or an enhanced mineralization of OM. Both processes are temperature controlled (Kirschbaum 2006). Evidence for a decreased soil C input is given by a decrease in root biomass between 1997 and 2003, whereas aboveground biomass yield or root biomass turnover (as indicated by the $\delta^{13}\text{C}$ signature) did not change over time. Additionally, enhanced decomposition of binding agents (root biomass, fungal hyphae) due to higher temperatures in particular during winter (Tab. 3.1) may have led to an enhanced activity of microbes at that time. As shown by the Jarvis-Stuart temperature function (Fig. 2.3), a slight temperature increase of 1°C during off season could have a large effect on the decomposition rates of OM. As temperature sensitivity of OM decomposition increases with decreasing temperatures, a warming during autumn or winter has a higher effect on OM decomposition than a similar temperature increase during summer (Kirschbaum 2000). Kirschbaum et al. (1995) provided evidence that a temperature increase of 1°C could lead to a 10% SOC loss at an annual mean T_{air} of 5°C . The here observed 6.3% temperature induced increase in microbial activity could therefore have contributed to the observed soil C loss (Fig. 2.3, Tab. 3.1). This is in line with the study of Knorr et al. (2005) who found a higher temperature sensitivity of non-labile SOC than of labile SOC, implying that the long-term positive feedback of soil decomposition in a warming world may be even stronger than predicted by global models.

The mean C loss in the top 15 cm between the 4th April 1998 and the 16th June 2004 was 1.23 kg C m^{-2} and 0.89 kg C m^{-2} for E- and A-plots, respectively. Assuming that respiration was responsible for the C loss this would result in $\text{CO}_2\text{-C}$ equivalents of 16.9 and $12.1 \text{ mg C m}^{-2} \text{ h}^{-1}$ for E and A plots, respectively. Given that the average measured ecosystem respiration (R_{eco}) rates between 1998 and 2006 were $188.9 \text{ mg C m}^{-2} \text{ h}^{-1}$ for the E plots and $163.4 \text{ mg C m}^{-2} \text{ h}^{-1}$ for the A plots, then this C loss corresponds to 8.9 and 7.4% of the mean CO_2 fluxes for E and A plots, respectively. Observed spatial and in particular temporal variations in R_{eco} are usually higher than 10%, thus the additional CO_2 emissions caused by an enhanced mineralization could easily have been masked within the standard deviation. The observed C loss is comes along with increased N_2O emissions in all plots between 1998 and 2001 (Kammann et al. 2008). This further supports the hypothesis of an increased mineralization of SOM, as during the decay of SOM also the organic N becomes mineralized, which may promote N_2O production.

Bellamy et al. (2005) in the United Kingdom and Schipper et al. (2007) in New Zealand also describe C losses in recent years as observed here. This underlines the importance to find out if this C loss is possibly a world-wide, recent phenomenon related to global climate change. Schipper et al. (2007) observed a mean C loss of $0.11 \text{ kg m}^{-2} \text{ yr}^{-1}$ under long-term pastoral management, which is a lower C loss rate

than observed in this study ($0.17 \text{ kg m}^{-2} \text{ yr}^{-1}$ in the top 15 cm). Bellamy et al. (2005) found a decrease in soil C for various soil types (5662 sites) with a mean rate of $0.6\% \text{ yr}^{-1}$ relative to the existing C content between 1978 and 2003. For permanent grassland sites with C contents between $30\text{--}50 \text{ g kg}^{-1}$ (which corresponds to the Giessen-FACE site) annual C loss rates of $1.2 \text{ g kg}^{-1} \text{ yr}^{-1}$ in 0–15 cm were recorded (Bellamy et al. 2005). This is close to the C loss measured in the Giessen-FACE, where the mean C loss was $1.05 \text{ g kg}^{-1} \text{ yr}^{-1}$ in the top 15 cm. However, the different investigation periods might limit the comparability of different studies. Bellamy et al. (2005) based their calculations on samples taken at two times, approximately 30 years apart, assuming a linear SOC loss. For example, assuming that the C loss took place within 15 years without any changes afterwards, the real loss rates would double. Therefore, more frequent long-term observations are needed to examine the soil C dynamics in more detail.

Bellamy and colleagues argued that climate change and the associated increase in temperature could be the reason for the large-scale C loss, but no evidence was given in their paper. In a recently published study of Smith et al. (2007) two model scenarios were applied to the data set published by Bellamy et al. (2005) to investigate the reported changes in SOC in more detail. In the first scenario only the direct climate impacts on SOC were considered, whereas in the second scenario indirect effects by atmospheric CO_2 -driven changes in NPP were assumed. The model results for grassland soils suggested a change of $-0.03\% \text{ yr}^{-1}$ for England and Wales in the first scenario, whereas in the second scenario an increased NPP resulted in an increase in SOC of $0.03\% \text{ yr}^{-1}$, based on current assumptions on the effect of elevated CO_2 on soil C storage via an enhanced NPP. In this modeling study elevated CO_2 did not only balance the C loss but even caused a net increase in SOC via an increased NPP. However, as argued earlier, the experimental evidence for such an assumption is still weak, and it is not supported by the findings of this study where no increase in soil C storage was observed in the CO_2 enriched plots. Therefore, more research is needed to investigate the interactive effects of elevated CO_2 and warming to enable reasonable predictions for soil C dynamics under a warmer and CO_2 -enriched climate.

The term “stability” in context of ecosystem research spans several meanings, ranging from constancy, indolence and elasticity to cyclical stability, where the system always varies within a certain range (Klötzli 1990). Amundson (2001) pointed out that soil C is rather a dynamic pool than a static reservoir. Six et al. (2002) indicated several protection levels and an upper limit of the soil C pool size, i.e. a saturation level. It is well known that SOC stocks of agricultural systems are sensitive to management practices, e.g. tillage leads to a significant SOC loss. Therefore, a cyclical stability may explain the observed soil C pool dynamics, where SOC varies within a certain range that is determined by a maximum and a minimum SOC content (Fig. 4.1). Likely, soils act as a C sink until saturation is reached and the weakly protected C pool increases (Six et al. 2002). “Accidental” disturbances,

e.g. freeze-thaw cycles, could trigger SOM mineralization. Once the decomposition of SOM starts, the increased availability could further promote mineralization (i.e. a priming effect, Kuzyakov (2002)), until a new level is reached where the remaining SOM is sufficiently protected. The subdivision into a protected and a dynamic C pool is compatible with the classification of recalcitrant and labile C pools, although this corresponds to different chemical compounds (Bosatta and Ågren 1991).

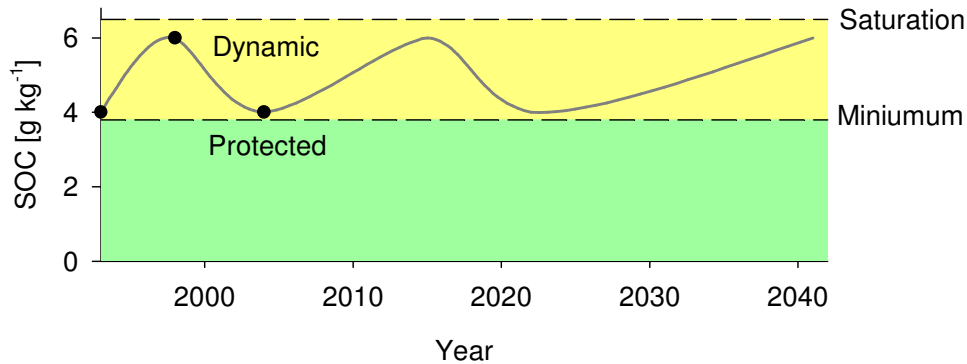


Fig. 4.1 Theoretical periodic changes on a decadal scale, where saturation is the highest possible SOC content and minimum refers to the protected SOC content beneath which a further decrease is unlikely.

Evidence for dynamic changes in SOC is given by soil samples collected in 1993 (data not shown) which indicate a lower C content similar to the C content 2004. Thus, it is possible that a C stock increase took place between 1993 and 1997/1998 but decreased again later. Long-term studies with regard to soil C dynamics in natural (grassland) ecosystems are scarce. To my knowledge only one study is available on continuous grassland. In this 35-yr long-term study (1945-1980) in the first 15 years SOC increased, but afterwards no further changes in SOC were observed (Goulding and Poulton 2007). However, the detection power of small SOC changes is limited (Smith 2004), and a high number of samples must be collected at each sampling date to achieve statistical evidence. Therefore, FACE-studies, where the spatial area is limited, are rather improper for a detailed evaluation of SOC dynamics. "Natural" cycles that lead to changes in the soil C pool would have major consequences for soil C monitoring, because the time point where the soil samples are collected would strongly affect the results. In context of climate change research this again highlights the importance of long-term monitoring studies over several decades.

4.3 Soil C input under elevated CO₂

Root biomass

In the Giessen-FACE ecosystem C enters the soil mainly via root decay and rhizodeposition. An enhanced root growth either by increasing root biomass or root turnover could result in an enhanced rhizodeposition (Canadell et al. 1996) and could then lead to a higher soil C input. In this study root biomass was on average not different under ambient CO₂ and the moderate CO₂ enriched plots E1-E3, but in plot E4 increases in root biomass up to 65% above ambient were observed. Many studies reported an increase in root biomass under elevated CO₂ (Rogers et al. 1994; Van Vuuren et al. 1997; Jastrow et al. 2000). However, in those studies atmospheric [CO₂] was at least enriched to 550 ppm. The results might indicate that a certain CO₂ concentration, i.e. higher than 440 ppm, is needed to supply enough extra carbon to build up a higher belowground plant biomass. No changes in the vertical distribution of root biomass were observed under elevated CO₂ (Fig. 3.5), which differs to the findings of Van Vuuren (1997) who observed a greater stimulation of root growth in the top layers.

Plants must compete against other plants and microbes to cover their N demand, which can be achieved by increasing their root system (Thornley 1998) or increasing their nitrogen-use efficiency (Finzi et al. 2002). The progressive N limitation (PNL) hypothesis predicts that increased C supply under elevated CO₂ leads to a higher N-demand in N-limited ecosystems (Luo et al. 2004). The Giessen-FACE soil is an N-limited ecosystem; therefore PNL can be expected to take place (Hu et al. 2006). The higher root biomass under [CO₂] +30% may be an indication that PNL is operational in this ecosystem. This is not the case under [CO₂] +20% which may indicate that the internal supply mechanisms for available N may be sufficient to support enhanced biomass production under elevated CO₂ (Kammann et al. 2005; Janze 2006). On the other hand, under elevated [CO₂] +20% N-use efficiency may have increased, which is supported by N-yield results after aboveground biomass clipping (Kammann et al. 2007). Nevertheless, it is possible that PNL will, temporally delayed, come into play under [CO₂] +20% in the next years.

In an earlier parallel study on the Giessen-FACE site with a slightly different sampling technique (i.e. same soil sampler but roots were washed out from the soil) a higher root biomass was observed under elevated CO₂ between 2001 and 2003, but the differences were not significant for the upper soil layer (Janze 2006). The inconsistent results can be explained by (1) changes over time; possibly the CO₂ enrichment led to an increase in root biomass in the beginning of the experiment but then adjusted again to a similar level as in the control plots. Or (2), there was no consistent behavior because of the strong spatial variability at the site, which is a more reasonable explanation. To address this problem, more samples would be needed per sampling date, but the space within the research plots is limited and

disturbances have to remain as small as possible. This could be solved by several extended samplings when the experiment will be finally terminated.

Due to the extraction method of roots from the soil in this study (i.e. roots were picked out manually with tweezers until virtually no roots remained in the sample) the total amount of roots, especially fine roots, was underestimated. Therefore, care must be taken when comparing the root biomass yield with data obtained by a different method, for example if roots were washed out of the soil. But as this method was applied to all samples collected between 2004 and 2007, differences between the E- and A-plots or changes over time can indeed be identified.

$\delta^{13}\text{C}$ signature of plant biomass

The significantly lower $\delta^{13}\text{C}$ signatures of plant biomass from CO_2 enriched plots compared to ambient plots confirmed that this fumigation strategy was successful (Tab. 3.3, Fig. 3.2); the measured plant $\delta^{13}\text{C}$ signatures fell within the range of values predicted by the Farquhar equation (Farquhar et al. 1982). Any differences from the given atmospheric CO_2 concentration would have resulted in deviations from the predicted plant $\delta^{13}\text{C}$ signature. The differences in plant $\delta^{13}\text{C}$ signature between the plots E1-E3 and plot E4 are due to the different CO_2 enrichment regimes (+20% and +30%). To archive an enrichment of 500 ppm (i.e. +130 ppm), relatively more fossil-fuel derived CO_2 must be applied than in the moderate, 440 ppm treatments (i.e. +70 ppm), so that the actual air $\delta^{13}\text{CO}_2$ signature is lower in plot E4 (Tab. 2.1). Despite the comparatively small atmospheric $\delta^{13}\text{CO}_2$ difference between ambient and elevated plots (Tab. 2.1) the ^{13}C signal could be traced in several ecosystem components such as plant leaves and roots, soil C pools, soil air CO_2 and R_{eco} . In particular the $\delta^{13}\text{C}$ signature switch of the CO_2 from -25‰ to -48‰ after 6 years of CO_2 -enrichment caused a further decrease in $\delta^{13}\text{C}$ that provided the opportunity for a second observation period under elevated CO_2 unaffected by a CO_2 -step increase.

All newly grown leaves after the second harvest in September 2004 showed a clear depletion in ^{13}C , compared to the first harvest in June 2004. The lower $\delta^{13}\text{C}$ signature of aboveground biomass in 2005 vs. 2006 was likely due to differences in water availability because precipitation and soil moisture were lower in 2006 (Fig. 3.1, Fig. 3.2). Water stress decreases the discrimination against ^{13}C because plants keep their stomata closed and the intracellular CO_2 concentration reaches lower values (Farquhar et al. 1982). Thus, the decreased availability of water likely resulted in a higher $\delta^{13}\text{C}$ signature of plant biomass in 2006.

Differences in $\delta^{13}\text{C}$ between roots and leaves could either be due to fractionation during C exchange between plant organs and/or along respiratory pathways (Badeck et al. 2005) or due to their different age and changing climatic conditions. As aboveground biomass is harvested twice annually in June and September, the leaves cannot be older than 9 or 3 month, respectively. Root biomass, on the other hand, partly exists in the soil for several years. Consequently, the $\delta^{13}\text{C}$ signature of

leaves corresponds more closely to the short-term air $\delta^{13}\text{C}$ signature of a few months, whereas the root $\delta^{13}\text{C}$ signature reflects the atmospheric $\delta^{13}\text{C}$ signature of several years.

The input of organic matter via decomposition of senescent roots is the primary source of C input into the soil for the Giessen-FACE site. Thus, root turnover plays an important role for soil C sequestration as it determines the input of organic matter to the soil (van Veen et al. 1991). CO_2 -induced changes in root turnover time could significantly alter the input of organic matter to the soil. Studies that focus on the effect of elevated CO_2 on root life span or turnover report either an accelerated root turnover (Fitter et al. 1997; Godbold et al. 2006) or no changes in root turnover (Higgins et al. 2002; Matamala et al. 2003). In calcareous grassland even a CO_2 -induced increase of +48% in median root life span took place in 12-18 cm depth (Arnone et al. 2000). In the CO_2 enriched plots root turnover could be roughly estimated via changes in $\delta^{13}\text{C}$ signature over time³; in the Giessen-FACE this was at most three years (Fig. 3.3). Although in the present data set it was not possible to compare the root turnover between ambient and elevated CO_2 , comparison of root $\delta^{13}\text{C}$ of $[\text{CO}_2] +20\%$ and $[\text{CO}_2] +30\%$ (Fig. 3.3) does not support the hypothesis of an enhanced turnover with increasing atmospheric $[\text{CO}_2]$. Similar tracer-techniques were used in forest ecosystems under FACE, where fine root turnover varied between 1.2 to 9 years (Matamala et al. 2003). Gill and Jackson (2000) calculated a mean annual root turnover of 0.55 yr^{-1} for temperate grasslands, with a strong impact of precipitation and temperature on the turnover rate. Differences to the Giessen-FACE might be due to the isotope method. Strand et al. (2008) suggested that isotope-based techniques likely underestimate root turnover by 60%, i.e. a root turnover time of approximately 3 years in the Giessen-FACE should be taken as an upper limit. However, studies on the effect of elevated CO_2 on root production, mortality or life span are limited and more data are needed to generalize the effects and explain different experimental results (Arnone et al. 2000).

The application of the ^{13}C label in the CO_2 enriched plots resulted in less depletion in root $\delta^{13}\text{C}$ signature with increasing depth (Fig. 3.4), indicating a slower root turnover with depth. This is in line with Joslin et al. (2006) who carried out a similar study in a forest ecosystem and found a more rapid root turnover near the soil surface. The faster root turnover in the upper soil layers resulted in faster adaptation of roots to the more negative $\delta^{13}\text{C}$ signature. However, the decreased root turnover with soil depth leads to a lower C input per unit root biomass with depth. For the ambient plots in the year 2005 also a significant effect of depth on $\delta^{13}\text{C}$ occurred, but the signature decrease within the soil profile was by far smaller than in the CO_2 enriched plots and must have other reasons than adaptation to a new $\delta^{13}\text{C}$ signature, since the control plots were not affected by the enrichment- CO_2 (Jäger et al. 2003).

³ i.e. when $d\delta^{13}\text{C}/dt = 0$

$\delta^{13}\text{C}$ signature of soil organic carbon

The CO_2 enrichment with ^{13}C depleted CO_2 led to a decrease in soil $\delta^{13}\text{C}$ signature of organic C (Fig. 3.15). This shows that the experimental setup worked properly and that the new C could be traced in the soil. The newly fixed C could be traced in various soil fractions, despite the fact that the ecosystem received a comparatively low CO_2 enrichment, and the isotope signature of the initial enrichment- CO_2 signature was with -25‰ less negative than in other FACE-studies (e.g. the Swiss-FACE). The successful establishment of a second investigation period after several years, where step increase effects (Klironomos et al. 2005) are less likely, provides a new tool in the planning and running of future FACE-experiments.

However, problems occurred for the samples collected in June 2007, where also the ambient plots showed a depletion in soil $\delta^{13}\text{C}$ signature. As no such decrease occurred in the plant biomass, a contamination of the A-plots with the enrichment- CO_2 of -48‰ can be excluded. The lower $\delta^{13}\text{C}$ signatures might be due to a problem with the calibration of the mass spec, as the decrease had the same magnitude under both CO_2 treatments and occurred also in the soil aggregate fractions. But reanalysis resulted in similar results. Therefore, the values from June 2007 were not considered for the calculation of the soil C input, because the $\delta^{13}\text{C}$ signature decrease would lead to a higher $\Delta\delta^{13}\text{C}$ between 2004 and 2007, which would then lead to an overestimation of the soil C input. Instead, the data from June 2006 were used in the calculation of the C input. The signature switch in 2004 led only to marginal ^{13}C depletion of the soil C pools until June 2006. Therefore, the observation period after the signature switch should be extended to at least 4 years to get a clear SOC ^{13}C depletion, especially if the C input rates are as low as they seem to be.

The highest ^{13}C depletion in SOC was observed in plot E4, which is in line with the lower $\delta^{13}\text{C}$ signature of plant biomass in comparison to E1-E3. In the CO_2 enriched plots the largest decrease in $\delta^{13}\text{C}$ occurred in the upper soil layer, but then lessened with soil depth, indicating a lower input of new C with depth. The $\delta^{13}\text{C}$ gradient within the soil profile (Fig. 3.16) is at least partly caused by the decrease in $\delta^{13}\text{C}$ of atmospheric CO_2 from -6.5 to -8‰ since the industrial revolution, causing more recently incorporated SOM near the soil surface to be -1.5‰ more negative (Boutton 1996; Francey et al. 1999). This is further supported by the results of Ladyman and Harkness (1980) who reported a correlation between the increase of $\delta^{13}\text{C}$ with soil depth and the increasing age and degree of SOM decay. Furthermore, several other hypothesis have been proposed, e.g. the preferential decomposition of certain components which preserve ^{13}C enriched components (Boutton 1996), the different mobility and sorption of DOC with variable $\delta^{13}\text{C}$ signature (Ehleringer et al. 2000), and isotopic fractionation during respiration (Ågren et al. 1996). However, the recently published findings of Boström et al. (2007) do not support the hypothesis that isotopic discrimination during microbial respiration causes a ^{13}C enrichment of SOM. Possibly, a combination of several factors caused the enrichment of ^{13}C with depth in the soil profile.

The CO₂ induced ¹³C depletion of SOC occurred in all aggregate fractions (Fig. 3.17), which shows that all aggregate fractions received part of the newly fixed C. However, differences in δ¹³C between the fractions (Fig. 3.18) are not only the result of elevated CO₂ or a different amount of newly fixed C, but also due to the degree of organic matter decomposition (Ågren et al. 1996), i.e. the aggregate life time. For example under ambient CO₂, the less negative δ¹³C signature was found in the SC fraction, with all other fractions having a similar isotope signature. Therefore, the isotope signature of the fractions tells little about the amount of newly fixed C. To estimate the input of new C, i.e. the fraction of new C or the amount of newly fixed C, this “inherent” δ¹³C difference must be considered.

The similar δ¹³C signature of free and SM-associated microaggregates (see section 3.5.3) suggests that the free microaggregates formed mostly within the small macroaggregates. This points towards a disruption or disturbance in the formation of new microaggregates within the LM fraction. Six et al. (2000) found that a shortcut in the life cycle of macroaggregates by physical disturbances like tillage inhibits the formation of microaggregates. Microaggregates form within macroaggregates when fine POM becomes encrusted with clay particles and microbial products (Six et al. 1998; Six et al. 1999). Thus, there is evidence that the breakup of LM disturbed the formation of microaggregates within the large macroaggregate fraction.

The finding of a lower δ¹³C signature in both the Mic-SM and the SM fractions compared to the Mic-LM and LM fractions indicates a higher turnover rate of SM-associated C and a higher C input into this fraction. This is in contrast to the results of Jastrow and Miller (1997) who observed a higher turnover rate of the LM-C compared to SM-C. The difference to this study is likely related to the observed change in soil aggregate structure.

The more depleted δ¹³C signature in the Mic-LM or Mic-SM fractions compared to the respective LM or SM fractions was unexpected because one would expect a lower signature in the total LM or SM fraction. Macroaggregates contain in addition to microaggregates also OM, which has a lower signature than microaggregate-C. Therefore, the δ¹³C signature of macroaggregates should be lower than the signature of the incorporated microaggregates. The lower δ¹³C signature of macroaggregate-associated microaggregates indicates the incorporation of a large proportion of new C into the newly formed microaggregates.

Fraction of new C

To evaluate the effect of elevated CO₂ on the input of new C a comparison is made between the [CO₂] +20% and [CO₂] +30% treatment, although there was only one repetition for [CO₂] +30%. For the ambient plots where no label was applied the C_{new} input could not be calculated.

The fraction of new C (*f*C_{new}) increased with increasing atmospheric [CO₂]. After 8 years of elevated CO₂ *f*C_{new} was 7% (0-7.5 cm) and 11% (7.5-15 cm) higher in plot

E4 than in the moderate CO₂ enriched plots E1-E3 (Tab. 3.10, Tab. 3.11). A higher fC_{new} in combination with a constant SOC under elevated CO₂ indicates an accelerated soil C turnover with increasing atmospheric [CO₂] (Hungate et al. 1997). The higher fC_{new} in plot E4 corresponds to the higher root biomass of this plot compared to the ring pairs 1-3 (Fig. 3.5). This finding shows that despite a higher soil C input no enhanced soil C sequestration took place. This is likely due to the absence of stabilization of the additional new C within aggregates because no CO₂ induced increase in soil aggregation occurred compared to ambient CO₂. Apparently the input of new C equals mineralization of old C, which is in line with Kuzyakov (2002) who suggested that an increased C input may cause a priming effect which would accelerate mineralization of recalcitrant SOM. Therefore, the results of this study show that despite higher C input rates no increase in the soil C pool can be expected without a concomitant protection of new C against microbial decay.

In plot E4 a surprisingly high fC_{new} was found in the Mic fractions in 15-30 and 30-45 cm and in the LM fraction in 30-45 cm depth, respectively. This might be due to a relocation of C percolating from upper to deeper soil layers, but no measurements on DOC were performed in the soil profile to confirm this assumption.

The high proportion of new C in the SC fraction could be at least partly due to the wet sieving technique, because all the water that was used for the sieving is collected in one pan together with the SC fraction. Likely, soluble C associated with micro- and macroaggregate fractions became diluted in the water and thereby entered the SC fraction. This is further supported by a pulse labeling experiment carried out at the site, where the by far highest ¹³C enrichment occurred in the SC fraction.

The incorporation of new C into the free microaggregates, or into microaggregates during the formation of macroaggregates, is important for the stabilization of new C in the soil (Six et al. 2000). A disturbance in the formation of new microaggregates would have major consequences for the long term C storage, as SOC within microaggregates has an approximately three times higher turnover rate than the SOC stored in macroaggregates (Jastrow and Miller 1997). The isotope signature and the fC_{new} give information about the formation of microaggregates in the soil. The largest fC_{new} was found in the free microaggregates, followed by the Mic-SM and, with a by far lower fC_{new} , in the Mic-LM fraction (Tab. 3.14). This points out that the LM breakup reduced the formation of new microaggregates with this soil fraction, but it did not prevent the formation of microaggregates in the SM fraction. Thus, despite the disturbances in the life cycle of large macroaggregates the formation of microaggregates and microaggregate-C sequestration still operated in the FACE-plots.

Input of new C

The C input measured in 0-45 cm between 1998 and 2006 was 93.5 ± 35.9 and $80.7 \text{ g m}^{-2} \text{ yr}^{-1}$ for $[\text{CO}_2] +20\%$ and $[\text{CO}_2] +30\%$, respectively. This is close to the results reported from the Swiss-FACE (van Kessel et al. 2006), where the mean input of new C in 0-50 cm corresponded to $85 \text{ g m}^{-2} \text{ yr}^{-1}$. However, a comparison with other studies is difficult because of the different experimental setup (Tab. 4.1). Differences in C input rates are amongst other things influenced by the varying amount of N-application (van Groenigen 2006). Surely, N is required for C sequestration, but this does not seem to happen proportionally. The coupling of the C- and N-cycles implies that C sequestration will only occur if the C:N-ratio of ecosystem components increases, the proportion of high C:N-ratios components increases, or an increase in total ecosystem N will take place (Rastetter et al. 1997). Rastetter et al. (1997) found in a modeling study that responses to elevated CO_2 appear (1) instantaneously via increased NPP and plant C:N-ratio, (2) on a yearly scale with increasing uptake effort for available N, (3) on a decadal scale where N moves from SOM to plants, and (4) on a century scale where total ecosystem N increases. In the Giessen-FACE nine years of elevated CO_2 caused higher C:N-ratios of aboveground plant biomass and an increase in the N-use efficiency (Kammann 2007, personal communication). Therefore, a net ecosystem C increase is likely restrained by the availability of N but might take place after the adaptation of the nutrient cycle, which could last several decades (Rastetter et al. 1997).

In both $+20\%$ and $+30\%$ CO_2 treatments the C input was higher in the first period than in the second period (Tab. 3.12, Tab. 3.13). This may indicate that one cannot expect a positive long-term effect of elevated CO_2 on the C input rates. However, care must be taken when comparing both periods as the first period spans six years whereas the second period spans only 2 years. Therefore, this aspect should be re-examined when the second observation period has extended to at least four years.

It is not clear if the decline in C input during the second period was caused by a decrease in soil C input or by enhanced mineralization of recently fixed C. The reduced belowground biomass between 1998 and 2003 (Kammann 2007, personal communication) may have influenced the C input during the second period. The differences in mean aboveground biomass grown under elevated CO_2 between the first (716 g m^{-2}) and the second (688 g m^{-2}) observation period were only marginal. For plot E4 no above- or belowground biomass data were available for the first period, but here the C input differences between both periods were much smaller than under $[\text{CO}_2] +20\%$. A fast mineralization of newly incorporated C would furthermore reduce the soil C input. A possible increase in SOM mineralization during the second observation period enhances soil respiration, which is confirmed by a comparison of the mean R_{eco} rates between 1999 and 2003 ($636 \pm 50 \text{ mg CO}_2 \text{ m}^{-2} \text{ h}^{-1}$) and the second period (2004-2006; $677 \pm 70 \text{ mg CO}_2 \text{ m}^{-2} \text{ h}^{-1}$). During the second period R_{eco} was 7% higher compared to the first period ($p < 0.1$, paired t-test). However, besides changes in mineralization R_{eco} is largely influenced by climatic conditions which differ between the years and therefore limit comparability between the two time periods.

During the second observation period the newly fixed C was predominantly sequestered into the deeper soil layers, whereas the highest root biomass occurred in the top layer. This supports the hypothesis that an enhanced mineralization annihilates the input of new C to the uppermost soil layer, which is in line with a lower soil aggregation in the uppermost soil layer compared to 7.5-15 cm depth (Fig. 3.6). In the deeper soil layer a better physical protection within macroaggregates probably increased the amount of new C (Tab. 3.12).

The effects of the CO₂ enrichment on the C input rates were rather inconsistent in both observation periods. In the first observation period a higher C input occurred under [CO₂] +20%, whereas in the second period the C input was by far higher under [CO₂] +30%. For the entire soil profile the absolute amount of new C sequestered between 1998 and 2006 was with 94 g m⁻² yr⁻¹ for [CO₂] +20% and 81 g m⁻² yr⁻¹ for [CO₂] +30% about equal for both CO₂ treatments, indicating no higher C input with increasing atmospheric [CO₂]. This seems to be in contrast to fC_{new} which was higher in plot E4 (Tab. 3.10, Tab. 3.11). The calculation of the C input rates considers the amount of C present in the soil (i.e. fC_{new} multiplied with the SOC content), which was lower in plot E4 than in the plots E1-E3. Therefore, the lower amount of C incorporated into plot E4 was caused by the lower SOC content, although the *relative* amount of new C was higher in this plot.

The high C input into the SM fraction during the first observation period was due to the breakup of large macroaggregates into the smaller soil particles. Thereby the SM fraction increased, which resulted in a higher absolute amount of new C bound in this fraction. The relation between the absolute amount of C input into a certain fraction correlates with the abundance of the respective aggregate class in the soil.

The amounts of newly sequestered C into the macroaggregate-associated microaggregates were 9.1 (Mic-LM) and 29.7 g m⁻² yr⁻¹ (Mic-SM) in 0-7.5 cm, which corresponded to 44% and 84% of the C input into the LM and SM fractions, respectively. This is close to the values reported for agro-ecosystems, where the C stabilized in microaggregates accounted for 40% and 68% of new macroaggregate-C (Kong et al. 2005). The preferential stabilization of C in the Mic-SM fraction makes it the most sensitive fraction to evaluate the soil C input (Kong et al. 2005), which is also true for the Giessen-FACE soil. This is also in line with other studies (Denef et al. 2004; del Galdo et al. 2006) who found the Mic-SM fraction to be a sensitive fraction for changes in SOC content.

4.4 Effects of elevated CO₂ on the autotrophic and heterotrophic components of soil and ecosystem respiration

Ecosystem respiration and soil air CO₂ concentration

Monitoring the soil air CO₂ concentration (soil air [CO₂]), ecosystem respiration (R_{eco}) and the $\delta^{13}\text{C}$ signature provides insight into the mineralization of SOC, the respiratory processes, the biological activity and the associated C dynamics.

Clear annual dynamics of R_{eco} , with highest respiration rates during the main vegetation period (Fig. 3.23) point out the influence of plant-derived C on R_{eco} . During these times R_{eco} was directly linked to soil air [CO₂] in the top 5 cm (Fig. 3.23). Additionally, R_{eco} also contained the respired CO₂ of aboveground biomass which was unaffected by soil air [CO₂] and contributed to the high respiration rates during summer. During dry periods R_{eco} was more related to the concentrations deeper in the soil profile, which corresponded to trace gas dynamics observed in the same grassland soil (Müller et al. 2004). Therefore, at times of low soil moisture the contribution of soil CO₂ from deeper soil layers to R_{eco} will be higher than at times of high soil moisture.

The mean CO₂-induced increase in R_{eco} of 13% during the years 2004 to 2006 (Fig. 3.23) points out that part of the extra carbon under elevated CO₂ was respired shortly after entering the ecosystem. Aeschliemann et al. (2005) reported for the Swiss-FACE an increase in R_{eco} of up to 39% under elevated CO₂ (600 ppm). The increase of soil respiration under elevated CO₂ (Kammann et al., unpublished data) led to the conclusion that the increase of R_{eco} was mainly due to an increase of R_{soil} . The lower $\delta^{13}\text{C}$ values in soil air and R_{eco} during the period of active plant growth (Fig. 3.29) indicate a predominant impact of R_{plant} on R_{eco} . If the additional C gain under elevated CO₂ is lost quickly by an increased respiration, no higher C input under elevated CO₂ will occur. The soil C pool can only increase if the additional C input under elevated CO₂ is not entirely lost via a stimulated ecosystem respiration. But the absence of a CO₂-induced increase in the soil C pool shows that any additional C input is dominantly lost via stimulated respiration.

The fast increase in soil air [CO₂] at the beginning of the growth period (Fig. 3.23) reflects a sudden temperature-induced activation of plant growth/photosynthesis and soil respiration. The highest [CO₂] occurred during spring, mainly as a result of increased respiration and following N fertilization but also because of the high soil moisture conditions that decelerate the gas diffusion within the soil profile. In summer the soil air [CO₂] decreased, which was due to a faster diffusion of CO₂ to the atmosphere, as indicated by an increased R_{eco} . Similar dynamics in soil air [CO₂] were observed in grassland soils in Switzerland (Hesterberg and Siegenthaler 1991) and in the Sonoran Desert, Arizona (Parada et al. 1983). The soil air [CO₂] is the

result of CO₂ production and the diffusion of CO₂ from the soil to the atmosphere (Fang and Moncrieff 1999). The diffusion of CO₂ from the soil to the atmosphere is much faster in soil air than in the liquid phase, thus the CO₂ diffusion is decelerated at times of high soil moisture. The strong impact of soil moisture via reduced gas diffusion is further supported by the obviously higher soil air [CO₂] in the wettest ring pair 2. Hence, a CO₂ induced increase in soil respiration must not necessarily lead to a higher soil air [CO₂]. This is in line with the finding of a significant increase in (ecosystem) respiration under elevated CO₂, without a concomitant significant increase in soil air [CO₂].

$\delta^{13}\text{CO}_2$ signature and components of soil respiration

The large $\delta^{13}\text{C}$ differences in soil air CO₂ between E- and A-plots at times when plant growth is minimal, i.e. during winter, prove that a considerable amount of recently fixed C is respired. This shows how important it is to follow a year-round CO₂-enrichment strategy in temperate grassland ecosystems. Similar isotope measurements in an agro-ecosystem (corn/winter wheat) showed even more pronounced annual dynamics in the $\delta^{13}\text{C}$ signature of soil air CO₂ (Schüßler et al. 2000).

In the Giessen-FACE the $\delta^{13}\text{C}$ of soil air CO₂ did not show a continuous decrease following the signature switch in July 2004 (Fig. 3.23). Therefore, the soil air ¹³CO₂ signature adapted to the new signature within less than two month. This points out that the respired CO₂ is dominantly derived from recently fixed C. This finding is in line with results obtained in a forest ecosystem exposed to elevated CO₂, where a depletion in $\delta^{13}\text{C}$ of soil air CO₂ was visible after a few days after the start of the CO₂ enrichment, but after four month no further depletion occurred (Bernhardt et al. 2006). The fast adaptation of CO₂ to the new signature is crucial for the successful partitioning of respiration into its autotrophic and heterotrophic sources and also proves that the labeling was successful.

The soil CO₂ originates from an autotrophic and a heterotrophic source differing in their isotope signature. Therefore, changes in the relative contribution of autotrophic and heterotrophic sources lead to changes in $\delta^{13}\text{CO}_2$. The temporal dynamics in soil air $\delta^{13}\text{CO}_2$ of A- and E-plots indicate that a moderate CO₂ enrichment did not change the soil C dynamics or the relative contribution of root and microbial derived CO₂. As plant biomass had the most negative $\delta^{13}\text{C}$ signature in this ecosystem, decreases in $\delta^{13}\text{CO}_2$ of soil air and R_{eco} during the growth period indicate a higher contribution of plant derived C. It is well known that photosynthesis drives (ecosystem) respiration (Johnson et al. 2002; Högberg and Read 2006; Larsen et al. 2007). Craine et al. (1999) for example found a 40% reduction in soil CO₂ efflux in a grassland ecosystem that was independent from temperature after two days of shading.

After the signature switch in June 2004 root biomass as a main source of R_{soil} continuously decreased in $\delta^{13}\text{C}$, whereas soil air $\delta^{13}\text{CO}_2$ adapted very fast (see above). This was likely due to the signature difference between the structural C of

plant tissue and that of labile substrates i.e. starch, lipids or sugars that are the main substrates of respiration, although no measurements of these compounds were carried out in this study. In contrast to $\delta^{13}\text{C}$ of soil air CO_2 , it took three years until the structural C was substituted by new C and the root $\delta^{13}\text{C}$ signature reached a new steady state. For the Giessen-FACE grassland ecosystem the $\delta^{13}\text{CO}_2$ values proved that the respired CO_2 originated predominantly from recently fixed C, because it adapted within a few days to the new $\delta^{13}\text{C}$ signature. Therefore, the root ^{13}C signature was not an appropriate value for the label of the plant source of R_{soil} . Hence, the $\delta^{13}\text{C}$ signature of aboveground biomass was used in the partitioning model, as it adapted to the new $\delta^{13}\text{C}$ signature within 3 months.

In the ambient plots the $\delta^{13}\text{C}$ signature difference of the two sources (i.e. plants and bulk soil C) was too small to successfully apply the two-component mixing model (Phillips and Gregg 2001). A possible CO_2 -effect on the components of respiration could therefore only be investigated in the $[\text{CO}_2] +20\%$ and $[\text{CO}_2] +30\%$ enriched plots. The approximately 1‰ lower $\delta^{13}\text{CO}_2$ signature in soil air CO_2 in plot E4 compared to E1-E3 is in line with the lower $\delta^{13}\text{C}$ signature of plant biomass under $[\text{CO}_2] +30\%$ (Galimov 1966).

The observed temporal dynamics of f_{root} to R_{soil} with highest values during spring time and lowest values during the winter month (Fig. 3.26) follow the plant growth activity. In particular during spring, when plant growth starts, root activity is high and a predominant proportion of CO_2 production is related to root respiration. The higher contribution of R_{root} during the growing season is in line with the results obtained by Hesterberg and Siegenthaler (1991), who found an enhanced relative contribution of R_{root} to R_{soil} during spring time in a temperate grassland. The annual $\delta^{13}\text{CO}_2$ dynamics occurred at all soil depths, but the amplitude decreased with increasing depth (Fig. 3.24). Therefore, it seems that the changes in the relative contribution of the two soil air CO_2 sources were less pronounced with increasing soil depth. Lower amplitudes with increasing depth are a characteristic pattern of soil temperature (Fig. 3.24) or soil moisture dynamics.

In the top 15 cm, plant and rhizosphere respiration (f_{root}) contributed on average 55% (E1-E3) and 45% (E4) to the soil CO_2 production (Tab. 3.17). This is close to the value reported by Hanson et al. (2000) who estimated from a review of existing literature that R_{root} contributed 60% to the total soil CO_2 production for non-forest vegetation under ambient atmospheric $[\text{CO}_2]$. The finding of a lower fraction of root-derived CO_2 on R_{soil} with increasing atmospheric $[\text{CO}_2]$ was not expected, because the availability of root-derived labile C substrates is known to increase under elevated CO_2 (Pendall et al. 2004) either by increased root exudation rates per unit root biomass or by enhanced root biomass (Phillips et al. 2006). Therefore, f_{root} was expected to increase with increasing atmospheric $[\text{CO}_2]$. However, the lower contribution of f_{root} to R_{soil} together with a higher fraction of new C ($f_{\text{C}_{\text{new}}}$) in plot E4 indicates a higher bonding of new, FACE-derived C to the soil C pool and a concomitant mineralization of old C, as the total C pool did not increase. The finding of an enhanced mineralization of old C in deep soil layers caused by the supply of

fresh plant-derived C was recently published by Fontaine et al. (2007). The changes in C turnover with increasing CO₂ concentration, i.e. old C is replaced by recently fixed C without an increase in the soil C pool, may affect the stability of C and therefore its residence time in the soil. So far the new C replaces the old C without a CO₂-induced net loss in soil C, but further samplings are necessary to assess if the new C is sequestered in the long term.

The annual dynamics of f_{root} were less distinctive in deeper soil layers (Fig. 3.28), indicating only small changes in R_{root} on R_{soil} over time with increasing depth. Furthermore, f_{root} increased with depth (Fig. 3.27). A possible discrimination against ¹³C in the metabolism of microbes would take place in the entire soil profile and is therefore not responsible for the lower ¹³CO₂ signatures and the higher f_{root} with increasing soil depth. Instead, the increase in f_{root} with depth was likely due to a higher turnover of substrates provided by the rhizosphere, as microbial activity (Tate 1979), SOC content, and root biomass all decrease with depth.

Depth effect on the isotopic composition of soil air CO₂

The decrease of the soil air $\delta^{13}\text{CO}_2$ signature with depth (Tab. 3.16) is in line with the model developed by Cerling et al. (1991) who showed that the isotope composition of soil air CO₂ is depth dependant and strongly influenced by the respiration rate. They found that the isotope signature changes mostly within the upper 30 cm, which corresponds to the depths monitored in this study. For the Giessen-FACE site the annual dynamics in the $\delta^{13}\text{CO}_2$ signature gradient led to a distinctive $\delta^{13}\text{CO}_2$ gradient during winter but to a homogenous $\delta^{13}\text{CO}_2$ profile during the vegetation period (Fig. 3.25). This is in line with the results of Dorr and Munnich (1980) and Reardon et al. (1979) who did not find an isotope gradient below 30 cm depth during summer when respiration rates were high. Similar results were also obtained for a grass-covered soil near Bern, Switzerland, where $\delta^{13}\text{CO}_2$ in 30 cm depth differed clearly from 80 cm in the winter month October to April, whereas no difference occurred during summer (Hesterberg and Siegenthaler 1991). Also at three sites in the Tucson Basin, Arizona, the $\delta^{13}\text{CO}_2$ signature decreased with depth (Parada et al. 1983). The seasonal variability might also explain contrasting findings from other studies where no long term sampling (i.e. at least over one year) was carried out.

The absence of a $\delta^{13}\text{CO}_2$ gradient during the summer month was likely due to a better diffusive mixing of soil gas in the profile during dry soil conditions. Under such conditions, CO₂ from deeper soil layers diffuses towards the surface and could alter the $\delta^{13}\text{C}$ gradient. This was further confirmed by the results obtained at the Giessen-FACE site by Müller et al. (2004), who found an increased amount of the trace gas N₂O that originated from deeper soil layers during drier soil conditions. Possibly the relative contribution of R_{root} on R_{soil} always increases with depth, but the gradient is annihilated by a better soil air mixing during the summer months. Nevertheless, there was no significant effect of soil moisture on the $\delta^{13}\text{CO}_2$ decrease with depth.

Changes in the isotopic signature of soil air CO₂ over time result from changes in respiration rates (Cerling 1984). In this study, (soil) temperature as a main factor for the control of respiration showed a significant impact on the soil air δ¹³CO₂ gradient. The δ¹³CO₂ gradient dynamics followed the soil temperature curve closely, although during winter 2004/2005 some discrepancies occurred (Fig. 3.25). The CO₂ enrichment was not the reason for the weak connection between the δ¹³CO₂ gradient and the soil temperature in winter 2004/2005, as the same discrepancies also occurred under ambient CO₂. However, Cerling (1984) did not distinguish between the sources of soil respiration. Unlike heterotrophic respiration, which can be expressed as a function of soil temperature and moisture (Byrne and Kiely 2006) plant respiration also depends on photosynthesis (Kuzyakov and Cheng 2001). Thus, an increase in photosynthesis could have increased root respiration, thereby disbanding the δ¹³CO₂ gradient during winter 2004/2005. To understand the mechanisms that lead to the annual dynamics of the δ¹³CO₂ gradient in the soil profile, a model including all processes and factors influencing the CO₂ respiration processes (McDowell et al. 2004) is needed.

δ¹³CO₂ signature and components of ecosystem respiration

Lower δ¹³C signatures of ecosystem-respired CO₂ during the growth period (Fig. 3.29) indicate a higher contribution of plant-derived C, which corresponds to the higher (aboveground) plant biomass at that time. The significant differences in δ¹³C of R_{eco} between the CO₂ treatments and the annual dynamics prove the successful use of the Keeling-plot technique to monitor the annual dynamics of R_{eco} and to compare both CO₂ treatments. Parallel annual dynamics in δ¹³C of R_{eco} under ambient and elevated CO₂ indicate no CO₂-induced changes in the soil C dynamics. The high spatial variability of δ¹³C of R_{eco} was likely due to the large impact of recently fixed C on R_{eco} and a significant effect of previous climatic conditions on δ¹³C of R_{eco} (Pataki et al. 2003).

Autotrophic and heterotrophic components of ecosystem respiration

Only a few studies are available that focus on the partitioning of ecosystem respiration into its autotrophic and heterotrophic sources. Moreover, the use of different methods, ranging from destructive methods where plant biomass was removed (Hu et al. 2008; Shurpali et al. 2008), empirical model analysis (Byrne and Kiely 2006) to non-invasive stable isotope techniques (Tu et al. 2001; Tu and Dawson 2005) exacerbates a comparison of the results.

In this study the mean contribution of R_{plant} to R_{eco} was 22% (Eqn. 9), whereas the highest contribution was observed during the summer months (31%), which is in line with the period of intense plant growth and high aboveground plant biomass (Tab. 3.19). The significant differences between the growth period and the off-season (R_{plant} was only 11% of R_{eco}) reflect the annual dynamics in plant growth and show the dominant contribution of microbial derived CO₂ from organic matter decay to R_{eco} during the winter period. In this study the contribution of R_{plant} to R_{eco} was by far

lower than the contribution of R_{root} to R_{soil} (i.e. 50%). Certainly, since R_{eco} contains in addition to soil respiration the plant-derived aboveground respiration (R_{leaf}), the contribution of R_{plant} to R_{eco} should be higher than that R_{root} to R_{soil} . Therefore, there must be either an overestimation of R_{root} to R_{soil} or an underestimation of R_{plant} to R_{eco} . A comparison with other methods (e.g. root exclusion or aboveground biomass removal) could help to solve this problem, although those destructive methods will probably alter the CO_2 fluxes compared to intact, non-disturbed systems.

A higher contribution of R_{plant} to R_{eco} during the growth period was also observed in an intensively managed grassland ecosystem using an empirical model based on abiotic factors (temperature, moisture) and the leaf area index (Byrne and Kiely 2006). In their study autotrophic respiration accounted for 38% between 15th September and 2nd May and 50% between 23rd May and 14th September. A natural abundance approach was used to separate R_{eco} into its components in an agricultural managed ecosystem (i.e. a shift from C3 to C4 vegetation), where R_{plant} was 44% of R_{eco} during the growth period (Griffis et al. 2005). In a mixed C3 grassland ecosystem grown on C4-soil, plant respiration contributed 69% to R_{eco} between December 2000 and February 2001 (Tu et al. 2001). In a destructive approach where leaves and plants were removed, Hu et al. (2008) found for two alpine meadow sites a contribution of autotrophic respiration to R_{eco} of 54% and 61%, respectively. In a root trenching experiment on canary grass in Finland, plant respiration accounted for 55% of R_{eco} (Shurpali et al. 2008).

The mean fraction of R_{plant} to R_{eco} obtained in this study (22%) was comparatively low. A comparison between the studies is difficult not only because of a missing standardized method, but also because of the different ecosystem types and management practices. The reliability of the methods might be limited either by far-ranging disturbances if plant biomass is removed (i.e. destruction of soil structure causing changes in soil moisture, aeration, and availability of SOM), uncertainties in source partitioning via the isotopic signature (Schnyder and Lattanzi 2005), or the limited possibility to revise model results. Variations could be due to different times of measurement (i.e. growth period vs. off-season), vegetation or the amount of fertilizer applied. The higher contribution of R_{plant} in the Byrne and Kiely study was likely due to the 7.5 times higher fertilizer application ($300 \text{ kg N ha}^{-1} \text{ yr}^{-1}$) compared to the Giessen-FACE site.

Above- and belowground components of ecosystem respiration

Over the entire observation period under $[\text{CO}_2] +20\%$, R_{soil} and R_{leaf} contributed 68% and 32% to R_{eco} , with a 4% higher R_{leaf} during the growth period than during the off-season. During several times in summer 2007, separate in-situ soil CO_2 efflux measurements were carried out on plots where the aboveground biomass was removed in 2005. The measurements showed that the contribution of R_{soil} to R_{eco} was 78% during the summer period from 15th June to 19th September 2007, and 68% during the off-season between 29th October to 11th December 2007 (Kammann 2008, personal communication). The results obtained by the second method might

be afflicted with an uncertainty due to methodical differences in R_{soil} and R_{eco} measurements (i.e. different chamber design and length of chamber cover) and the removal of aboveground biomass in the R_{soil} measurement plots. However, the values obtained at the Giessen-FACE site are close to the results obtained in an annual grassland ecosystem, where R_{soil} contributed 67% to R_{eco} (Tu et al. 2001).

The higher contribution of R_{leaf} to R_{eco} during the growth period is in line with the higher aboveground biomass at that time, although f_{leaf} varies widely during the year (Fig. 3.30). The effect of aboveground biomass removal on f_{leaf} was insignificant. However, the contribution of R_{leaf} to R_{eco} was expected to decrease, resulting in a higher $\delta^{13}\text{C}$ signature of R_{eco} , i.e. closer to the $\delta^{13}\text{C}$ signature of R_{soil} . The absence of a $\delta^{13}\text{C}$ increase in R_{eco} following clipping could have been due to the time differences between the $\delta^{13}\text{C}$ measurement and biomass clipping (Tab. 7.1, Tab. 7.2). In the year 2005, where biomass clipping resulted in a small increase in f_{leaf} (Fig. 3.30), the samples of R_{eco} were collected four (first harvest) and three days (second harvest) after clipping. The biomass clipping in 2006 on the other hand resulted in a small decrease of leaf derived CO_2 . Here the gas samples of R_{eco} were collected at the same day. This suggests that the small amount of aboveground biomass left after clipping (5 cm above the ground) is quite active and thereby keeps the fraction of leaf respiration high. Furthermore, the high f_{leaf} after clipping and the differences between the years could be due to an immediate mobilization of storage substrates from stubble, rhizomes and roots, mobilized and respired to build up new leaves.

Relative contributions of leaf, root and soil respiration to R_{eco}

A combined approach of Keeling-plot analysis, soil air CO_2 measurements, and a subsequent use of the two-component mixing model enabled the separation of R_{eco} into aboveground respiration (R_{leaf} , Eqn. 8), root (R_{root}) and microbial-derived CO_2 (R_{bulk}). Although many studies are available on the partitioning of R_{soil} into its heterotrophic and autotrophic components (Hanson et al. 2000; Kuzyakov and Larionova 2005), studies that focus on the separation of R_{eco} are limited. To my knowledge only two other studies were carried out where a similar separation of R_{eco} was accomplished. One focused on an annual grassland ecosystem (Tu et al. 2001), whereas the other was carried out in a Californian redwood forest ecosystem (Tu and Dawson 2005). All results are presented in Tab. 4.2.

Tab. 4.2 Components of R_{eco} in the Giessen-FACE ($[\text{CO}_2] +20\%$), in an annual grassland, and in a Californian redwood forest ecosystem where no CO_2 enrichment was applied.

Component	Giessen-FACE	Annual grassland*	Redwood forest**
	% of R_{eco}		
R_{leaf}	32 ±23	33	25 ±10
R_{root}	29 ±18	36	33 ±20
R_{bulk}	38 ±20	31	42 ±22

(Tu et al. 2001)*; *(Tu and Dawson 2005)*

The differences between the annual grassland and the Giessen-FACE grassland were only marginal, with a 7% higher R_{bulk} in the Giessen-FACE study (R_{root} decreased by 7%). The Californian redwood forest ecosystem showed with 42% the highest fraction of R_{bulk} , followed by the old Giessen-FACE grassland and the annual grassland ecosystem, respectively. This could reflect differences in SOC or in the bacterial- and fungal community structure. The contribution of R_{root} was with 33% similar to the values reported for the two grassland ecosystems. Although R_{leaf} was higher in both grassland ecosystems, the difference to the Redwood forest ecosystem was still in the range of the standard deviation. However, because of the limited number of studies available on this topic (and none under elevated CO_2), a detailed discussion would be meaningless. In conclusion, the results of the Giessen-FACE study are well in the range of the values reported for the annual grassland and the forest site.

5 Conclusions and outlook

In the Giessen-FACE experiment elevated CO_2 did not lead to an increase in soil aggregation or in the soil C pool. Despite a higher input of organic matter due to the significant increase in root biomass under $[\text{CO}_2] +30\%$, no significant increase in either soil aggregation or the soil C content was observed. This was further confirmed by the CO_2 -induced increase in ecosystem respiration under $[\text{CO}_2] +20\%$, which proves that a significant part of the “extra”-C was respired instead of sequestered into the soil. The higher fraction of new C with increasing CO_2 together with the absence of an increase in the soil C pool indicates a higher C turnover under elevated CO_2 . This is in line with the findings of Gill et al. (2002) who found an unchanged soil C pool at elevated CO_2 where losses of old soil carbon offset increases in new carbon, and may indicate that soils under current $[\text{CO}_2]$ are nearly C saturated in the sense of Six et al. (2002). The experimental setup of FACE experiments is restricted by the fact that the C input of the ambient plots could not be measured because of the absence of a ^{13}C label. This problem can be solved by inserting into all FACE and control plots soil columns filled with C4 soil, which is ^{13}C enriched compared to soil where C3 plants were grown.

The loss of soil C between 1997 and 2004 took place in all soil aggregate classes and was associated with a change in the soil aggregate structure: large macroaggregates broke up into smaller aggregates. Most likely, the enhanced mineralization of organic matter released by the breakup of large macroaggregates promoted the C loss. The thereby induced priming effect, together with a significant increase in (winter) temperatures further promoted the mineralization of soil organic C. As the C loss also occurred under ambient CO_2 , a CO_2 -induced SOC loss via priming effects (of the initial CO_2 step-increase) can be excluded. The reasons for the breakup of the large macroaggregates remain uncertain. Likely candidates are (1) an increase in winter temperatures, and (2) a decrease in roots and fungal hyphae that act as macroaggregate binding agents, possibly associated with a shift in plant species composition. To revise the hypothesis of periodic changes in SOC and soil aggregation on decadal scales and, moreover, to examine if elevated CO_2 leads to an increase in SOC beyond the 9 yr observation period, it is crucial to continue the regular soil sampling. A more detailed examination of the soil C loss between 1998 and 2004 could be achieved by considering the eddy-covariance measurements at that time, i.e. the net ecosystem C balances during certain time periods (seasons or years). This may provide information on the C loss. For example, it may answer the question if the C loss only occurred in the FACE- and N-fertilization plots, or if it was a general side-wide phenomenon. If so, the time period of the C loss could be narrowed down and potential seasonal C-loss dynamics (i.e. a possible higher C loss during the warmer autumn/winter month) could possibly be identified.

The annual dynamics of the soil air $\delta^{13}\text{CO}_2$ signature together with the large $\delta^{13}\text{C}$ differences between ambient and elevated CO_2 prove the importance of a year-round CO_2 enrichment of the grassland site. A significant decrease in $\delta^{13}\text{CO}_2$ with depth indicated a relatively higher contribution of root-respired CO_2 with depth. The $\delta^{13}\text{CO}_2$ gradient with depth showed clear annual dynamics with shallowest gradients

during summer which was probably due to the better diffusive soil air mixing during the summer months.

The partitioning of soil respiration into plant and SOM-derived CO_2 revealed a higher contribution of root respiration under $[\text{CO}_2] +20\%$ (55%) than under $[\text{CO}_2] +30\%$ (45%). However, the lower contribution of R_{root} to R_{soil} under $[\text{CO}_2] +30\%$ together with a higher root C input in the $[\text{CO}_2] +30\%$ treatment may indicate a higher incorporation of new C to the soil C storage, and a concomitant shift in respired substrates towards older SOC sources.

The synchronous dynamics of soil air $\delta^{13}\text{CO}_2$ and ecosystem respired $\delta^{13}\text{CO}_2$ underlines the significant contribution of soil respiration to ecosystem respiration. Although uncertainties due to isotopic fractionation may occur, the contribution of soil respiration to R_{eco} was 68% whereas 32% were due to leaf respiration.

6 References

- Adu, J. K. and J. M. Oades (1978). Physical factors influencing decomposition of organic materials in soil aggregates. Soil Biology and Biochemistry **10**: 109-115.
- Aeschlimann, U., J. Nösberger, P. J. Edwards, M. K. Schneider, M. Richter and H. Blum (2005). Responses of net ecosystem CO₂ exchange in managed grassland to long-term CO₂ enrichment, N fertilization and plant species. Plant, Cell and Environment **28**: 823-833.
- Ågren, G. I., E. Bosatta and J. Balesdent (1996). Isotope discrimination during decomposition of organic matter: a theoretical analysis. Soil Science Society of America Journal **60**: 1121-1126.
- Allard, V., C. Robin, P. C. D. Newton, M. Lieffering and J. F. Soussana (2006). Short and long-term effects of elevated CO₂ on *Lolium perenne* rhizodeposition and its consequences on soil organic matter turnover and plant N yield. Soil Biology and Biochemistry **38**: 1178-1187.
- Amundson, R. (2001). The carbon budget in soils. Annual Review of Earth and Planetary Sciences **29**: 535-562.
- Andrews, J. A., K. G. Harrison, R. Matmala and W. H. Schlesinger (1999). Separation of root respiration from total soil respiration using carbon-13 labeling during free-air carbon dioxide enrichment (FACE). Soil Science Society of America Journal **63**: 1429-1435.
- Arnone, J. A., III, J. G. Zaller, E. M. Spehn, P. A. Niklaus, C. E. Wells and C. Körner (2000). Dynamics of root systems in native grasslands: effects of elevated atmospheric CO₂. New Phytologist **147**: 73-85.
- Badeck, F.-W., G. Tcherkez, S. Nogués, C. Piel and J. Ghashghaie (2005). Post-photosynthetic fractionation of stable carbon isotopes between plant organs - a widespread phenomenon. Rapid Communications in Mass Spectrometry **19**: 1381-1391.
- Balesdent, J. and A. Mariotti (1996). Measurement of soil organic matter turnover using ¹³C natural abundance. In: T. W. Boutton and S. Yamasaki, Mass Spectrometry of Soils, 83-111. Dekker, New York.
- Batjes, N. H. (1998). Mitigation of atmospheric CO₂ concentrations by increased carbon sequestration in the soil. Biology and Fertility of Soils **27**: 230-235.
- Behaydt, D., P. Boeckx, T. J. Clough, J. Vermeulen, R. R. Sherlock and O. Van Cleemput (2005). Methods to adjust for the interference of N₂O on ¹³C and ¹⁸O measurements of CO₂ from soil mineralization. Rapid Communications in Mass Spectrometry **19**: 1365-1372.
- Bellamy, P. H., P. J. Loveland, R. I. Bradley, R. M. Lark and G. J. D. Kirk (2005). Carbon loss from all soils across England and Wales 1978-2003. Nature **437**: 245-248.

- Bernhardt, E. S., J. J. Barber, J. S. Phipps, L. Taneva, J. A. Andrews and W. H. Schlesinger (2006). Long-term effects of free air CO₂-enrichment (FACE) on soil respiration. *Biogeochemistry* **77**: 91-116.
- Blanco-Canqui, H. and R. Lal (2004). Mechanisms of carbon sequestration in soil aggregates. *Critical Reviews in Plant Sciences* **23**: 481-504.
- Bosatta, E. and G. I. Ågren (1991). Dynamics of carbon and nitrogen in the organic matter of the soil: a generic theory. *The American Naturalist* **138**: 227-245.
- Boström, B., D. Comstedt and A. Ekblad (2007). Isotope fractionation and ¹³C enrichment in soil profiles during the decomposition of soil organic matter. *Oecologia* **153**: 89-98.
- Boutton, T. W. (1996). Stable carbon isotope ratios of soil organic matter and their use as indicators of vegetation and climate change. In: T. W. Boutton and S. Yamasaki, *Mass Spectrometry of Soils*, 47-82. Dekker, New York.
- Bowling, D. R., P. P. Tans and R. K. Monson (2001). Partitioning net ecosystem carbon exchange with isotopic fluxes of CO₂. *Global Change Biology* **7**: 127-145.
- Byrne, K. and G. Kiely (2006). Partitioning of respiration in an intensively managed grassland. *Plant and Soil* **282**: 281-289.
- Canadell, J., L. F. Pitelka and J. S. I. Ingram (1996). The effects of elevated CO₂ on plant-soil carbon below-ground: A summary and synthesis. *Plant and Soil* **187**: 391-400.
- Carney, K. M., B. A. Hungate, B. G. Drake and J. P. Megonigal (2007). Altered soil microbial community at elevated CO₂ leads to loss of soil carbon. *Proceedings of the National Academy of Sciences of the United States of America* **104**: 4990-4995.
- Cerling, E. T. (1991). On the isotopic composition of carbon in soil carbon dioxide. *Geochimica et Cosmochimica Acta* **55**: 3403-3405.
- Cerling, T. (1984). The stable isotopic composition of modern soil carbonate and its relationship to climate. *Earth and Planetary Science Letters* **71**: 229-240.
- Chapin III, F. S., P. A. Matson and H. A. Mooney (2002). *Principles of Terrestrial Ecosystem Ecology*. New York, Springer.
- Chung, H., D. R. Zak, P. B. Reich and D. S. Ellsworth (2007). Plant species richness, elevated CO₂, and atmospheric nitrogen decomposition alter soil microbial community composition and function. *Global Change Biology* **13**: 980-989.
- Comstedt, D., B. Boström, J. D. Marshall, A. Holm, M. Slaney, S. Linder and A. Ekblad (2006). Effects of elevated atmospheric carbon dioxide and temperature on soil respiration in a boreal forest using δ¹³C as a labeling tool. *Ecosystems* **9**: 1266-1277.
- Craine, J. M., D. A. Wedin and F. S. Chapin III (1999). Predominance of ecophysiological controls on soil CO₂ flux in a Minnesota grassland. *Plant and Soil* **207**: 77-86.

- Dämmgen, U., G. L. and S. Schaaf (2005). The precipitation and spatial variability of some meteorological parameters needed to determine vertical fluxes of air constituents. Landbauforschung Völkerode **55**: 29-37.
- De Gryze, S., L. Jassogne, H. Bossuyt, J. Six and R. Merckx (2006). Water repellence and soil aggregate dynamics in a loamy grassland soil as affected by texture. European Journal of Soil Science **57**: 235-246.
- del Galdo, I., W. C. Oechel and M. F. Cotrufo (2006). Effects of past, present and future atmospheric CO₂ concentrations on soil organic matter dynamics in a chaparral ecosystem. Soil Biology and Biochemistry **38**: 3235-3244.
- del Galdo, I., J. Six, A. Peressotti and M. F. Cortufo (2003). Assessing the impact of land-use change on soil C sequestration in agricultural soils by means of organic matter fractionation and stable C isotopes. Global Change Biology **9**: 1204-1213.
- Denef, K., H. Bubenheim, T. Lenhart, J. Vermeulen, O. Van Cleemput, P. Boeckx and M. C (2007). Community shifts and carbon translocation within metabolically-active rhizosphere microorganisms in grasslands under elevated CO₂. Biogeosciences **4**: 769-779.
- Denef, K., J. Six, R. Merckx and K. Paustian (2004). Carbon sequestration in microaggregates of no-tillage soils with different clay mineralogy. Soil Science Society of America Journal **68**: 1935-1944.
- Denef, K., J. Six, K. Paustian and R. Merckx (2001). Importance of macroaggregate dynamics in controlling soil carbon stabilization: short-term effects of physical disturbance induced by dry-wet cycles. Soil Biology and Biochemistry **33**: 2145-2153.
- Dexter, A. R. (1988). Advances in Characterization of Soil Structure. Soil and Tillage Research **11**: 199-238.
- Dorr, H. and K. O. Munnich (1980). Carbon-14 and carbon-13 in soil CO₂. Radiocarbon **22**: 909-918.
- Drissner, D., H. Blum, D. Tscherko and E. Kandeler (2007). Nine years of enriched CO₂ changes the function and structural diversity of soil microorganisms in a grassland. European Journal of Soil Science **58**: 260-269.
- Ehleringer, J. R., N. Buchmann and L. B. Flanagan (2000). Carbon isotope ratios in belowground carbon cycle processes. Ecological Applications **10**: 412-422.
- Ekblad, A. and P. Högberg (2001). Natural abundance of ¹³C in CO₂ respired from forest soils reveals speed of link between tree photosynthesis and root respiration. Oecologia **127**: 305-308.
- Elliott, E. T. (1986). Aggregate structure and carbon, nitrogen, and phosphorus in native and cultivated soils. Soil Science Society of America Journal **50**: 627-633.
- Eviner, V. T. and F. S. Chapin III (2002). The influence of plant species, fertilization and elevated CO₂ on soil aggregate stability. Plant and Soil **246**: 211-219.

- Fang, C. and J. B. Moncrieff (1999). A model for soil CO₂ production and transport 1: model development. Agricultural and Forest Meteorology **95**: 225-236.
- Farquhar, G., M. H. O. O'Leary and J. A. Berry (1982). On the relationship between carbon isotope discrimination and the intercellular carbon dioxide concentration in leaves. Australian Journal of Plant Physiology **9**: 121-137.
- Feng, X., L. L. Nielsen and M. J. Simpson (2007). Responses of soil organic matter and microorganisms to freeze-thaw cycles. Soil Biology and Biochemistry **39**: 2027-2037.
- Finzi, A. C., E. H. DeLucia, J. G. Hamilton, D. D. Richter and W. H. Schlesinger (2002). The nitrogen budget of a pine forest under free air CO₂ enrichment. Oecologia **132**: 567-578.
- Fitter, A. H., J. D. Graves, J. Wolfenden, G. K. Self, T. K. Brown, D. Bogie and T. A. Mansfield (1997). Root production and turnover and carbon budgets of two contrasting grasslands under ambient and elevated atmospheric carbon dioxide concentrations. New Phytologist **137**: 247-255.
- Fitter, A. H., G. K. Self, T. K. Brown, D. S. Bogie, J. D. Graves, D. Benham and P. Ineson (1999). Root production and turnover in an upland grassland subjected to artificial soil warming respond to radiation flux and nutrients, not temperature. Oecologia **120**: 575-581.
- Fontaine, S., S. Barot, P. Barré, N. Bdioui, B. Mary and C. Rumpel (2007). Stability of organic carbon in deep soil layers controlled by fresh carbon supply. Nature **450**: 277-280.
- Francey, R. J., C. E. Allison, D. M. Etheridge, C. M. Trudinger, I. G. Enting, M. Leuenberger, R. L. Langenfelds, E. Michel and L. P. Steele (1999). A 1000-year precision record of $\delta^{13}\text{C}$ in atmospheric CO₂. Tellus **51B**: 170-193.
- Galimov, E. M. (1966). Carbon isotopes of soil CO₂. Geochemica international **3**: 889-897.
- Gill, A. R., H. W. Polley, H. B. Johnson, L. J. Anderson, H. Maherall and R. B. Jackson (2002). Nonlinear grassland response to past and future atmospheric CO₂. Nature **417**: 279-282.
- Gill, R. A. and R. B. Jackson (2000). Global patterns of root turnover for terrestrial ecosystems. New Phytologist **147**: 13-31.
- Godbold, D. L., M. R. Hoosbeek, M. Lukac, M. F. Cotrufo, I. A. Janssens, R. Ceulemans, A. Polle, E. J. Velthorst, G. Scarascia-Mugnozza, P. De Angelis, F. Miglietta and A. Peressotti (2006). Mycorrhizal hyphal turnover as a dominant process for carbon input into the soil organic matter. Plant and Soil **281**: 15-24.
- Goulding, K. and P. Poulton (2007). Long-term research in the UK - lessons learned from the Rothamsted Classical Experiments. In: Hideborn Alm, K., Success Stories of Agricultural Long-term studies **9**: 8-12.

- Griffis, T. J., J. M. Baker and J. Zhang (2005). Seasonal dynamics and partitioning of isotopic CO₂ exchange in a C3/C4 managed ecosystems. *Agricultural and Forest Meteorology* 132: 1-19.
- Hansen, J., M. Sato, P. Kharecha, G. Russell, D. W. Lea and M. Siddall (2007). Climate change and trace gases. *Philosophical Transactions of the Royal Society* 365: 1925-1954.
- Hanson, P. J., N. T. Edwards, C. T. Garten and J. A. Andrews (2000). Separating root and soil microbial contributions to soil respiration: a review of methods and observations. *Biogeochemistry* 48: 115-146.
- Harms, V. (1998). *Biomathematik, Statistik und Dokumentation*. Harms Verlag, Kiel.
- Harris, D., W. R. Horwath and C. van Kessel (2001). Acid fumigation of soils to remove carbonates prior to total organic carbon or carbon-13 isotopic analysis. *Soil Science Society of America Journal* 65: 1853-1856.
- Hartley, I. P., A. F. Armstrong, R. Murthy, G. Barron-Gafford, P. Ineson and O. K. Atkin (2006). The dependence of respiration on photosynthetic substrate supply and temperature: integrating leaf, soil and ecosystem measurements. *Global Change Biology* 12: 1954-1968.
- Heinz, S. K. (2000). Auswirkungen von erhöhtem Kohlendioxid auf die oberirdische Biomasse und den Kohlenstoffhaushalt eines Dauergrünlandes. Master thesis, Department of Plant Ecology, Justus-Liebig-University Gießen.
- Hesterberg, R. and U. Siegenthaler (1991). Production and stable isotopic composition of CO₂ in a soil near Bern, Switzerland. *Tellus* 43B: 197-205.
- Hicks, B. B., D. D. Baldocchi, T. P. Meyers, R. P. Hosker Jr. and D. R. Matt (1987). A preliminary multiple resistance routine for deriving dry deposition velocities from measured quantities. *Water, Air and Soil Pollution* 36: 311-330.
- Higgins, P. A. T., R. B. Jackson, J. M. Des Rosiers and C. B. Field (2002). Root production and demography in a California annual grassland under elevated atmospheric carbon dioxide. *Global Change Biology* 8: 841-850.
- Högberg, P., N. Buchmann and D. J. Read (2006). Comments on Kuzyakov's review Sources of CO₂ efflux from soil and review of partitioning methods. *Soil Biology and Biochemistry* 38: 2997-2998.
- Högberg, P., A. Nordgren, N. Buchmann, A. F. S. Taylor, A. Ekblad, M. N. Högberg, G. Nyberg, M. Ottosson-Löfvenius and D. J. Read (2001). Large-scale forest girdling shows that current photosynthesis drives soil respiration. *Nature* 411: 789-792.
- Högberg, P. and D. J. Read (2006). Towards a more plant physiological perspective on soil ecology. *Trends in Ecology and Evolution* 21: 548-554.
- Hovenden, M. J., P. C. D. Newton, R. A. Carran, P. Theobald, K. E. Wills, J. K. Vander Schoor, A. L. Williams and Y. Osanai (2008). Warming prevents the elevated CO₂-induced reduction in available soil nitrogen in a temperate, perennial grassland. *Global Change Biology* 14: 1-7.

- Hu, Q.-W., Q. Wu, G.-M. Cao, D. Li, R.-J. Long and Y.-S. Wang (2008). Growing Season Ecosystem Respirations and Associated Component Fluxes in Two Alpine Meadows on the Tibetan Plateau. Journal of Integrative Plant Biology **50**: 271-279.
- Hu, S., C. Tu, X. Chen and J. B. Gruver (2006). Progressive N limitation of plant response to elevated CO₂: a microbiological perspective. Plant and Soil **289**: 47-58.
- Hungate, B. A., E. A. Holland, R. B. Jackson, F. Stuart Chapin, III, H. A. Mooney and C. B. Field (1997). The fate of carbon in grasslands under carbon dioxide enrichment. Nature **388**: 576-579.
- IPCC, 2007: Climate Change 2007: The Physical Science Basis. Contribution of Working Group I to the Fourth Assessment. Report of the Intergovernmental Panel on Climate Change, Solomon, S., D. Qin, M. Manning, Z. Chen, M. Marquis, K.B. Averyt, M. Tignor and H.L. Miller (eds.), Cambridge University Press, Cambridge, United Kingdom and New York, NY, USA, 996 pp.
- IPCC, 2007: Climate Change 2007: Impacts, Adaptation and Vulnerability. Contribution of Working Group II to the Fourth Assessment. Report of the Intergovernmental Panel on Climate Change, M.L. Parry, O.F. Canziani, J.P. Palutikof, P.J. van der Linden and C.E. Hanson (eds.), Cambridge University Press, Cambridge, United Kingdom, 976 pp.
- IPCC, 2007: Climate Change 2007: Mitigation. Contribution of Working Group III to the Fourth Assessment Report of the Intergovernmental Panel on Climate Change, B. Metz, O.R. Davidson, P.R. Bosch, R. Dave, L.A. Meyer (eds), Cambridge University Press, Cambridge, United Kingdom and New York, NY, USA.
- Jäger, H.-J., S. W. Schmidt, C. Kammann, L. Grünhage, C. Müller and K. Hanewald (2003). The university of Giessen free-air carbon dioxide enrichment study: description of the experimental site and of a new enrichment system. Journal of Applied Botany **77**: 117-127.
- Janze, S. (2006). Auswirkungen von erhöhtem CO₂ auf die Vegetation eines Grünlandes. PhD thesis, Department of Plant Ecology, Justus-Liebig University Gießen.
- Jastrow, J. D. (1996). Carbon Dynamics of Aggregate-Associated Organic Matter Estimated by Carbon-13 Natural Abundance. Soil Science Society of America Journal **60**: 801-807.
- Jastrow, J. D. (1996). Soil aggregate formation and the accrual of particulate and mineral-associated organic matter. Soil Biology and Biochemistry **28**: 665-676.
- Jastrow, J. D., J. E. Amonette and V. L. Bailey (2007). Mechanisms controlling soil carbon turnover and their potential application for enhancing carbon sequestration. Climatic Change **80**: 5-23.
- Jastrow, J. D. and R. M. Miller (1997). Soil aggregate stabilization and carbon sequestration: feedbacks through organomineral associations. In: R. Lal, J.

- M. Kimble, R. F. Follett and B. A. Stewart, Soil Processes and the Carbon Cycle, CRC Press LLC, Boca Raton.
- Jastrow, J. D., R. M. Miller, R. Matamala, R. J. Norby, T. W. Boutton, C. W. Rice and C. E. Owensby (2005). Elevated atmospheric carbon dioxide increases soil carbon. Global Change Biology **11**: 2057-2064.
- Jastrow, J. D., R. M. Miller and C. E. Owensby (2000). Long-term effects of elevated atmospheric CO₂ on below-ground biomass and transformation to soil organic matter in grassland. Plant and Soil **224**: 85-97.
- Johnson, D., J. R. Leake, N. Ostle, P. Ineson and D. J. Read (2002). *In situ* ¹³CO₂ pulse-labelling of upland grassland demonstrates a rapid pathway of carbon flux from arbuscular mycorrhizal mycelia to the soil. New Phytologist **153**: 327-334.
- Joslin, J. D., J. B. Gaudinski, M. S. Torn, W. J. Riley and P. J. Hanson (2006). Fine-root turnover patterns and their relationship to root diameter and soil depth in a ¹⁴C-labeled hardwood forest. New Phytologist **172**: 523-535.
- Kammann, C. (2001). Die Auswirkung steigender atmosphärischer CO₂-Konzentrationen auf die Flüsse der Klimaspurengase N₂O und CH₄ in einem Grünlandökosystem. PhD thesis, Department of Plant Ecology, Justus-Liebig University Gießen.
- Kammann, C., L. Grünhage, U. Grütters, S. Janze and H.-J. Jäger (2005). Response of aboveground grassland biomass and soil moisture to moderate long-term CO₂ enrichment. Basic and Applied Ecology **6**: 351-365.
- Kammann, C., L. Grünhage and H.-J. Jäger (2001). A new sampling technique to monitor concentrations of CH₄, N₂O and CO₂ in air at well- defined depths in soils with varied water potential. European Journal of Soil Science **52**: 1-7.
- Kammann, C., L. Grünhage, C. Müller, S. Jacobi and H.-J. Jäger (1998). Seasonal variability and mitigation options for N₂O emissions from differently managed grasslands. Environmental Pollution **102**: 179-186.
- Kammann, C., L. Grünhage, C. Müller and H.-J. Jäger (2007). More than 8 years of CO₂ enrichment increased the N-use efficiency but also N₂O emissions in a temperate grassland ecosystem. Verhandlungen der Gesellschaft für Ökologie, Verlag Die Werkstatt, Göttingen.
- Kammann, C., C. Müller, G. L and J. H. J (2008). Elevated CO₂ stimulates N₂O emissions in permanent grassland. Soil Biology and Biochemistry **40**: 2194-2205.
- Kandeler, E., A. R. Mosier, J. A. Morgan, D. G. Milchunas, J. Y. King, S. R. Rudolph and D. Tscherko (2007). Transient elevation of carbon dioxide modifies the microbial community composition in a semi-arid grassland. Soil Biology and Biochemistry **40**: 162-171.
- Keeling, C. D. (1958). The concentration and isotopic abundances of atmospheric carbon dioxide in rural areas. Geochimica et Cosmochimica Acta **13**: 322-334.

- Ketterings, Q. M., J. M. Blair and J. C. Y. Marinissen (1997). Effects of earthworms on soil aggregate stability and carbon and nitrogen storage in a legume cover crop agroecosystem. Soil Biology and Biochemistry **29**: 401-408.
- Kirschbaum, M. U. F. (1995). The temperature dependence of soil organic matter decomposition, and the effect of global warming on soil organic C storage. Soil Biology and Biochemistry **27**: 753-760.
- Kirschbaum, M. U. F. (2000). Will changes in soil organic carbon act as a positive or negative feedback on global warming? Biogeochemistry **48**: 21-51.
- Kirschbaum, M. U. F. (2006). The temperature dependence of organic-matter decomposition -still a topic of debate. Soil Biology and Biochemistry **38**: 2510-2518.
- Klironomos, J. N., M. F. Allen, M. C. Rillig, J. Piotrowski, S. Makvandi-Nejad, B. E. Wolfe and J. R. Powell (2005). Abrupt rise in atmospheric CO₂ overestimates community response in a model plant-soil system. Nature **433**: 621-624.
- Klötzli, F. A. (1990). Stabilität: Konstanz und Elastizität. In: F. A. Klötzli, Ökosysteme -Aufbau, Funktion, Störungen, 76-87, Gustav Fischer Verlag, Stuttgart.
- Klumpp, K., R. Schäufele, F. A. Lattanzi, W. Feneis and H. Schnyder (2005). C-isotope composition of CO₂ respired by shoots and roots: fractionation during dark respiration? Plant, Cell and Environment **28**: 241-250.
- Knorr, W., I. C. Prentice, J. I. House and E. A. Holland (2005). Long-term sensitivity of soil carbon turnover to warming. Nature **433**: 298-301.
- Kong, A. Y., J. Six, D. C. Bryant, R. F. Denison and C. van Kessel (2005). The relationship between carbon input, aggregation, and soil organic carbon stabilization in sustainable cropping systems. Soil Science Society of America Journal **69**: 1078-1085.
- Kool, D. M., H. Chung, K. R. Tate, D. J. Ross, P. C. D. Newton and J. Six (2007). Hierarchical saturation of soil carbon pools near a natural CO₂ spring. Global Change Biology **13**: 1282-1293.
- Kuzyakov, Y. (2002). Review: factors affecting rhizosphere priming effects. Zeitschrift für Pflanzenernährung und Bodenkunde **165**: 382-396.
- Kuzyakov, Y. (2006). Sources of CO₂ efflux from soil and review of partitioning methods. Soil Biology and Biochemistry **38**: 425-448.
- Kuzyakov, Y. and W. Cheng (2001). Photosynthesis controls of rhizosphere respiration and organic matter decomposition. Soil Biology and Biochemistry **33**: 1915-1925.
- Kuzyakov, Y. and G. Domanski (2000). Carbon input by plants into the soil. Review. Zeitschrift für Pflanzenernährung und Bodenkunde **163**: 421-431.
- Kuzyakov, Y. and A. A. Larionova (2005). Root and rhizomicrobial respiration: A review of approaches to estimate respiration by autotrophic and heterotrophic organisms in soil. Journal of Plant Nutrition and Soil Science **168**: 503-520.

- Ladyman, S. J. and D. D. Harkness (1980). Carbon isotope measurement as an index of soil development. Radiocarbon **22**: 885-891.
- Lal, R. (2004). Soil carbon sequestration to mitigate climate change. Geoderma **123**: 1-22.
- Larsen, K. S., A. Ibrom, C. Beier, S. Jonasson and A. Michelsen (2007). Ecosystem respiration depends strongly on photosynthesis in a temperate heath. Biogeochemistry **85**: 201-213.
- Long, S. P., E. A. Ainsworth, A. D. B. Leakey and P. B. Morgan (2005). Global food insecurity. Treatment of major food crops with elevated carbon dioxide or ozone under large-scale fully open-air conditions suggests recent models may have overestimated future yields. Philosophical Transactions of the Royal Society **360**: 2011-2020.
- Lovelock, C. E., S. F. Wright and K. A. Nichols (2004). Using glomalin as an indicator for arbuscular mycorrhizal hyphal growth: an example from a tropical rain forest soil. Soil Biology and Biochemistry **36**: 1009-1012.
- Ludlow, M. M., J. H. Troughton and R. J. Jones (1976). A technique for determining the proportion of C₃ and C₄ species in plant samples using stable natural isotopes of carbon. Journal of Agricultural Science **87**: 625-632.
- Luo, Y. (2001). Transient ecosystem responses to free-air CO₂ enrichment (FACE): experimental evidence and methods of analysis. New Phytologist **152**: 3-8.
- Luo, Y., W. S. Currie, J. S. Dukes, A. C. Finzi, U. Hartwig, B. A. Hungate, R. E. McMurtrie, R. Oren, W. J. Parton, D. E. Pataki, M. R. Shaw, D. R. Zak and C. B. Field (2004). Progressive nitrogen limitation of ecosystem responses to rising atmospheric carbon dioxide. BioScience **54**: 731-739.
- Luo, Y., D. Hui and D. Zhang (2006). Elevated CO₂ stimulates net accumulations of carbon and nitrogen in land ecosystems: a meta-analysis. Ecology **87**: 53-63.
- Luo, Y., R. B. Jackson, C. B. Field and H. A. Mooney (1996). Elevated CO₂ increases belowground respiration in California grassland. Oecologia **108**: 130-137.
- Luo, Y. and X. Zhou (2006). Separation of source components of soil respiration. In: Luo, Y. and X. Zhou, Soil respiration and the environment, 187-214, Elsevier.
- Matamala, R., M. A. Gonzales-Meler, J. D. Jastrow, R. J. Norby and W. H. Schlesinger (2003). Impacts of fine root turnover on forest NPP and soil C sequestration potential. Science **302**: 1385-1387.
- McDowell, N. G., D. R. Bowling, B. J. Bond, J. Irvine, B. E. Law, P. Anthoni and J. R. Ehleringer (2004). Response of the carbon isotopic content of ecosystems, leaf, and soil respiration to meteorological and physiological driving factors in a *Pinus ponderosa* ecosystem. Global Biogeochemical Cycles **18**: GB1013 doi:10.1029/2003GB002049.
- Montealgre, C. M., C. van Kessel, J. M. Blumenthal, H.-G. Hur, U. A. Hartwig and M. J. Sadowsky (2000). Elevated atmospheric CO₂ alters microbial population structure in a pasture ecosystem. Global Change Biology **6**: 475-482.

- Müller, C., R. J. Stevens, R. J. Laughlin and H.-J. Jäger (2004). Microbial processes and the site of N₂O production in a temperate grassland soil. Soil Biology and Biochemistry **36**: 453-461.
- Newton, P. C. D., H. Clark, G. R. Edwards and D. J. Ross (2001). Experimental confirmation of ecosystem model predictions comparing transient and equilibrium plant responses to elevated CO₂. Ecology Letters **4**: 344-347.
- Niklaus, P. A., J. Alpehi, D. Ebersberger, C. Kampichler, E. Kandeler and D. Tschirko (2003). Six years of *in situ* CO₂ enrichment evoke changes in soil structure and soil biota of nutrient-poor grassland. Global Change Biology **9**: 585-600.
- Niklaus, P. A., M. Wohlfender, R. Siegwolf and C. Körner (2001). Effects of six years atmospheric CO₂ enrichment on plant, soil, and soil microbial C of a calcareous grassland. Plant and Soil **233**: 189-202.
- Ohlsson, K. E. A., B. Singh, S. Holm, A. Nordgren, L. Lövdahl and P. Högberg (2005). Uncertainties in static closed chamber measurements of the carbon isotope ratio of soil-respired CO₂. Soil Biology and Biochemistry **37**: 2273-2276.
- Oztas, T. and F. Fayetorbay (2003). Effect of freezing and thawing processes on soil aggregate stability. Catena **52**: 1-8.
- Parada, C. B., A. Long and S. N. Davis (1983). Stable-isotopic composition of soil carbon dioxide in the Tucson-Basin, Arizona, U.S.A. Isotope Geoscience **1**: 219-236.
- Pataki, D. E. (2005). Emerging topics in stable isotope ecology: are there isotopic effects in plant respiration? New Phytologist **167**: 321-323.
- Pataki, D. E., J. R. Ehleringer, L. B. Flanagan, D. Yakir, D. R. Bowling, C. J. Still, N. Buchmann, J. O. Kaplan and J. A. Berry (2003). The application and interpretation of Keeling plots in terrestrial carbon cycle research. Global Biogeochemical Cycles **17**: 2001GB001850.
- Pendall, E., S. W. Leavitt, T. Brookes, B. A. Kimball, P. J. Pinter, Jr, G. W. Wall, R. L. LaMorte, G. Wechsung, F. Wechsung, F. Adamsen, A. D. Matthias and T. L. Thompson (2001). Elevated CO₂ stimulates soil respiration in a FACE wheat field. Basic and Applied Ecology **2**: 193-201.
- Pendall, E., A. R. Mosier and J. A. Morgan (2004). Rhizodeposition stimulated by elevated CO₂ in a semiarid grassland. New Phytologist **162**: 447-458.
- Petit, J. R., J. Jouzel, D. Raynaud, N. I. Barkov, J.-M. Barnola, I. Basile, M. Bender, J. Chappellaz, M. Davis, G. Delaygue, M. Delmotte, V. M. Kotlyakov, M. Legrand, V. Y. Lipenkov, C. Lorius, L. Pépin, C. Ritz, E. Saltzman and M. Stievenard (1999). Climate and atmospheric history of the past 420,000 years from the Vostok ice core, Antarctica. Nature **399**: 429-436.
- Phillips, D. A., T. C. Fox and J. Six (2006). Root exudation (net efflux of amino acids) may increase rhizodeposition under elevated CO₂. Global Change Biology **12**: 561-567.

- Phillips, D. L. and J. W. Gregg (2001). Uncertainty in source partitioning using stable isotopes. Oecologia **2001**: 171-179.
- Pulleman, M. M. and J. C. Y. Marinissen (2004). Physical protection of mineralizable C in aggregates from long-term pasture and arable soil. Geoderma **120**: 273-282.
- Rastetter, E. B., G. I. Ågren and G. R. Shaver (1997). Responses of N-limited ecosystems to increased CO₂: a balanced-nutrition, coupled-element-cycles model. Ecological Applications **7**: 444-460.
- Reardon, E. J., G. B. Allison and P. Fritz (1979). Seasonal chemical and isotopic variations of soil CO₂ at trout creek, Ontario. Journal of Hydrology **43**: 355-371.
- Rillig, M. C., E. R. Lutgen, P. W. Ramsey, J. N. Klironomos and J. E. Gannon (2005). Microbial accompanying different arbuscular mycorrhizal fungal isolates influence soil aggregation. Pedobiologia **49**: 251-259.
- Rillig, M. C., S. F. Wright, M. F. Allen and C. B. Field (1999). Rise in carbon dioxide changes soil structure. Nature **400**: 628.
- Rillig, M. C., S. F. Wright, B. A. Kimball, P. J. Pinter, G. W. Wall, M. J. Ottman and S. W. Leavitt (2001). Elevated carbon dioxide and irrigation effects on water stable aggregates in a Sorghum field: a possible role for arbuscular mycorrhizal fungi. Global Change Biology **7**: 333-337.
- Robinson, D. and C. M. Scrimgeour (1995). The contribution of plant C to soil CO₂ measured using ¹³C. Soil Biology and Biochemistry **27**: 1653-1656.
- Rogers, H. H., G. B. Runion and S. V. Krupa (1994). Plant responses to atmospheric CO₂ enrichment with emphasis on roots and the rhizosphere. Environmental Pollution **83**: 155-189.
- Saggar, S., C. Hedley and A. D. Mackay (1997). Partitioning and translocation of photosynthetically fixed ¹⁴C in grazed hill pastures. Biology and Fertility of Soils **25**: 152-158.
- Schipper, L. A., W. T. Baisden, R. L. Parfitt, C. Ross, J. J. Claydon and G. Arnold (2007). Large losses of soil C and N from soil profiles under pasture in New Zealand during the past 20 years. Global Change Biology **13**: 1138-1144.
- Schlesinger, W. H. and J. Lichter (2001). Limited carbon storage in soil and litter of experimental forest plots under increased atmospheric CO₂. Nature **411**: 466-469.
- Schnyder, H. and F. A. Lattanzi (2005). Partitioning respiration of C3-C4 mixed communities using the natural abundance ¹³C approach -testing assumptions in a controlled environment. Plant Biology **7**: 592-600.
- Schüßler, W., R. Neubert, I. Levin, N. Fischer and C. Sonntag (2000). Determination of microbial versus root-produced CO₂ in an agricultural ecosystem by means of δ¹³CO₂ measurements in soil air. Tellus **52B**: 909-918.

- Shurpali, N. J., N. P. Hyvönen, J. T. Huttunen, C. Biasi, H. Nykänen, N. Pekkarinen and P. J. Martikainen (2008). Bare soil and reed canary grass ecosystem respiration in peat extraction sites in Eastern Finland. Tellus **60B**: 200-209.
- Six, J., H. Bossuyt, S. Degryze and K. Denef (2004). A history of research on the link between (micro) aggregates, soil biota, and soil organic matter dynamics. Soil and Tillage Research **79**: 7-31.
- Six, J., P. Callewaert, S. Lenders, S. De Gryze, S. J. Morris, E. G. Gregorich, E. A. Paul and K. Paustian (2002). Measuring and understanding carbon storage in afforested soils by physical fractionation. Soil Science Society of America Journal **66**: 1981-1987.
- Six, J., A. Carpentier, C. van Kessel, R. Merckx, D. Harris, W. R. Horwath and A. Lüscher (2001). Impact of elevated CO₂ on soil organic matter dynamics as related to changes in aggregate turnover and residue quality. Plant and Soil **234**: 27-36.
- Six, J., R. T. Conant, E. A. Paul and K. Paustian (2002). Stabilization mechanisms of soil organic matter: Implications for C-saturation of soil. Plant and Soil **241**: 155-176.
- Six, J., E. T. Elliott and K. Paustian (1999). Aggregate and soil organic matter dynamics under conventional and no-tillage systems. Soil Science Society of America Journal **63**: 1350-1358.
- Six, J., E. T. Elliott and K. Paustian (2000). Soil macroaggregate turnover and microaggregate formation: a mechanism for C sequestration under no-tillage agriculture. Soil Biology and Biochemistry **32**: 2099-2103.
- Six, J., E. T. Elliott, K. Paustian and J. W. Doran (1998). Aggregation and soil organic matter accumulation in cultivated and native grassland soils. Soil Science Society of America Journal **62**: 1367-1337.
- Six, J. and J. D. Jastrow (2002). Organic matter turnover. In: Lal, R. Encyclopedia of Soil Science: 936-942, Taylor & Francis, Boca Raton.
- Smith, P. (2004). How long before a change in soil organic carbon can be detected? Global Change Biology **10**: 1878-1883.
- Smith, P., S. J. Chapman, W. A. Scott, W. A. Black, H. I. J. Black, M. Wattenbach, R. Milne, C. D. Campbell, A. Lilly, N. Ostle, P. E. Levy, D. G. Lumsdon, P. Millard, W. Towers, S. Zaehle and J. U. Smith (2007). Climate change cannot be entirely responsible for soil carbon loss observed in England and Wales, 1978-2003. Global Change Biology **13**: 2605-2609.
- Soe, A. R. B., A. Giesemann, T.-H. Anderson, H.-J. Weigel and N. Buchmann (2004). Soil respiration under elevated CO₂ and its partitioning into recently assimilated and older carbon sources. Plant and Soil **262**: 85-94.
- Sollins, P., P. Homann and B. A. Caldwell (1996). Stabilization and destabilization of soil organic matter: mechanisms and controls. Geoderma **74**: 65-105.
- Stocker, R., P. W. Leadley and C. Körner (1997). Carbon and water fluxes in a calcareous grassland under elevated CO₂. Functional Ecology **11**: 222-230.

- Strand, A. E., S. G. Pritchard, M. L. McCormack, M. A. Davis and R. Oren (2008). Irreconcilable differences: fine-root life spans and soil carbon persistence. Science **319**: 456-458.
- Taneva, L., J. S. Phippen, W. H. Schlesinger and M. A. Gonzales-Meler (2006). The turnover of carbon pools contributing to soil CO₂ and soil respiration in a temperate forest exposed to elevated CO₂ concentration. Global Change Biology **12**: 983-994.
- Tate, R. L. (1979). Microbial activity in organic soils as affected by soil depth and crop. Applied and Environmental Microbiology **37**: 1985-1090.
- Taub, D. R., B. Miller and H. Allen (2008). Effects of elevated CO₂ on the protein concentration of food crops: a meta-analysis. Global Change Biology **14**: 565-575.
- Tcherkez, G., S. Nogues, J. Bleton, G. Cornic, F. Badeck and J. Ghashghaie (2003). Metabolic origin of carbon isotope composition of leaf dark-respired CO₂ in french bean. Plant Physiology **131**: 237-244.
- Thornley, J. H. M. (1998). Grassland Dynamics: An Ecosystem Simulation Model. Oxon, CAB International.
- Tisdall, J. M. and J. M. Oades (1982). Organic matter and water-stable aggregates in soils. Journal of Soil Science **33**: 141-163.
- Treseder, K. K. (2005). Nutrient acquisition strategies of fungi and their relation to elevated atmospheric CO₂. In: S. F. Wright and R. Zobel, Roots and soil management - Interactions between roots and soil, 145-162, Soil Science Society of America, Madison.
- Trueman, R. J. and M. A. Gonzales-Meler (2005). Accelerated belowground C cycling in a managed agriforest ecosystem exposed to elevated carbon dioxide concentrations. Global Change Biology **11**: 1258-1271.
- Tu, K. and T. Dawson (2005). Partitioning ecosystem respiration using stable carbon isotope analyses of CO₂. In: L. B. Flanagan, J. R. Ehleringer and D. E. Pataki, Stable Isotopes and Biosphere-Atmosphere Interactions, 125-153, Elsevier.
- Tu, K. P., T. Dawson and F. Ponti (2001). Partitioning ecosystem respiration using stable carbon isotopes in a mixed C3 annual grassland. Eos, Transactions, American Geophysical Union **82**, Fall Meeting, Abstract B11A-04.
- van Groenigen, K.-J. (2006). Element interactions limit soil carbon storage. Proceedings of the National Academy of Sciences of the United States of America **103**: 6571-6574.
- van Groenigen, K.-J., D. Harris, W. R. Horwath, U. A. Hartwig and C. van Kessel (2002). Linking sequestration of ¹³C and ¹⁵N in aggregates in a pasture soil following 8 years of elevated atmospheric CO₂. Global Change Biology **8**: 1094-1108.
- van Kessel, C., B. Boots, M.-A. de Graaff, D. Harris, H. Blum and J. Six (2006). Total soil C and N sequestration in a grassland following 10 years of free air CO₂ enrichment. Global Change Biology **12**: 2187-2199.

- van Kessel, C., J. Nitschelm, W. R. Horwath, D. Harris, F. Walley, A. Lüscher and U. Hartwig (2000). Carbon-13 input and turn-over in a pasture soil exposed to long-term elevated atmospheric CO₂. Global Change Biology **6**: 123-135.
- van Veen, J. A. and P. J. Kuikman (1990). Soil structural aspects of decomposition of organic matter by micro-organisms. Biogeochemistry **11**: 213-233.
- van Veen, J. A., E. Liljeroth, L. J. A. Lekkerkerk and S. C. van de Geijn (1991). Carbon fluxes in plant-soil systems at elevated atmospheric CO₂ levels. Ecological Applications. **1**: 175-181.
- Van Vuuren, M. M. I., D. Robinson, A. H. Fitter, S. D. Chasalow, L. Williamson and J. A. Raven (1997). Effects of elevated atmospheric CO₂ and soil water availability on root biomass, root length, and N, P and K uptake by wheat. New Phytologist **135**: 455-465.
- White, R., S. Murray and M. Rohweder (2000), Pilot analysis of global ecosystems: grassland ecosystems, World Resources Institute, Washington D.C.
- Wright, S. F. and A. Upadhyaya (1998). A survey of soils for aggregate stability and glomalin, a glycoprotein produced by hyphae of arbuscular mycorrhizal fungi. Plant and Soil **198**: 97-107.
- Xu, C., G. Lin, K. L. Griffing and R. N. Sambrotto (2004). Leaf respiratory CO₂ is ¹³C-enriched relative to leaf organic components in five species of C3 plants. New Phytologist **163**: 499-505.
- Zaller, J. G. and J. A. Arnone, III (1999). Earthworm responses to plant species' loss and elevated CO₂ in calcareous grassland. Plant and Soil **208**: 1-8.

Danksagung

Ich danke allen, die mir bei der Durchführung dieser Arbeit behilflich waren, insbesondere:

Prof. Jäger für die Betreuung meiner Dissertation, das mir entgegengebrachte Vertrauen und vor allem das exzellente Arbeitsklima am Institut, sowie der Bereitstellung (aller-) letzter Finanzreserven für Aufbereitung und Analyse noch unbedingt notwendiger (!) Proben.

Mein Dank gilt Prof. Christoph Müller für die konstruktiv-kritischen Anmerkungen (*“Get used to disappointment”*⁴) und die uneingeschränkte Unterstützung und wissenschaftliche Betreuung meiner Arbeit.

Des weitern danke ich Dr. Claudia Kammann für das Lesen meiner Arbeit und das bereitwillige zur Verfügung stellen von Ökosystematmungsdaten und insbesondere den „long-time storage“ alter Bodenproben, die einen wichtigen Beitrag zu meiner Dissertation lieferten.

Special thanks go to Johan Six and Karolien Deneef for a great collaboration and the opportunity to accomplish part of the lab work at the UC Davis and the University of Gent. I also want to thank Jan Vermeulen for the fast ¹³C analyses of my samples.

Gedankt sei auch Christin Barthelmie für die hervorragende Laborarbeit („*Tick Tack...*“) und auch sonst Mädchen für alles, und nicht zuletzt PD Dr. Grünhage für die Erhebung von meteorologischen Daten. Mein Dank gilt auch Jochen Senkbeil und Jürgen Franz für ihre kontinuierliche und mühevollen Datenerhebung bei Wind und Wetter und ihre Bemühungen, zumindest einige der Bodenluftsonden mit dem Balkenmäher zu verschonen.

Auch danke ich der Physikwerkstatt für ihr schnelles Reparieren bzw. Ändern von sämtlichen dem Bodenbohrer zugehörigen Metallteilen.

Danken möchte ich auch meinem Mann Thomas für das Lesen meiner Arbeit und seinem Verständnis für die vielen nächtliche Ausflüge in den GC Container sowie für das Sammeln von Bodenproben und das Erledigen weiterer Schweissarbeiten von unbedingt und sofort (!) benötigten Teilen.

Mein ganz besonderer Dank gilt meinen Eltern, die mich sehr unterstützt haben und mir stets den Rücken von anderen Dingen frei gehalten haben.

⁴ William Goldmann, *The princess bride*

7 Appendix

7.1 Date of aboveground biomass clipping

Tab. 7.1 Dates of aboveground biomass clipping of the first and second harvest between 2004 and 2006.

Year	2004	2005	2006
first harvest	1 st Jun 2004	13 th Jun 2005	29 th May 2006
second harvest	6 th Sep 2004	13 th Sep 2005	11 th Sep 2006

7.2 Drying-Wetting Cycles between 1997 and 2004

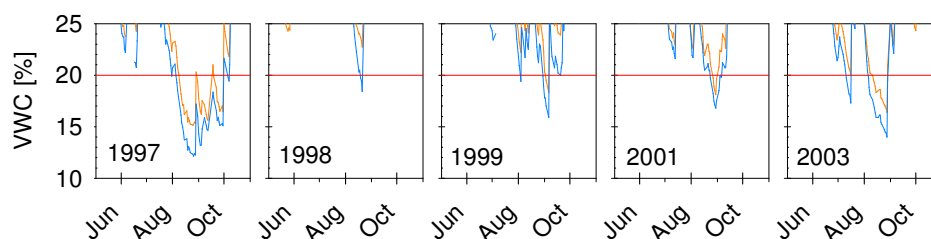


Fig. 7.1 Drying-wetting events of the upper 15 cm of soil between 1997 and 2004, values are presented as means of the ring pairs 1-3 separately for each CO₂ treatment.

7.3 List of gas samples

A list of all gas samples that were used in this study are presented in Tab. 7.2. For the ring pairs 1-3 in total 4679 samples were taken at 100 days to determine the CO₂ concentration, whereas 1209 samples collected on 26 days were measured for their ¹³C signature. For the soil profile of ring pair 4 2680 samples were taken for [CO₂] measurements on 92 days, whereas 645 samples collected on 23 days were analyzed for their ¹³C signature. At 22 days in total 900 gas samples were taken during the ecosystem respiration measurements and analyzed for their δ¹³C signature.

Tab. 7.2 (Soil) gas samples collected between August 2004 and December 2006 to measure the CO₂ concentration or the δ¹³C signature

Date	[CO ₂] Ring pairs 1-3	[CO ₂] Ring pair 4	δ ¹³ C Ring pairs 1-3	δ ¹³ C Ring pair 4	δ ¹³ C R _{eco}
06/Aug/2004			45		
02/Sep/2004			44		
01/Oct/2004		27		26	
07/Oct/2004			46		
13/Oct/2004				27	
05/Nov/2004	46				
12/Nov/2004		25			
15/Nov/2004				28	
18/Nov/2004			46		
22/Nov/2004	47				
10/Dec/2004		27			
22/Dec/2004	44				
24/Dec/2004		45			
05/Jan/2005				27	
07/Jan/2005		28			
12/Jan/2005	46				
27/Jan/2005	45				
09/Feb/2005	42			27	
14/Feb/2005		27			
21/Feb/2005			45		
28/Feb/2005	47				
02/Mar/2005		24			18
08/Mar/2005	45				
09/Mar/2005		27			
10/Mar/2005			47		
11/Mar/2005				28	
12/Mar/2005	47				
13/Mar/2005		27			
16/Mar/2005	45				
17/Mar/2005		28			
18/Mar/2005	45				
19/Mar/2005		28			
28/Mar/2005	47				
31/Mar/2005		28			
04/Apr/2005	47				18
06/Apr/2005				28	
08/Apr/2005		28			
11/Apr/2005			45		
13/Apr/2005	47	27			
18/Apr/2005	48				
21/Apr/2005	47	27			
22/Apr/2005					18
23/Apr/2005	48				
26/Apr/2005		27			

Date	[CO ₂] Ring pairs 1-3	[CO ₂] Ring pair 4	δ ¹³ C Ring pairs 1-3	δ ¹³ C Ring pair 4	δ ¹³ C R _{eco}
28/Apr/2005	48				
29/Apr/2005		27	42		
02/May/2005	47				
06/May/2005	46				
09/May/2005		29			
11/May/2005	47				
17/May/2005			46		
18/May/2005				29	
19/May/2005	47				
20/May/2005		29			
02/Jun/2005		22			
03/Jun/2005	47				
08/Jun/2005	46	27			
10/Jun/2005			47	29	
12/Jun/2005					18
15/Jun/2005			48		
17/Jun/2005	48	30			18
21/Jun/2005	48	29			
24/Jun/2005	48	30			
28/Jun/2005		30			
06/Jul/2005	48				
15/Jul/2005	48	30			
26/Jul/2005					18
27/Jul/2005	47				
30/Jul/2005		30			
08/Aug/2005	46				
11/Aug/2005	46	30			
15/Aug/2005			48		
16/Aug/2005				30	
17-Aug-2005					18
19/Aug/2005	48	30			
24/Aug/2005		30			
25/Aug/2005	46				
02/Sep/2005					18
11/Sep/2005	48				
12/Sep/2005		30			
16/Sep/2005					72
19/Sep/2005			48		
21/Sep/2005	48				
23/Sep/2005		30			
04/Oct/2005	48				
10/Oct/2005		30			
11/Oct/2005	48				
24/Oct/2005			48	29	
26/Oct/2005	47	30			
31/Oct/2005	47				
03/Nov/2005	46				

Date	[CO ₂] Ring pairs 1-3	[CO ₂] Ring pair 4	$\delta^{13}\text{C}$ Ring pairs 1-3	$\delta^{13}\text{C}$ Ring pair 4	$\delta^{13}\text{C}$ R _{eco}
21/Nov/2005			48	27	
23/Nov/2005	46	28			
29/Nov/2005					18
08/Dec/2005	45	28			
19/Dec/2005			48	30	
21/Dec/2005	44	29			
24/Dec/2005		29			
02/Jan/2006	46	29			
14/Jan/2006	46	29			
20/Jan/2006					18
26/Jan/2006		29			
27/Jan/2006	44				
30/Jan/2006			48	29	
01/Feb/2006	47	30			
14/Feb/2006	48	30			
16/Feb/2006	48	29			
19/Feb/2006	48	28			
21/Feb/2006					18
24/Feb/2006	48	30			
26/Feb/2006			45	21	
14/Mar/2006	45	30			
24/Mar/2006	45				
04/Apr/2006	48	30			
06/Apr/2006			47	27	
07/Apr/2006					90
08/Apr/2006	48	30			
17/Apr/2006	46	30			
19/Apr/2006	48	30			
21/Apr/2006	48	30			
23/Apr/2006	47	30			
25/Apr/2006	47	30			
27/Apr/2006	45	30			
30/Apr/2006	48	30			
02/Mai/2006			48		72
04/May/2006	47	29			
05/May/2006				29	
08/May/2006	48	30			
11/May/2006	48	30			
15/May/2006	47	30			
18/May/2006	48	30			
24/May/2006	47	30			
26/May/2006			47	30	
28/May/2006					72
29/May/2006	46	30			72
01/Jun/2006			46	29	
03/Jun/2006	47	30			
05/Jun/2006	47	29			

Date	[CO ₂] Ring pairs 1-3	[CO ₂] Ring pair 4	$\delta^{13}\text{C}$ Ring pairs 1-3	$\delta^{13}\text{C}$ Ring pair 4	$\delta^{13}\text{C}$ R _{eco}
08/Jun/2006	46	28			
16/Jun/2006	47	30			
19/Jun/2006	47	30			
23/Jun/2006	48	29			
28/Jun/2006	48	29			
04/Jul/2006	48	30			
06/Jul/2006			48	28	
07/Jul/2006					54
08/Jul/2006	48	30			
13/Jul/2006	45	29			
19/Jul/2006	48	29			
24/Jul/2006	48	29			
28/Jul/2006	48	29			
31/Jul/2006	48				
03/Aug/2006	47	29			
07/Aug/2006	48	30			
08/Aug/2006					54
09/Aug/2006			44	29	
11/Aug/2006	48	30			
16/Aug/2006	47	30			
16/Aug/2006	47	30			
29/Aug/2006	44	30			
06/Sep/2006	48	30			
10/Sep/2006					54
11/Sep/2006					54
13/Oct/2006	48	30			
15/Oct/2006			48	29	
17/Oct/2006	45	30			54
24/Oct/2006	46	28			
01/Nov/2006	48	26			
07/Nov/2006	44	29			
20/Nov/2006	45	28			
27/Nov/2006	48	29			
01/Dec/2006			47	29	54
04/Dec/2006	46	30			
11/Dec/2006	45	30			

7.4 Bulk density

Tab. 7.3 Bulk density determined in July 2005 and June 2006, values are presented separately for each plot as 2005/2006 averages with the standard deviation.

Depth [cm]	A1	A2	A3	E1	E2	E3	E4
	[g cm ⁻³]						
0-7.5	1.13 ±0.09	0.94 ±0.06	0.99 ±0.10	1.06 ±0.03	1.03 ±0.12	1.01 ±0.02	0.98 ±0.05
7.5-15	1.27 ±0.09	1.06 ±0.07	1.08 ±0.05	1.19 ±0.01	1.16 ±0.07	1.13 ±0.03	1.11 ±0.08
15-22.5	1.37 ±0.11	1.25 ±0.10	1.27 ±0.10	1.29 ±0.04	1.31 ±0.02	1.29 ±0.04	1.26 ±0.05
22.5-30	1.50 ±0.02	1.51 ±0.04	1.49 ±0.00	1.37 ±0.02	1.46 ±0.00	1.47 ±0.02	1.35 ±0.04
30-37.5	1.54 ±0.07	1.60 ±0.04	1.53 ±0.00	1.37 ±0.02	1.54 ±0.01	1.53 ±0.00	1.46 ±0.05
37.5-45	1.55 ±0.04	1.58 ±0.10	1.65 ±0.02	1.45 ±0.00	1.67 ±0.02	1.63 ±0.05	1.58 ±0.01